AD NUMBER: AD0854310
LIMITATION CHANGES
TO: Approved for public release; distribution is unlimited.
FROM: Distribution authorized to US Government Agencies only; Export Controlled; 1 Apr 1969. Other requests shall be referred to Air Force Rocket Propulsion Laboratory, Edwards AFB, CA 93523
AUTHORITY
AFRPL ltr dtd 29 Sep 1971

AFRPL-TR-69-57

AD854310

VOL. 6, NO. 2

APRIL 1969

SOLID ROCKET STRUCTURAL INTEGRITY

ABSTRACTS

STRUCTURAL INTEGRITY INFORMATION CENTER

COLLEGE OF ENGINEERING
UNIVERSITY OF UTAH
SALT LAKE CITY, UTAH

106

SOLID ROCKET

STRUCTURAL INTEGRITY INFORMATION CENTER

is sponsored by the

Air Force Rocket Propulsion Laboratory
Research and Technology Division
Edwards Air Force Base, California
Air Force Systems Command
United States Air Force

Release of this document
by the
Defense Documentation Center
to the
Clearing House for Federal Scientific and Technical Information
is not
authorized

SI 69-016 AFRPL-TR-69-57

Vol. 6, No. 2

SOLID ROCKET STRUCTURAL INTEGRITY ABSTRACTS

F. R. Wagner
Technical Editor

E. D. Cluff
Administrative Editor

April 1969

SOLID ROCKET
STRUCTURAL INTEGRITY INFORMATION CENTER
University of Utah

The Solid Rocket Structural Integrity Abstracts are prepared at the Solid Rocket Structural Integrity Information Center, College of Engineering, University of Utah, Salt Lake City, Utah 84112, under the Technical Direction of Dr. M.L. Williams. The Program is supported by the Air Force Rocket Propulsion Laboratory, Research and Technology Division, Air Force Systems Command, United States Air Force, Edwards, California 93523, under Contract Number F04611-67-0042, AFSC Project Number 3059.

TABLE OF CONTENTS

TABLE OF CONTENTS (contd.)

TABLE OF CONTENTS (contd.)

THE BALLISTIC INTERFACE IN GRAIN CONFIGURATION FOR STRUCTURAL ANALYSIS*

John S. Billheimer

Senior Engineering Specialist
Research & Technology Department
Aerojet-General Corporation
Sacramento, California

Abstract

Solid propellant grain designs submitted for structural analysis have many features which are not favorable to good structural design and make the analysis of stress rather difficult. Presumably there are valid ballistic reasons for these configurations, but it is wondered if closer communication between ballistician and structural analyst would not give a better selection of grain design. The factors leading to a ballistics first, structural review are discussed: quantitativeness of sacrifice in ballistic performance versus probabilistic nature of comparative structural examination, the internal vector surface displacement of ballistic analysis versus the cylindrical chamber coordinates of structural analysis, and traditions of responsibility. The principles of grain design are expressed in terms of the first and second derivative of the burning surface area with respect to distance burnt, the degree of exposure of the chamber wall to propellant flame, and the manner of support of the grain by the case. Examples in star-wagonwheel-dendrite, dogbone and anchor, slotted, conocyl, finocyl, multiperforated and free-standing charge configurations are given. Realization of the morphological order of ballistic grain design should make it easier for the structures analyst to plan his computing capability, and devise trade-off principles for guidance of the original ballistic selection.

Contents

I. Introduction: Ballistic and Structural Objectives

The history of grain design for solid propellant rockets is a contest between maximization of ballistic performance with sharply angular grain designs and relaxation of surfaces for structural integrity. The ballistic design of the grain is based on the mathematical regression in burning normal to all exposed surfaces, and can be rigorously solved by analytical geometry. Structural analysis is more complex, depending on an assumption of material behavior, and can be numerically solved only for somewhat restricted cases of cross-section geometry and end effects.

* Security Order PRA/SA AFRPL dtd. 3 Feb 1969

Furthermore, the measure of deviation from an ideal performance curve (pressure or thrust-time curve) can be computed in a simulated trajectory to yield a definite change in range, or change in payload at fixed range. This phenomenon is described by the "configuration efficiency" of the grain design. The configuration efficiency is obtained by integrating the thrust-time curve to a specified cut-off point or action time, often 10% of average thrust to that point, depending on aerodynamic drag and staging. This actual impulse is divided by that which would have been obtained if all propellant present were converted to impulse at the maximum pressure (presumbly that for which the case and nozzle are designed), as if there were no geometrical problem of charge design, i.e., a square performance curve at the maximum pressure withstood by the case. Using the single figure of merit, i.e. the configuration efficiency, or the longer calculation of actual flight simulation for range or payload, the grain design can be systematically optimized for maximum performance in terms of chamber dimensions, propellant ballistic properties, and the geometrical parameters of the configuration. If a grain design does not give the maximum ballistic performance available, it can be unequivocably subjected to revision. The criteria of performance evaluation: configuration efficiency, progressive, neutral and regressive slope, positive and negative second derivative, tail-off and sliver, as well as typical grain designs, are defined in Figure 1 and 2. These are highly quantitative and subject to computer evaluation.[7]

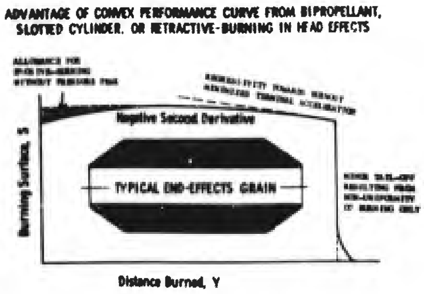

Figure 1

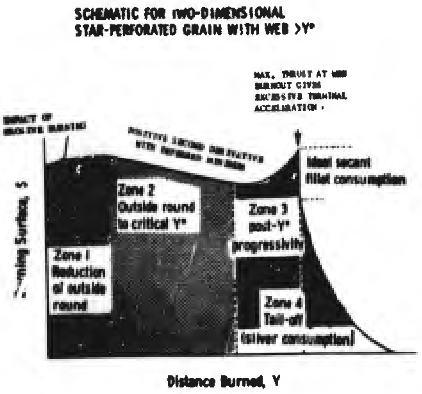

Figure 2

A. Structural Analysis is Less Decisive than Ballistic for Grain Designs

Structural analysis is not so fortunate. Even if the grain design is one for which numerical analysis is available, the relative applicability of elastic or viscoelastic characterization of propellant behavior and the experimental measurement of appropriate coefficients is not conclusive. When the deformation or stress has been calculated, the criteria for failure, immediate or cumulative, must be postulated. Although it is admitted that a propellant charge that gives superior ballistic performance is useless if it has failed structurally, the prediction of structural failure is a qualified concept, involving statistical concepts whereas the loss of ballistic performance is a demonstrable sacrifice in range or payload, the customer's immediate measure of propulsion.

Consequently the history of grain design is one of quantitative ballistic optimization, frequently automated and tied in with a trajectory measure of merit,[6] while the structural integrity is expressed as a statistical qualification, recognized when it is severe, but usually influencing only a request for improved mechanical properties, seldom initiating a major revision of the (ballistic) grain design.[9,78]

Being thus dominated by ballistic considerations, the structural analyst has a sincere need for understanding of the ballistic description and selection criteria which define the structural form.

The fact that propellant burns in straight lines (planes regress to planes, cylindrical surfaces regress to cylindrical surfaces, etc), reduces ballistic grain design to an exercise in geometry. The fact that one desires to obtain the maximum loading in a cylindrical envelope while maintaining an essentially constant (burning) mass flow rate and thermal protection of the chamber wall with a uniform layer of propellant, results in the familiar star, wagonwheel and similar single-perforated grain configurations. The ballistic performance of these configurations is a maximum when all internal fillet angles are sharp, and sides of propellant wedges are parallel to the sector boundaries. Geometrically this analysis originates on the inner bore surface, and projects vectorially into the propellant, with the chamber wall (a circular boundary) being only an incidental boundary condition defining the interruption of the burning surface, and the inception of tailoff or pressure decay.

Structurally, however, the grain cross-section would be subject to a field solution, relating the inner bore and all contained propellant to the circular outer boundary, and thus may be represented numerically by an orthogonal grid of stress/strain flow lines. Rounded fillets and curved boundaries would be the natural solution, as can readily be demonstrated in photoelastic or contour mapping models. The angular features of ballistic optimization are anathema. It is recognized that the ballistic sacrifice in filleting, or otherwise stress relieving a grain configuration is small, but it is real and expressible numerically as in a loss of range, whereas the structural benefit so incurred is problematical, of unquestioned good, but the absolute amount required not decisively established.

B. Nomenclature and Coordinate Systems in Grain Design

In an attempt to give meaning to the configurations usually submitted for structural evaluation the nomenclature of ballistic grain design will be introduced, and the principles of control of the first and second derivative of the burning surface area for ballistic optimization established. The nomenclature of ballistic description will be compared to that of structural analysis and the conversion for the familiar star-perforation with various values of positive and negative wedge angles, various slots and fillet shapes is discussed. A ready conversion between the ballistic and structural analysis of a grain is suggested as essential to a balanced optimization. In a truly integrated design loop this would replace the present ballistic optimization followed by structural veto required by the separate design sequences. A common coordinate system is not essential, and may not be desirable. For numerical efficiency of the separate ballistic and structural routines, an analytical transformation or grid generator is essential to effective balance of ballistic and mechanical properties of propellant in optimizing the charge configuration. Although two-dimensional in this presentation, the principles established apply equally to three-dimensional charge configurations. However, the state-of-the-art in either ballistic optimization or structural analysis may not be sufficiently advanced to warrant an integrated design procedure at this time. A quantitative trade-off can be established on an intermittent basis and interface requirements of a continuous ballistic/structural revision cycle tested in intermittent cycle.

The following will establish the analytical principles of grain design for the planning of future ballistic/structural optimization cycles. The nomenclature employed is based on the morphological classification of solid propellant grain configurations developed by Billheimer.[7]

C. The Status of Structural Analysis of Propellant Grains

The status of design automation for structural analysis of solid propellant grains has been reviewed by Parr.[48] Despite the advances made under the program of the ICRPG Mechanical Behavior Working Group on the definition of mechanical properties of propellants and the development of structural analysis computer programs, three problems remain to thwart an integrated ballistic/structural analysis: (1) the time, temperature and history dependence of the mechanical properties of real propellants, (2) the very large storage and running time requirements of three-dimensional stress analysis computer programs, and (3) the cumulative and critical, not just average, nature of structural failure, in which the petty computation near a discontinuity-which would be ignored in the preliminary design estimation of many engineering aspects - may be critical to inception and growth of a failure in a propellant grain.

The following material will attempt to define the logic by which a grain configuration comes into being, i.e., ballistic criteria. In view of the highly automated nature of ballistic optimization of propellant grain design, and the disproportionately higher cost of structural analysis by finite element techniques, it is important that the structural analyst have some understanding of the principles of ballistic design, and the restraints on configuration alteration that limit ballistic response to the structural notice of criticality. In almost every case, the factors of ballistic optimization (neutrality of performance curve, minimization of sliver, support from and thermal protection of the chamber wall) are in direct opposition to the desirable features of structurally relaxed grains. Unfortunately the quantitative penalties in range associated with ballistic degradation of a grain configuration are difficult to compare to the probabilistic estimates of failure risk in the structural integrity analysis. Grain designs are constantly being sought wherein the ballistic compensatory effects are located in areas that do not produce structural sensitivity, but this perversity seems almost to be a topological fundamental.

The mechanical nature of propellant has been defined in a series of review articles in the Structural Integrity Abstracts.[96] These have included Parr[49] in a survey of numerical methods of solution of solid propellant structural integrity problems, based primarily on elastic solutions. Hilton[35] has described the viscoelastic aspects of the problem, and Fitzgerald[25] has presented the practical engineering approach to the time-temperature transformation in relaxation behavior of propellants including memory effects. The nature of a solid propellant as a structural material has been discussed by Britton,[11] and more recently Parr[50] has summarized the current status of finite element grain structural analysis computer programs.

Brisbane and Becker[10] have established both the mathematical principles and illustrated solutions for "axisymmetric solid propellant rocket motors and other similar geometries with certain non-axisymmetric loads and support conditions which are expressible as a finite Fourier series in the circumferential coordinate."

Melette[42] combines these capabilities into an automated viscoelastic grain structural analysis program, which can respond among other things to a defined ignition transient pressure loading curve. The grain is represented by an equivalent figure of revolution, however, and uses simulated photoelastic stress concentration factors[26] to evaluate configurated bores.

The organization of the subject in such papers, and in the Structural Integrity Abstracts, is appropriately according to the coordinates (dimension and time) of analytical solution. This is necessary to the technical progress of the structural analysis techniques. It does not, however, afford a ready reference to the application-oriented types of grain designs, for which structural analyses are desired. In general, the more the actual configuration of the cross-section and end-effects of the grain are acknowledged in their ballistic form, the less advanced in a materials property sense is the solution capability. That is, the state-of-the-art will permit the rigorous dynamic analysis of a one-dimensional specimen, the exact static finite element solution of a figure of revolution with finite ends, or the empirical photoelastic or numerical approximation of a configurated cross-section such as in a ballistically-designed star-perforated charge.[48]

To the ballistician, who is preoccupied with which star (or wagonwheel or dendrite or other particular grain configuration) gives the optimum ballistic performance in terms of symmetry number, web thickness, fillet radius, wedge angle, etc., the concern is not so much with the absolute predictability of the real mechanical properties as with the relative structural durability of variations in the detail geometrical parameters. This discussion will attempt to define the origin of the various grain configurations, the relative advantages (ballistically) of the design parameters, and the almost inevitable contest between the angularity of optimized ballistic configuration and the filleted forms resulting from structural relaxation. The explicitness of ballistic sacrifice and the intangibility of structural gain require development of a rigorous mathematical expression of the objectives of ballistic grain design to be processed against the structural criteria. These principles of grain design are presented herein.

II. Scope and Constraints of Solid Propellant Grain Design

A. Introduction: Types of Grain Designs

Grain design is a crucial step in the preparation of a solid propellant rocket occurring immediately after and feeding back into mission analysis. It links the properties of the propellant through topology and interior ballistics to the dimensions of the case, and thus establishes the operating pressure and thrust-time history for nozzle and chamber design. This permits detail thermal and structural design of the case, leading to weights determination and confirmation of the mission capability.

The term "grain" derives from gun propellants, where a "charge" was made up of a great number of randomly arranged perforated cylinders whose pressure-time history depended more on empirical flame spread than on the "shape factor" of individual grains.[13,33]

In modern rockets, there are only one or a few pieces of propellant, occasionally cartridge loaded or segmented but usually cast directly into the case in a single mass and (1) providing an insulating function to the case, and (2) deriving structural support directly from the case.

Grain designs are traditionally end-burning, internal-external burning (tubular), or internal burning (case-bonded).[3,64] The case-bonded grains are further divided into two-dimensional (satisfying neutrality in a cross-section independent of length), and three-dimensional (using axial shortening to compensate for increasing internal radius to obtain a constant total burning surface area).

The two-dimensional designs generally have names descriptive of their perforations, as star-, wagonwheel-, dendrite-, anchor-, dogbone-perforated, multiperforated (sectionally or annular) and longitudinally-slotted cylindrically perforated.[5,52,56,75,80] Graphical design charts and analytical computer programs[29,72,73,76,77] exist for most two-dimensional grain designs. The web thicknesses of these cited grains, except for the slotted grain[69] which does not fully protect the chamber wall, are less than one-half of the charg radius. With length-to-diameter ratios of chamber of 2:1 or greater at these web thicknesses, "end-effects" of either unrestricted free-burning ends or interception of radial burning by head-closure contours is treated as a correction in the two-dimensional design system[73,76].

The three-dimensional designs generally have web thicknesses greater than one-half of the radius and often length-to-diameter ratios of the chamber of 2:1 or less. In this case an internal-burning cylinder is used in the high mass flow aft section of the chamber and the configuration detail (slots, stars, cones) is placed in the forward section. By this means the exposure of chamber wall to regulate the effective burning surface area is not as severe in terms of insulation requirement as would apply in the high gas velocity aft portions. Such designs are known as the stake (end-slotted circular-bore cylinder), conocyl (cone-in-cylinder)[15], finocyl (fin-in-cylinder), "star-in-a-pocket,"[95] "winged slot,"[83] and the cone-ended or segmented cylinder.[54,55,62] Each of these configurations depends as much on the chamber envelope (length-to-diameter ratio and head-closure contour) as on the internal perforation for the form of the performance curve. Such designs do not generalize in morphological sequence as tidily as the two-dimensional grain design taxonomy. Some facilities therefore eschew any descriptive names or parametric computer programs, preferring to use only specific designations (literal codes). These designs are evaluated by generalized vector displacement computer routines accepting definition only as a system of spherical, cylindrical, and prismatic sections.[51,86-93]

B. Volumetric Loading and Simultaneous Burnout at the Chamber Wall

Practical grain design may use any combination of these methods to secure an arrangement of propellant surface that will recede from the initial free surface in accordance with Piobert's law (solid propellants burn normal to all exposed surfaces)[43] *towards preferentially a simultaneous exposure of the chamber confining surface (propellant is burnt in an endothermic process in the solid phase and is thus its own best insulator of the remaining propellant and underlying chamber wall)*[12, 34, 63, 65] *to minimize the insulation duty.*

The ideal solution to this topological problem is a series of "onion skin" layers of propellant of successively decreasing burning rate so that the mass flow rate is a constant from a small initial ignition surface to a final burnout equivalent to the chamber wall.[80] Practically this is approached in research grains by a core of relatively fast propellant, which burns out axially with transition to a radial layer of intermediate burning rate and finally by appropriate interfacial boundaries to a relatively slow layer approximating the chamber inner surface.[1,23,85]

Although this tripropellant charge gives "100% volumetric loading without sliver," the difficulty of attaining adequate ratios of burning rate while maintaining competitive specific impulse in all propellant layers limits this ultimate solution. Practically, the cross-sectional loading for internal-burning (single or bipropellant) charges is limited by the simple principle that the port space (aft-end internal flow space) must generally be greater than the nozzle throat proper to secure accurate thrust alignment (propellant throttling is less reproducible than a refractory nozzle throat). The first controlled firings with port-to-throat less than one were reported at JPL in the Loki program.[58a] Thus as throat area becomes an increasing fraction of the chamber cross-section (high thrust relative to duration or operation at low chamber pressures), the possible loading fraction in the propellant chamber is decreased so as not to produce a port-to-throat area ratio less than one. (Actually initial port-to-throat less than one is achieved in some motors by designing an initially progressive burning surface area - distance burnt curve, so as to incorporate considerable erosive-burning without incurring an excessive pressure peak, but this is a principle of detail design discussed elsewhere.)

C. Dimensional Analysis and Environmental Restraints

The volumetric loading discussion above has illustrated a close relationship between the topological design of the grain, the thrust-duration profile of the mission, and the operating pressure and length-to-diameter ratio of the chamber. Dimensional analysis shows that a designer seeking a high thrust, low duration will preferentially select a propellant of relatively high inherent burning rate, operate it in a motor with relatively high chamber pressure and length-to-diameter ratio, in conjunction with configuration of low web thickness; while conversely, for a long duration with relatively low thrust, he will use a low burning rate, low chamber pressure, relatively short length-to-diameter ratio and a grain design of high web thickness.[6,19]

When total impulse is divided by the cube of duration, and substitution is made for web thickness = burning rate x duration, and the resultant web/diameter ratio is expressed as a reduced web or web-to-charge radius ratio (w), then a "dimensionless" parameter F/t^2 is obtained. This is proportional to the cube of the ratio of burning rate to reduced web, multiplied by the first power of the L/D ratio, and the ratio of chamber pressure relative to a reference pressure, raised to a power depending on the burning rate - pressure exponent of the propellant and the slope of the nozzle optimization area ratio curve.

Figures 3 and 4[19] show the distribution of sources of solid propellant rockets and the types of configurations used, respectively, as a function of this F/t^2 parameter.

DISTRIBUTION OF SOURCES FOR SOLID PROPELLANT ROCKET MOTORS AS A FUNCTION OF F/tb^2 FEASIBILITY INDEX FOR 127 OPERATIONAL MOTORS

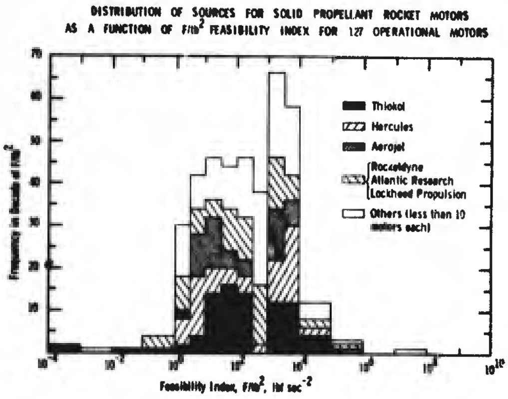

Figure 3

DISTRIBUTION OF GRAIN DESIGN TYPES AS A FUNCTION OF F/tb^2 FEASIBILITY INDEX FOR 127 OPERATIONAL MOTORS

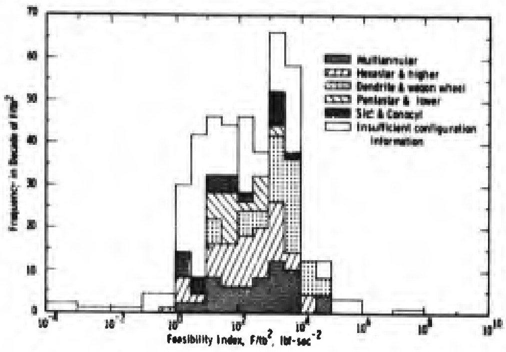

Figure 4

Missions are characterized by F/t^2 values which range from 1 to 10^4 lbf sec^{-2} for all operational motors, but can be blocked within a specific decade for identification of type of grain design, burning rate, and chamber pressure normally used in a particular mission such as an ICBM, Sustaining Rocket, Tactical Booster or Interceptor Missile. The launch mode which is a familiar classification of rockets, as air-to-air, surface-to-air, etc. is not a significant criteria of internal design, except as it may define the value of F/t^2 or secondarily affect the aerodynamic envelope (the L/D ratio).

An exception to this is the effect of launch conditions on environment. It would be ideal if the environmental requirements could be taken into direct account in grain design. However, aside from virtually outlawing cartridge loaded and multiperforated grains,[80] the qualitative nature of environmental criteria compared to the quantitative rigor of mission performance criteria (as specific impulse, peak pressure, hardware weights, thrust-time curve, velocity increment) preclude design of the grain for other than competitive mission satisfaction, and environmental requirements are satisfied by choice of propellant.[18] Fortunately the skill of propellant formulation permits partial separation of ballistic (thermodynamic composition) from mechanical (polymer cross-linkage) factors, although both are highly dependent on solids loading, so that the design of a grain for ballistic satisfaction and adjustment of mechanical properties for environmental requirements are separable procedures. Certain grain designs would be preferred for structural integrity, but until unlimited burning rate at competitive specific impulse is achieved, ballistic performance will continue to dictate grain design.

D. Scope and Design Constraints

Although there are many design factors in the evaluation of a grain design, such as structural analysis, ignition transient, and unstable burning, this discussion will be limited to the quasi-steady-state burning of fully ignited, uniform temperature, homogeneous grains.

Theoretically, the configuration of a propellant charge to deliver a specified thrust performance is limited only by the imagination and ingenuity of the designer. However, there are a number of very real constraints that restrict the designer's freedom and generally channel the design into one or two fairly well defined classes. Among the principal constraints are the available burning rate range,[2,17,22,47] the processing characteristics of the propellant, the mechanical properties of the finished propellant,[9,78] the environment to which the motor will be exposed, the complexity and cost of the core or mold,[32,45] the size and shape of the motor being designed,[31] and the sliver and tailoff characteristics inherent in a candidate configuration.[8]

The general classes of configurations are defined and their characteristics and areas of applicability described. This includes both free standing (trap supported) and case bonded designs. These two methods of support demand vastly different propellant mechanical properties. The former requires a high modulus, "stiff" propellant since the grain is supported at a few discrete points, and the storage, handling, and flight loads must be distributed through the grain.[80] With the case bonded systems,[4] formulations capable of large extensions, sometimes as much as 100% or more of original length, are required This requirement stems principally from the large differences between the coefficients of thermal expansion of the propellants and the case materials to which they are bonded. Since the propellant changes dimensions with temperature change much more rapidly than the chamber, most of the change in volume of the propellant must be absorbed by changes in volume of the internal perforation. This magnifies the basic propellant strain and can lead to very high local bore strains at temperatures significantly lower than the cure temperature, particularly if the bore is highly configurated. Case bonding also requires a relatively low modulus propellant to keep the bond stresses at the grain-chamber interface within acceptable limits.[11,79]

The characteristics, advantages and disadvantages of the possible candidate configurations are discussed. In addition to the mechanical properties mentioned above, this includes consideration of the limitations imposed by processing and the techniques of design construction, assembly, processing, and removal of the core or mold used to shape the propellant charge. The core may be a single-piece, solid, reusable tool. Alternatively it may range to mechanically dismantleable designs, where the core may be assembled inside the chamber and removed in two or more sections, or ultimately to systems where a portion of the core is left permanently inside the grain to be ejected on firing.[11a,32,37a,41,42c,45,57a,80a] The effects of factors such as the range of propellant burning rates available and the other propellant ballistic properties such as pressure and temperature sensitivities on the choice of design is included. The sliver formation and tailoff characteristics of the various configurations will also be discussed.[8] Techniques for automatic grain design through the use of computers are described.[61]

E. Ballistic Evaluation After Shaping of the Grain

Once the shape of the propellant charge has been selected, the problem shifts to one of estimating the performance to be expected for comparison with the originally specified requirements and possible revision of the design. In essence this is an extremely simple problem. Most designs are amenable to the quasi-steady-state approach where the mass balance changes in inventory of combustion products in the enlarging bore can be ignored. The mass balance then reduces to "what is burned off the propellant surface goes out of the nozzle," and many cases can be handled on this simple basis.[57] However, even this simple problem can often become quite complex in its execution, not only because the determination of the burning surfaces as the propellant is consumed can offer some very complicated three dimensional geometry problems, but because the exposed propellant burns at rates dependent on the local environment existing at various locations in the motor.

Erosive burning is one of the major factors complicating the problem. The flow of gases past a burning propellant face tends to increase the propellant burning rate primarily by augmenting the rate of heat transfer from the combustion products to the propellant surface.[38] At the same time the local static pressure is reduced, tending to lower the burning rate. The result is a new equilibrium pressure dependent on the erosive characteristics of the propellant and its pressure sensitivity.[14] Net burning rates thus vary significantly from one end of the motor to the other and often large differences occur in the expected performance. Although this phenomenon is dissipated after the bore cross-section becomes large enough to reduce the internal gas velocities, it results in changes to the grain configuration that can significantly alter performance and materially change the sliver. Various methods of accounting for erosive burning are used including the empirical constants of the equation of Lenoir and Robillard, which is of more theoretical interest than practical determination in actual motors. Comparison of the erosive burning characteristics of the various classes of propellants and the effects of burning rate variations from specific formulations have been made.[30]

III. Basic Analysis of the Star Perforated Grain

A. Introduction - Distribution of Grain Designs Actually Used

The most highly developed grain design analytically, and the most frequently used in 127 operational motors developed in the Western World[19] is the star-perforated charge.[36,52] Since the ideal number of rays for neutrality is 5.7 (corresponding to a sector angle of one radian), the design can be subdivided into star-perforated charges with 6 or more rays (hexastar and higher - 37 motors), and 5 or less rays (pentastar and lower - 32 motors). This subdivision is important since the lower symmetry number stars tend to have web thickness greater than their lateral burning distances (one half of the breadth of the protrusions) and to require and effects (three-dimensional burning) to attain neutrality. The higher symmetry number stars are, on the other hand, satisfied in neutrality in the two-dimensional cross-section, so are independent of length-to-diameter ratio in burning surface area calculations. This is usually the starting point for analytical grain design studies. Other grain configurations of higher periphery and lesser web thickness, such as the wagonwheel- and dendrite- perforated (32 instances) are developed from the high symmetry star configuration and will be discussed later.[67,68,69] In the converse sense, the relatively thick-webbed slotted cylinder designs (16 instances) are evolved from the low symmetry stars and will be presented thereafter. These latter designs develop further into three-dimensional configurations, which will be introduced after the two-dimensional treatment is fully established. These four classes of grain configurations, along with 16 instances of multi-annular or multitubular charges, make up the bulk of the two-dimensional cylindrical-type grain designs employed in operational motors as listed in the CPIA Solid Rocket Motor Manual.[82]

The following section will introduce the precise behavior of the surface regression in the star-perforated grain[8,36,37,39,70,71] in terms of symmetry number, web thickness, vertex or wedge angle, and fillet construction. Understanding of the behavior of these elements, and the principle of zoning the burning in accordance with changes in the first and second derivative of the burning surface area[8] is fundamental to all of the more complicated designs to follow, from 7 degrees of freedom in the star, to 10 in the wagonwheel, 17 in the dendrite,[76] and 20 in the broken-back forked wagonwheel.[81] The multi-propellant and three-dimensional designs are not usually defined in the parametric system but are analyzed by component parts and summed over all surface ares.[51]

B. Analytical Definition of the Star-Perforated Grain in Ballistic and Structural Application

Figure 5 shows the "stop-fire" of an actual star-perforated grain, at the moment of chamber wall exposure, demonstrating the slivers remaining under each protrusion.[21] Figure 6 illustrates the graphical construction of the burnback lines for four principal types of surface intersections. This behavior is due to the presence of a combustion zone only a few hundred millimeters in thickness, comparable to the dimensions of a typical oxidizer particle, which follows with the accuracy of chemical milling the exact contour of the solid surface. This is the source of the computer-predictable reliability of solid propellant grain design. Thus trigonometric expressions are readily written for the position of the burning surface at any distance burnt for a specified configuration, and these can be differentiated to obtain the optimum symmetry number and fillet angle for neutrality or other key design variables. Figure 7 shows the right halfsector of an

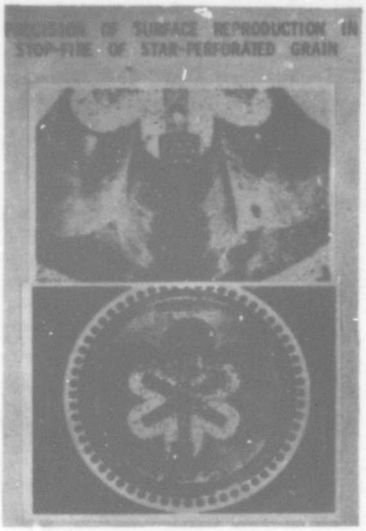

Figure 5

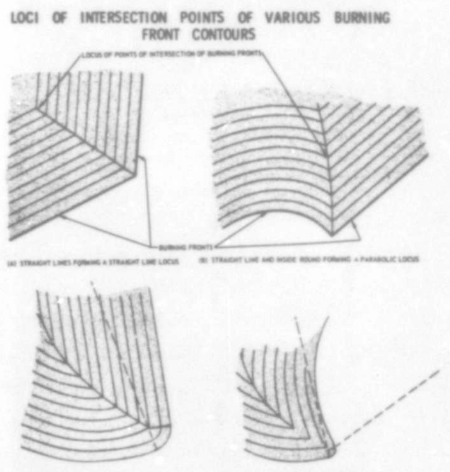

Figure 6

ideal star-perforated grain before rounding or fillets. Defining a vertex radius (R_s) and an inner radius (R_i), the law of cosines gives two relations which permit expression

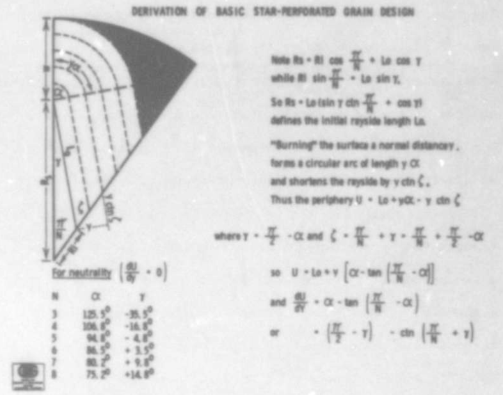

Figure 7

of the initial rayside length (L_o) as a function of the sector half-angle (π/N) or symmetry number (N), the fillet half-angle (γ), and this vertex radius (R_s), which is by definition the complement of the reduced web thickness in a charge of unit radius before introduction of stress relief fillets. (In structural nomenclature, this design would be a "negative wedge angle star" whose included angle would equal 2γ).

"Burning" of this surface for a normal distance (y) will form a circular arc of length ($y\alpha$) and shorten the rayside by the segment (y ctn ζ). Thus, the periphery becomes

$$U = L_o + y\alpha - y \text{ ctn } \zeta$$

noting that $\gamma = \frac{\pi}{2} - \alpha$ and $\zeta = \frac{\pi}{N} + \gamma = \frac{\pi}{N} + \frac{\pi}{2} - \alpha$

then $U = L_o + y\,[\alpha - \tan(\frac{\pi}{N} - \alpha)]$

so that the slope of the "geometric performance curve" $dU/dy = \alpha - \tan(\pi/N - \alpha)$. Setting this equal to zero and solving for α or γ, the neutrality control condition becomes

$$\alpha = \tan(\frac{\pi}{N} - \alpha) \quad \text{or} \quad \frac{\pi}{2} - \gamma = \text{ctn}(\frac{\pi}{N} + \gamma).$$

It is seen that for N of 3, 4, or 5, the tangential fillet angle (α) exceeds 90° and hence the rayside cannot exist without a negative value of the vertex angle (γ). Hence, in the sharp pointed star, only symmetry of 6 or higher (3.5° vertex half angle or greater) is possible for a neutral periphery-distance burnt relation.[52]

In Figure 8, a rotation of the reference axis has been made Φ degrees to the right, producing a "secant fillet" of included angle (Φ) and radius (R_s). This adds an arc ($R_s + y$)

INTRODUCTION OF SECANT AND TANGENT FILLETS

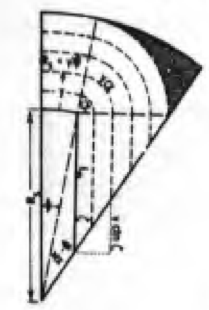

Rotating the prior figure ϕ degrees to the right, introduces a secant fillet of included angle ϕ and web inner radius Rs, adding an arc (Rs + y) ϕ to the periphery and substituting $\left(\frac{\pi}{N} - \phi\right)$ for $\frac{\pi}{N}$ in periphery.

$$U = (Rs + y)\,\phi + Lo + y\left[\alpha - \tan\left(\frac{\pi}{N} - \phi - \alpha\right)\right]$$

$$= Rs\,\phi + Lo + y\left[\phi + \alpha - \tan\left(\frac{\pi}{N} - \phi - \alpha\right)\right],$$

so the neutrality control expression becomes

$$\phi + \alpha = \tan\left(\frac{\pi}{N} - \phi - \alpha\right),$$

and the previous table becomes

N	$\phi + \alpha$	$\gamma - \phi$	$\phi_{slot(\gamma=0)}$	$\gamma_{\phi = 10^0}$
3	125.5°	-35.5°	35.5°	--
4	106.8°	-16.8°	16.8°	--
5	94.8°	- 4.8°	4.8°	5.2°
6	86.5°	+ 3.5°	--	13.5°

Figure 8

THE POSITIVE WEDGE ANGLE OR BROAD-POINTED STAR GRAIN

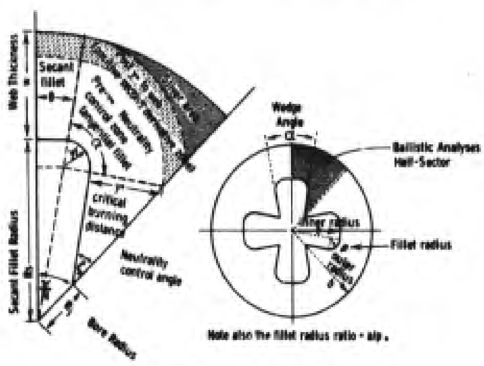

Figure 9

to the burning periphery and substitutes ($\pi/N - \phi$) where π/N formerly appeared in the periphery relations. Thus, the periphery equation becomes $U = R_s\phi + L_o + y\,[\phi + \alpha - \tan(\pi/N - \phi - \alpha)]$ and the neutrality control expression becomes

$$\phi + \alpha = \tan\left(\frac{\pi}{N} - \phi - \alpha\right).$$

In this case, the critical angular difference ($\gamma - \phi$) can be satisfied in neutrality by $\gamma = 0$ (producing a pseudo-slotted grain when the secant fillet is given the prescribed value ϕ = 35.5° for N = 3, ϕ = 16.8° for N = 4, and ϕ = 4.8° for N = 5). Similarly, for a negative wedge angle (positive 2γ) with a secant fillet angle of 10°, the neutrality condition would be satisfied by γ = 5.2°, in N = 5, γ = 13.5° in N = 6, etc. Charts of this correlation for various values of symmetry number, secant fillet angle, and "regressivity coefficient" or slope of the performance curve are available [37,39] or solutions may be obtained directly from the expressions above.

It is apparent that, when the secant fillet angle is above a certain critical value in each symmetry number, the vertex angle (γ) can be negative without the tip of the wedge crossing over the sector boundary. A particular condition of this design is defined in Figure 9, where the tangential fillet angle (α) is arbitrarily held at 90°, and the rayside is parallel to the radius through the secant fillet/tangent fillet boundary. This is shown in a small insert in the same figure, where the structural nomenclature b = outer radius of charge, a = inner radius of web, α = wedge angle, and ρ = fillet radius is used. [26] The corresponding nomenclature for the ballistic analysis is shown on the enlarged half-sector, which is really a special case of the secant-filleted star from the previous figure with the tangential fillet angle set at 90°.

Performing the obvious trigonometric relations including provision for the tangential fillet radius (y_f in the ballistic nomenclature), the reduced web $\omega = (b-a)/b$, and the secant fillet angle (ϕ) is obviously half the stated wedge angle. Then for the secant fillet radius $R_s = R_c - w$, the tangential fillet radius $y_f = \rho$ and the inner radius R_1 is obtained from the expression $y_f \csc(\pi/N - \phi)$, and the initial rayside $L_o = (R_s - y_f) - y_f \operatorname{ctn}(\frac{\pi}{N} - \phi)$. In this case the burning periphery is given by

$$U = (R_s + y)\,\phi + y\alpha + L_o - y \operatorname{ctn}\left(\frac{\pi}{N} - \phi\right)$$

and

$$dU/dy = \phi + \alpha - \operatorname{ctn}\left(\frac{\pi}{N} - \phi\right)$$

So the neutrality control expression becomes simply

$$\phi + \alpha = \operatorname{ctn}\left(\frac{\pi}{N} - \phi\right)$$

It is apparent that in the positive wedge angle design, as defined with tangential fillet angle of 90° and independent of the radius of the tangential fillet (y_f or ρ), there is a unique value of the positive wedge angle (2ϕ) for each value of symmetry number, and that this cannot even be satisfied with a positive value of ϕ below symmetry of 6 in the neutral-burning condition. Thus, all positive wedge angle designs having symmetry of 5 or below will necessarily have progressive burning (positive slope) performance curves and not be applicable to high mass ratio, acceleration-limited rockets unless this two-dimensional periphery relation is mitigated by the end-effects of burning in short length-to-diameter ratio motors, or by multipropellant charges of differing burning rate layers, etc. The ballistic significance of the fillet angle in obtaining an optimum performance curve is developed in the following section. Each such design should also be subjected to a photoelastic stress concentration test before final selection.[20,26] The nomenclatures of ballistic and structural analysis are compared in Figure 10.

COMPARISON OF STRUCTURAL AND BALLISTIC NOMENCLATURE IN POSITIVE WEDGE ANGLE STAR WITH TANGENTIAL FILLET ANGLE 90°

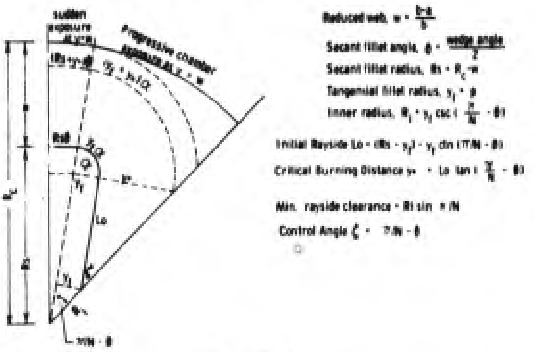

Figure 10

C. Vertex Angle - Progressivity, Neutrality, and Regressivity[61]

The effect of vertex angle (γ) on the performance curve of the ideal (unfilleted) star-perforated grain design is shown in Figure 11. This is a symmetry of 8 star with reduced web 0.35, tangential fillet angle ($\alpha = \frac{\pi}{2} - \gamma$) of 85, 80, and 75°, with zero value of secant fillet angle (ϕ), and trivial value of tangential fillet radius (y_f). Since there are 7 degrees of freedom, the rayside (L_o) is necessarily dependent and decreases with the decrease in fillet angle (increase in vertex angle). This produces a "regressive," "neutral," and "progressive" performance curve respectively.* Although the loading factor decreases systematically as the rayside rotates (0.887, 0.844, 0.810 respectively), the configuration efficiency is a maximum at neutrality (95.56%), and significantly less whether the peak pressure is at the beginning of the performance curve (regressive case, 94.29% configuration efficiency) or at the end of the curve (progressive case, 94.64% configuration efficiency).

Effect of Vertex Angle on Slope of Performance Curve

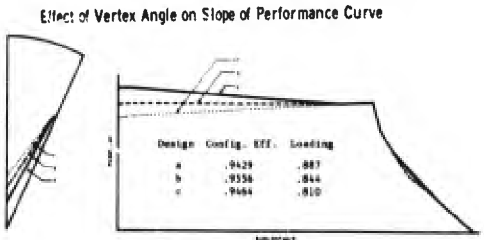

Figure 11

* For definitions, see the diagram in the Glossary

In the case of severe acceleration limits, the regressive curve might be used to accomplish as much acceleration as possible while the mass of the motor is large, i.e., allowing thrust to decrease proportionally as the residual mass of the rocket reduces. Even with the 4% increase in volumetric loading (0.844 to 0.887), it is doubtful whether the 1% loss in specific impulse (configuration efficiency 0.9556 to 0.9429) would be acceptable in terms of burnt velocity at constant maximum acceleration. Significant regressivity for the entire length of the curve is seldom employed, due to the necessity of carrying a chamber and nozzle capable of the maximum pressure experienced, while only enjoying the specific impulse efficiency of the average pressure.

Using the progressive option, an allowance could be made for erosive-burning without the risk of exceeding the design pressure in an "erosive-burning peak." However it will be shown later that this is better done by control of the outside round, which gives an initially deficient burning surface area (Zone I burning) during the erosive-burning period, without impairing the neutrality of the main portion of the performance curve (Zone II burning). It is seen that neutrality is actually the control of the tangential fillet angle to determine the length of the rayside compared to the sliver burnout arc. This is the *first principle of grain design* for maximum burnt velocity.

D. Tangential and Secant Fillet for Stress Relief at Point of Attachment

For stress reasons, it will be desirable to introduce a fillet at the point of attachment of the wedge to the case-bonded web. This may be done with a tangential fillet, which has its center just off the web surface and meets the rayside tangentially (Figure 12) or by a secant fillet whose center is at the axis of the charge and forms a small annular segment before attachment of the wedge (Figure 13). The web thick-

Introduction of a Tangential Fillet

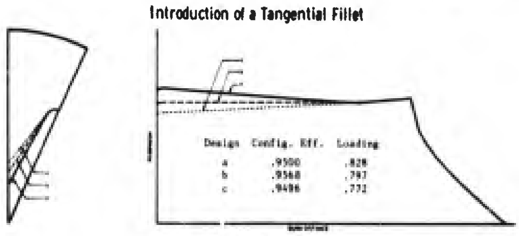

Figure 12

Shift of Slope with a Secant Fillet

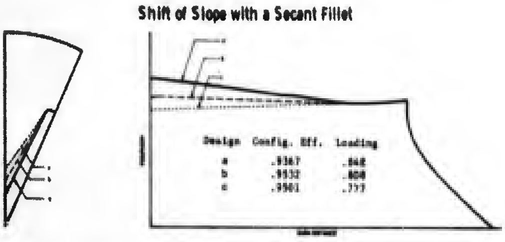

Figure 13

ness (0.350) and assortment of tangential fillet angles (85, 80 and 75°) are maintained the same in both cases. The tangential fillet radius is increased from its nominal value of 0.02 radius to 0.05 of the charge radius in the prior figure with a 6 to 4% loss in loading respectively, compared to the base case in the unfilleted star. The configuration efficiency [60] shows the usual peaking around neutrality, i.e., the enlargement of the tangential fillet radius has no significant effect on neutrality.

The secant fillet, on the other hand, causes a slightly more complex phenomenon. The loading for introduction of a 2.5° secant fillet decreases only half as much in the progressive case (a) as resulted from the tangential fillet, but the configuration efficiency obtained the lowest value cited. The second case (b) has almost the same volumetric loading and configuration efficiency whether the filleting is done in the secant or the tangent fashion. Finally in the third case (c) it is noted that loading is again about the same, and the configuration efficiency is slightly higher (95.01%) with the secant fillet than was obtained with the tangential fillet (94.96%). Most significant is that neutrality with the secant fillet has shifted from the b ($\alpha = 80°$) case to midway between the b and c cases ($\alpha \approx 78°$), reflecting the fact that not the tangential fillet angle α but the difference $\alpha - \phi$ appears in the neutrality control expression.

$$\phi - \gamma = \text{ctn}(\pi/N + \phi - \gamma) \quad \text{or} \quad \phi + \alpha = \tan(\pi/N - \phi - \alpha)$$

It has been necessary to use quantitative examples to show the significance of filleting in controlling the performance curve, and thus the velocity increment. It is noted that a 1% change in configuration efficiency is directly equivalent to a 1% change in specific impulse by analogy. However it would require a 6.5% change in volumetric loading factor ($1-0.935^{0.15} = 1-0.99$) for the same effect, assuming a loading exponent of 0.15 (which is typical of the threshold between fixed volume and open volume chambers). It is evident that configuration efficiency and the volumetric loading factor have a material effect on the choice of tangential fillet angle (α) for rayside orientation, while either the tangential fillet radius (y_f) or the secant fillet angle (ϕ) controls the wedge attachment stress relief, when constant burnt velocity control is being maintained in the design of the grain. This assumes that maximization of mass ratio and specific impulse, which are effectively combined in the expression ($I_s\rho^\alpha$) for propellant specific impulse and density tradeoff [28] or ζv_p^α for the analogous configuration efficiency and volumetric loading factor tradeoff, is the object of optimization.*

E. The Significance of the Secant Fillet

In the reinforcement theory of stress concentration in a star-perforated grain, it is postulated that deformation which would normally occur in the internal pressurization of a thick-walled cylinder is restrained by the presence of the protrusion, so that it must concentrate in the unreinforced portion (subtended by the secant fillet) in the proportion of the protrusion width to the secant fillet width. Since $y^* = $ web for reasonable ballistic performance, the stress concentration is thus approximated by the ratio of web thickness to secant fillet arc or w/ϕ radians. If the secant fillet angle (ϕ) is increased therefore for stress relief,[20,46] Figure 14 shows that the performance curve will be altered significantly. The usual spread of regressive, neutral and progressive performance has been foreshortened, since the center of the tangential fillet was moved towards the far sector boundary. That is, the critical distance (y^*) has been decreased, while the radial web remains unaltered.

Introduction of Broad Secant Fillet at Constant Web

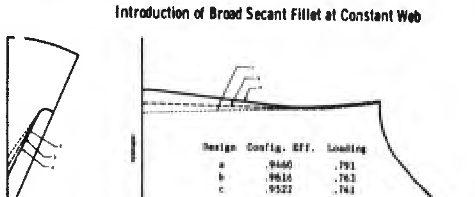

Figure 14

* The use of α established in the expression $I_s\rho^\alpha$ is not to be confused with the tangential fillet angle α used in grain design.

Thus, the lateral burning wedge (which contributes the regressive element to the total periphery) is being exhausted at an earlier time than the progressive element emanating from the several fillets, which endures until the burning front from the secant fillet reaches the chamber wall (web burnout time). The effect is an upwards turn in the performance curve (positive second derivative of the burning surface area with respect to the distance burnt characterizing Zone III or post - y* burning), regardless of the slope of the performance curve prior to y* (the Zone II or wedge-angle-controlled burning).[76]

F. Creation of the Wagonwheel Grain Design

In an effort to recoup the large loss of loading occurring in parallel displacement of the rayside with an increasing ϕ, and to correct for the upset of the y* = web limitation on the Zone III terminally progressive burning, the tangential fillet may be increased beyond 90°, producing the "positive wedge angle" star perforation previously shown in contrast to the conventional "negative wedge angle" (looking outward) of the basic star configuration (Figure 7). Unfortunately spatial limitation requires that the secant fillet also grow very rapidly to prevent physical cross-over of the protrusions. Under neutrality conditions, this loading factor becomes impractical for more than a very modest positive wedge angle. A break is therefore made in the rayside at the point of reasonable approach to the reference line (actually determined by the practical web of the casting core and the pressure equalization of the web and central flow spaces).

This extra degree of freedom (adding a breakround angle, breakround radius, and far rayside length) results in 10 independent variables. It permits the tangential fillet angle (α) to be set to permit the critical burning distance (y*) to approximate the web thickness at an appropriate secant fillet angle (ϕ) magnitude, and the neutrality to be satisfied by assignment of the breakround angle (β).

Loading is a maximum when the far rayside is approximately parallel to the reference axis producing a spoke-and-hub appearance, whence the term "wagonwheel" perforation (Figure 15).[66-68] The value of β thus becomes an implied dependent variable under conditions of maximization of loading

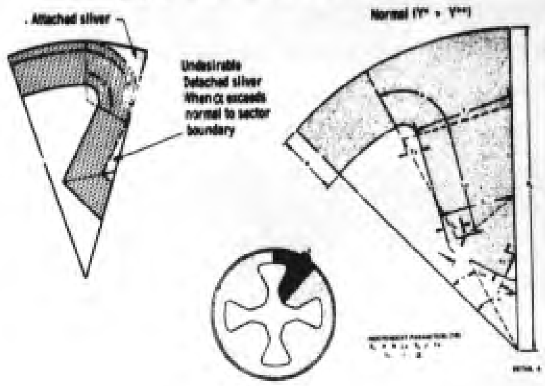

Figure 15

at neutrality, much as the vertex angle was the key optimization variable in the simple star configuration. Figures 16 and 17 show that interplays of tangential fillet angle (α) and breakround angle (β) produce comparable configuration efficiency and volumetric loading factor, and final evaluation would require both structural and mission analyses for resolution.[9]

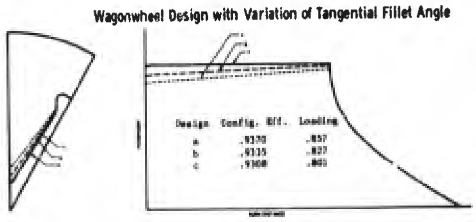

Figure 16

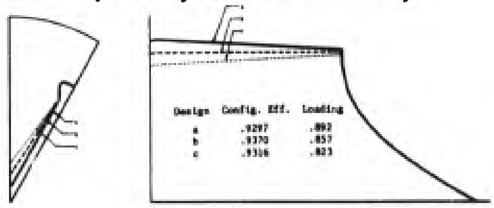

Figure 17

Up to this point, it has been established that y* must be almost as large as web to prevent post - y* terminal progressivity. It has been previously shown that y* much greater than web results in a large quantity of propellant remaining when the radial web burns through to the chamber wall. This "attached sliver" is consumed during the decreasing pressure period or tail-off, where nozzle thrust coefficient is reduced (assuming constant expansion area ratio). Thus attached sliver, although not physically lost, decreases the average specific impulse of the propellant,[24,40] and is a part of the penalties assessed in the configuration efficiency along with the deviation from neutrality during web-burn time. These are taken together to obtain the effective specific impulse to action time compared to that which would have been obtainable if all the propellant could have been burned in a "square curve" at the design pressure of the nozzle and chamber, i.e., as if there were no spatial problem of grain design.[60] Control is thus the *second principle of grain design.*

If an intentional displacement of the rayside along the length of a grain (all prior considerations have been constant cross-section) were made in variation of the three designs shown in Figure 18, which action would be said to violate the provision of y* = web for minimum sliver, there would be a significant terminal muting of the usual web-burnout thrust in the resulting composite mass flow (pressure-time) curve.

Displacement of Y* for Muting of Terminal Acceleration

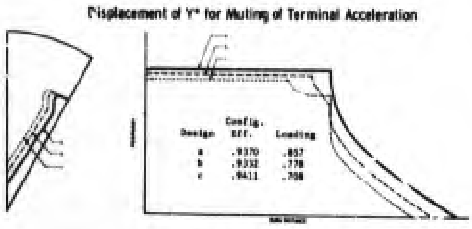

Figure 18

Numerous variations on the axial taper principle[16,44] to systematically mute the angular features of single cross-sections have been devised, but all follow logical application of principles stated above.

G. Development of the Dentritic-perforated Grain Design

The action taken above to form the wagonwheel configuration placed a greater proportion of the propellant lying along a sector boundary with the mean burning vector normal to that boundary than occurred in the star grain where the mean vector lay midway between the sector boundary and the charge circumference. The effective web thickness for a balance between the lateral and radial webs is also less than in the star configuration. To obtain even thinner webs, for a maximum surface area and a minimum burning time, a simple increase in symmetry number will not do, since this would result in excessive regressivity. Instead, the "eye" of the wagonwheel configuration is filled by a minor protrusion, which may be either star or wagonwheel in its form, and ideally nestles within a major wagonwheel protrusion, to form a constant width, branched channel, flow space, whence the term "dendrite-perforated" grain.[8,76]

Figure 19 shows the disproportionately high surface area and low web thickness obtained in this design, which unfortunately incures also relatively lower configuration efficiency and volumetric loading factor, due to the simple geometrical fact of imperfection in design of continuously supported angular and radial elements in an overall sectorial space with continuous flow space and without violation of detachable sliver or neutrality deviation prohibitions. This is clearer

Simple Dendrite Design Formed by Two Star Protrusions

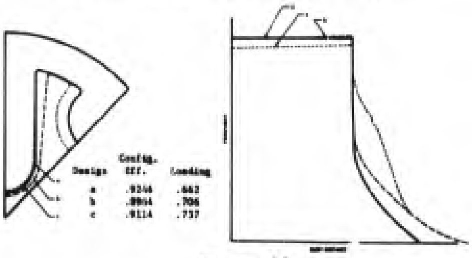

Figure 19

by inspection of the dimensions of the simple dendrite in Figure 20.

Dimensioning of Simple Dendrite Showing Significance de Round

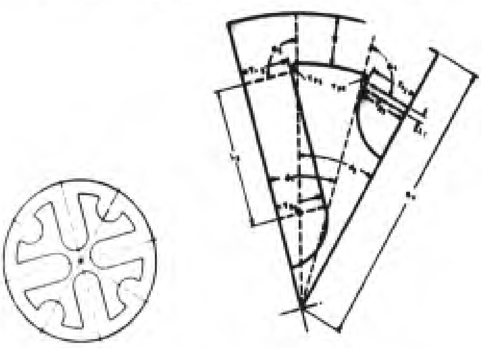

Figure 20

Actually much higher loading can be obtained by composing the dendrite-perforated grain from a wagonwheel-in-star (Figure 21) where the far rayside of the minor protrusion is made parallel to the opposing rayside of the major protrusion. If further the major protrusion is itself a wagonwheel form (Figure 22) with its outer rayside in turn parallel to the

DENDRITE COMPOSED OF WAGONWHEEL IN STAR PROTRUSION

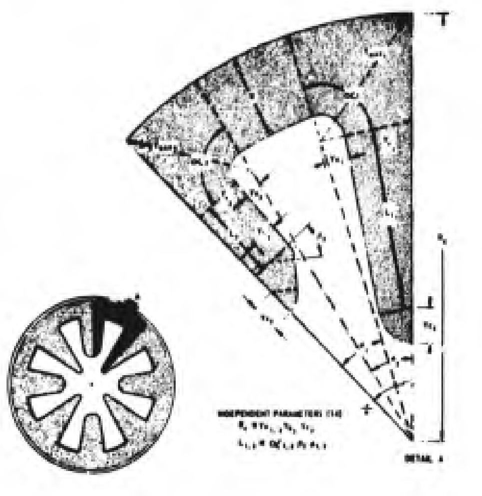

Figure 21

DENDRITE COMPOSED OF WAGONWHEEL IN WAGONWHEEL PROTRUSION

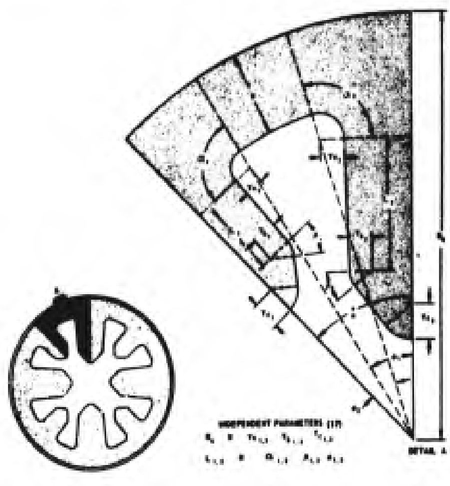

Figure 22

minor protrusion sector boundary, the generalized 17-degree of freedom dendrite grain is obtained. In practice, a computer program written for this design, by assigning insignificant values to the unwanted variables, is actually used in evaluation of the complete star-wagonwheel-dendrite two-dimensional case-bonded grain design system.[7,76] An even more general design is shown in Figure 23, where the "broken-back" on the major protrusion adds 3 more degrees of freedom (total of 20), while permitting a slightly better access to the sliver area and thus reducing tail-off losses.[73, 81]

GENERAL FORKED WAGON WHEEL (DENDRITE) CONFIGURATION INPUTS

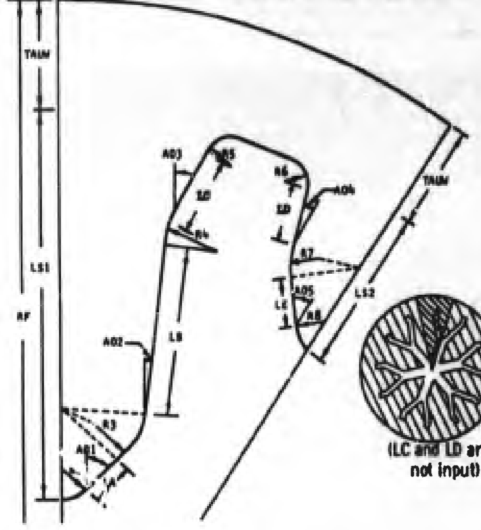

Figure 23

H. Configuration Efficiency and Volumetric Loading Factor for the Star-Wagonwheel-Dendrite Grain Design

The complete performance of the star-wagonwheel dendrite system can be summarized in Figure 24.[60] The configuration

CONFIGURATION EFFICIENCY AS A FUNCTION OF VOLUMETRIC LOADING FACTOR FOR GRAIN DESIGNS OF VARIOUS TYPICAL WEB THICKNESSES

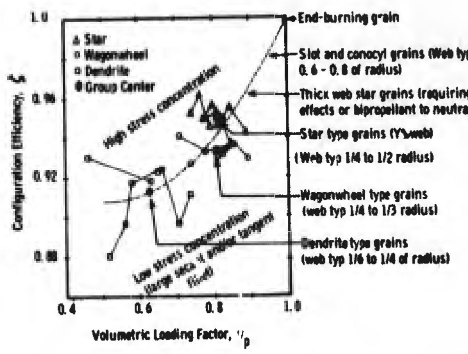

Figure 24

efficiency is given as a function of the volumetric loading factor for sets of dendrite type grains (the square symbols), wagonwheel type grains (the circular symbols), and star type grains (the triangular symbols). The tielines between the symbols represent the variation in properties as these sets go from regressive to neutral to progressive, which represents the range from angular wedge attachment (typically low configuration efficiency, high loading factor and stress concentration) to secant and/or tangentially filleted attachment (typically higher configuration efficiency, lower loading, but also lower stress concentration). A locus may be drawn through the group centers and connected to the ideal end-burning charge (100% configuration efficiency *and* loading factor, in principle). It may then be generally stated that as reduced web goes from 1/6 to 1/4 to 1/2 of the radius, the loading factor goes from 60 to 90 vol % while the configuration efficiency goes from 90 to 96% respectively, or an exchange exponent $\alpha \approx 0.15$ for the expression ζv_p^{α} = constant, as previously discussed.

Since this is approximately the threshold magnitude of the closed volume - open volume impulse-density exponent for burnt velocity maximization, it is evident that the choice of configuration is a sensitive balance of web thickness versus burning rate, burning rate versus the specific impulse and density, and web thickness versus the loading factor and configuration efficiency. These latter in turn vary with the symmetry number and rayside orientation for neutrality and sliver control, and finally the resultant fillet angles and radii determine the stress concentration factor, which presumably relates to the mechanical properties of the propellant and involves the solids loading, burning rate, specific impulse, etc.[6,9] Full execution of this loop is not yet a quantitative capability of preliminary design, although computer programs are used to generate the performance curve obtainable in systematic parameter variation of the ballistic factors discussed above, and these results are compared qualitatively with structural failure criteria and propellant formulation practices.

IV. Ballistic Optimization, Chamber Exposure, and Grain Support

A. The First and Second Derivative: The Laws of Ballistically Optimized Grain Design[76]

The above excursion establishes the first two laws of grain design for singly-connected, internal-burning, case-bonded two-dimensional grain designs. (Figure 25 shows the functional zones of ballistic analysis for the wagonwheel configuration).

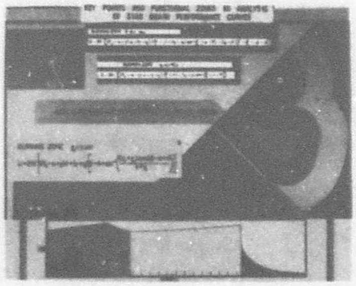

Figure 25

1. The first derivative of the burning surface area with respect to distance burnt shall approximate zero (neutral-burning) in the region between the exhaustion of the outside round (y_R) and the critical burning distance (y_*), which defines the Zone II of functional burning. This law will relate symmetry number, reduced web thickness, tangential fillet angle, secant fillet angle, and breakround angle (in approximately that order of decreasing significance) for maximization of the volumetric-loading-weighted configuration efficiency (combining the significance of neutrality, sliver, and volumetric loading in fixed or variable chamber volumes for maximum burnt velocity).

2. The second derivative of burning surface area with respect to distance burnt shall be negative during that period (Zone I burning) in which erosive-burning and/or axial pressure drop make static fore-end pressure greater than the ideal steady state relation to burning surface area (which is usually synchronized with Zone II where the second derivative is zero, and the slope is determined by first law considerations). This second derivative shall further not be positive during the post-y_* period when radial progressivity overshadows the residual wedge-burning. However, this may be excepted when axial shortening of the effective charge length by interception of curved head closure surfaces compensates for the increasing mean radius of the inner burning surface.

B. Chamber Wall Exposure and the Slotted Grain Design

The above designs by definition have not exposed chamber wall to propellant flame until web burnout, except for the "end-effects" noted in the waiver of post-ye burning in the second law above. Another concept of grain design employs the chamber wall to confine the burning surface area at any point in time. In the star-wagonwheel-dendrite case-protected designs, this occurs only after web burnout when the pressure is decreasing rapidly or on head closures where additional insulation is readily installed. The end-burning grain, on the other hand, has a linear rate of exposure of chamber wall with distance burnt, and is thus limited to low flame temperature propellants, short burning times, or relatively heavy-wall chambers.[58] Intermediate between the end-burner (100% volumetric loading and configuration efficiency, albeit ignoring considerable insulation penalties) and the truly internal burning grains (usually with web thicknesses less than one-half of the charge radius), are a large variety of "slotted" grain configurations. The condition which defines the ballistically functional slot in the classification of grain designs is given in Figure 26.

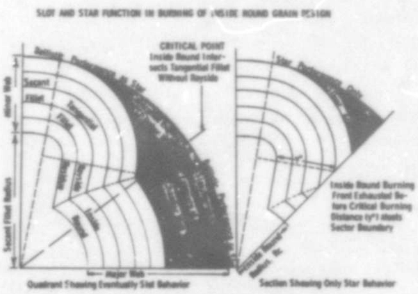

Figure 26

The most familiar in two-dimensional slotted grains is the slotted shell (slotted cylinder) shown in Figure 27. This is originally designed with a certain exposure time thickness (minor web), during which time it is progressive burning (equivalent to the Zone I erosive-burning absorbance period of star configurations). After the first chamber exposure, the radial burning front from the central bore and that from the incision fillet intersecting the chamber wall together curtail the length of the lateral burning front from

BUILT-UP INSULATION FOR SLOT COMPARED TO UNIFORM LINER FOR STAR

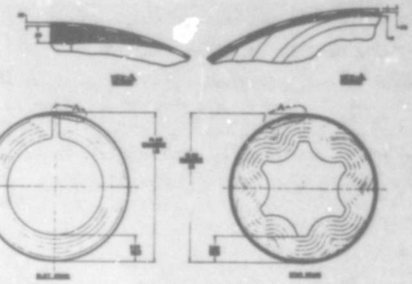

Figure 27

the sides of the incision, whereby a state of neutrality can be approximated. The exposure time of the chamber wall can be calculated, and the original depth of the incision adjusted for the necessary insulation pad compensating for ablation during this period, so that thermal duty on the chamber will be uniform over the grain, and not produce "hot spots" under the slots.

When optimized for first law neutrality (only about half as many slots are required, 2 or 3, as the symmetry number in a comparable star-perforated charge). For this the second derivative of burning surface area is constantly negative; that is, at a given slope of the performance curve, the second derivative continuously decreases giving a convex performance curve. This naturally provides for the absorbance of the initial erosive-burning peak, and for a terminal muting of thrust desirable in high mass ratio, acceleration limited systems. Thus the Second Law, in slotted grains, is satisfied continuously. The price of this ideal performance curve is, however, the exposed chamber wall duty. Thus the *Third Law of grain design is that the second derivative of burning surface area can be made continuously negative entirely to web burnout only by exposure of chamber wall as a neutrality control device.* Thus it follows that the concomitant insulation (measured in the exposure integral or integral of chamber exposure area with respect to time of burning), taking account of ablation rate for uniform thermal protection of the chamber wall, is a direct offset to penalties of sliver and positive second derivative impairment of configuration efficiency in the internal burning grain. No quantitative expression of the third law, comparable to the loading-factor-weighted configuration efficiency of the second law, has been achieved. This is evaluated only by comparative design with a comprehensive ablative insulation, thermal design, computer program.

C. Structural Support and the Slotted Grain

If the "fourth law" of grain design could be stated quantitatively, it would require that all propellant be supported from the chamber wall with a minimum of stress concentration: either internal pressurization, temperature cycling or flight acceleration. On the surface this favors the slotted grain, which relieves all differential cylindrical strain between chamber and propellant by means of the slot thru the web. However, in avoiding the stress concentration of the internally-convoluted grain, the slotted charge incurs disadvantages in exposure of the chamber wall under the slot, plus the necessity of restricting a portion of the slot faces to meet certain ballistic requirements, and in the limited web thickness of 0.7 - 0.8 of the charge radius for competitive volumetric loading of the chamber space.

This means that the design is used for relatively moderate thrust, long duration missions, or that exceptionally high burning rates must be made available.[19] The slotted grain is rather inflexible with respect to web thickness, and is critically dependent on the technologies of internal insulation, collapsible cores, and partial release between chamber wall and grain for critical stress areas. A sliverless, multi-propellant charge would theoretically seem the ideal solution for high loading, minimum stress, neutral-burning charge.

D. The Sliverless Bipropellant Grain Design

The ideal sliverless charge is based on the principle that a line of burning passing through an interface between propellants of differing burning rates, will refract as in the case of a stick placed in water, and if this interface is so oriented that after refracting, the line of burning is normal to the chamber wall, and furthermore the initial surface is so related to the burning rate ratio that all these lines of burning are exhausted at the same time, then a sliverless, internal-burning (bipropellant) grain has been achieved. This is shown in Figure 28 for symmetries of 2,3, and 4 giving progressive, neutral, and regressive performance, respectively.[7,53,59]

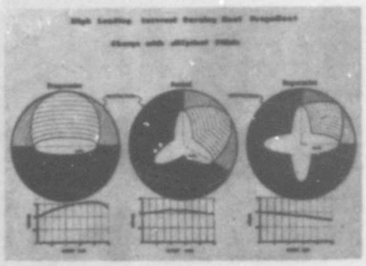

Figure 28

The method of construction of the interface and the shapes of performance curves obtainable are shown in Figure 29.

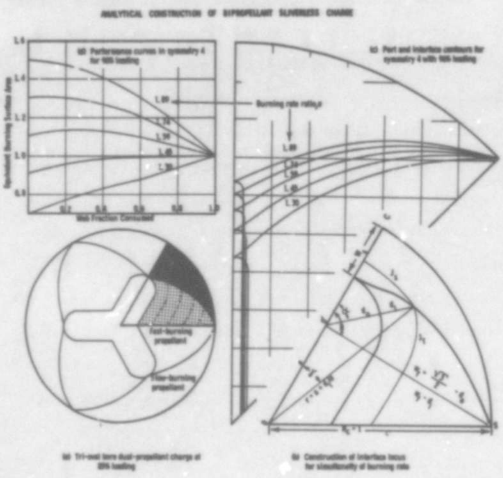

Figure 29

The physical web thickness of such bipropellant grains is typically 0.5 - 0.7 of the charge radius, compared to 0.3 - 0.4 for a single-propellant star-perforated grain of comparable neutrality. The latter is completely satisfied in two-dimensional section (independent of length-to-diameter ratio), with loading factors above 90% and a constantly negative second derivative of mass flow generation (otherwise attainable only by chamber wall exposure). Mechanical and ballistic reliability of bipropellant interface is no problem with proper process control, but the fabrication does involve the extra expense of two propellant processing and casting operations. Being of constant cross-section, the design permits the conventional aft-withdrawable casting core.

E. Collapsible Core, Integral Chambers, and Shift to Forward Exposure

With the advent of monocoque (integral) chambers developed via filament winding technology, integral core withdrawal became impossible. Simultaneously the high mass ratio, short length-to-diameter ratio ballistic missile power plant created an "all end-effects" attitude towards conventional two-dimensional star-perforated grain systems. Systematic heat transfer studies indicate that the "slots" for thick-web chamber-exposing grain designs should preferentially be located in the stagnation region of the forward head, rather than uniformly along the length of the grain (Figure 30). This produces the conocyl (or cone-in-cylinder) design,[15] and its variation for slightly greater degrees of freedom - the "star-in-a-pocket" or finocyl (fins in a flared cylindrical surface).[95]

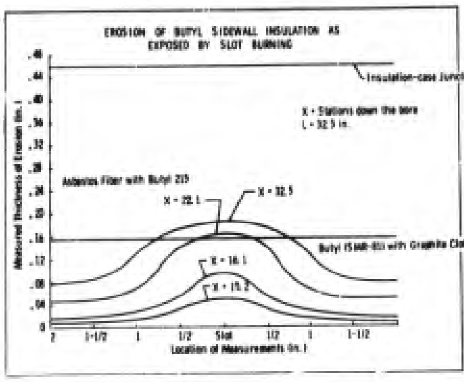

Figure 30

These designs frankly depend on the exposure of chamber wall (third law domain) for burning surface area control, but keep this exposure in the relatively low heat transfer regions of the forward part of the chamber. They display the desirable negative second derivative of the burning surface area characteristic of slotted or end-exposure grains (second law satisfaction), and furthermore have the unique property of conveying the greatest portion of this gas generation through a circular bore to the nozzle during the initial moments of burning. This has desirable thrust alignment, ignition transient, and erosive-burning characteristics. The casting cores are completely collapsible, frangible, or consumable.

Structurally the main body of the grain is a simple thick-webbed circular-bore cylinder. Figure 31 shows that neutrality is obtainable in a cone-ended circular bore grain design at an impractical 40% volumetric loading and 0.25 reduced web

EXTERNALLY-RESTRICTED CONE-ENDED INTERNAL-BURNING CHARGE

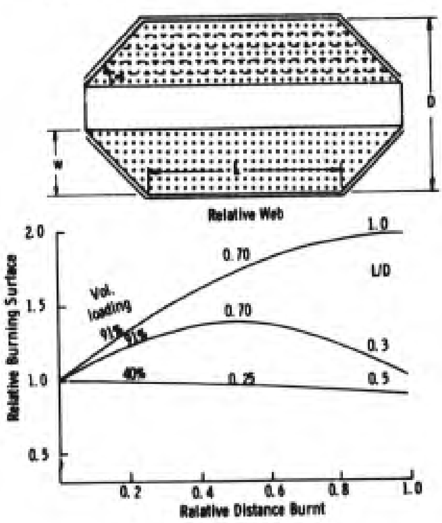

Figure 31

with L/D = 1/2, but that a highly progressive curve is obtained at higher webs and loading factors. The solution for total neutrality by end effects is indicated by the idealized design in Figure 32. In practice end-effects are used only

IDEAL HYPERBOLIC-ENDED EXTERNALLY-RESTRICTED NEUTRAL-BURNING CHARGE

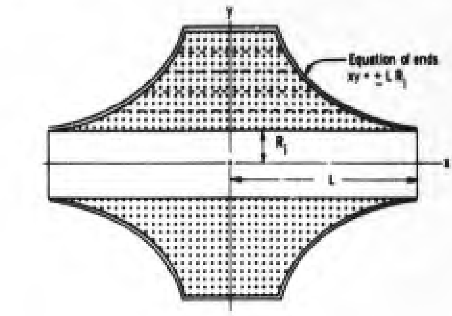

Figure 32

partially to compensate the increase in surface area of the inner bore burning, and conical slots are employed in the forward end to complete compensation of the burning surface area. This results in the conocyl grain of Figure 33, which has been proven in a wide variety of sizes and chamber proportions as shown in Figure 34. The stress concentration has been shifted from the internal bore to the case-attachment region of the flared end of the cylinder and the structural integrity is further aided by systematic partial release of the chamber-to-propellant bond in the critical regions, without impairing support of the whole. When the chamber envelope, the mission requirement, and the available burning rate permit it, the conocyl/finocyl type grain design is apparently an ultimate utilization of solid propellant. On the other hand, if burning rate is not adequate to the requirements of chamber dimensions and mission parameter, the previously discussed internally-convoluted grains must be used. The Fourth Law, if it could be formulated, would have something to do with the topological relation of chamber support of the burning surface area for maximum structural integrity.

F. Review of Cartridge Loading and Free-standing Grains

Many other grain designs have been postulated and a few have enjoyed temporary vogue. The original artillery grain was simply an internal-external burning cylinder with a single circular perforation. This is the origin of the term "grain design." To accomplish greater stability and reproducibility in the burning surface area, this was replaced by a smaller number of larger grains with seven equally-spaced circular perforations (the Rodman grain, circa the Civil War) as shown in Figure 35. A "sliver" is released when the burning from adjacent perforations cuts off support from the chamber as shown in the inset. In World War II the artillery rocket was developed, using an extruded, external-burning triform or cruciform grain (Figure 36), sometimes with cogs or lugs to space it in the chamber. Durations were only a few seconds, flame temperatures moderate, and weight fraction propellant typically 0.3.

INSULATION BUILD-UP LOCALIZED TO FORWARD STAGNATION AND NOZZLE APPROACH AREAS FOR CONOCYL CHARGE CONFIGURATION

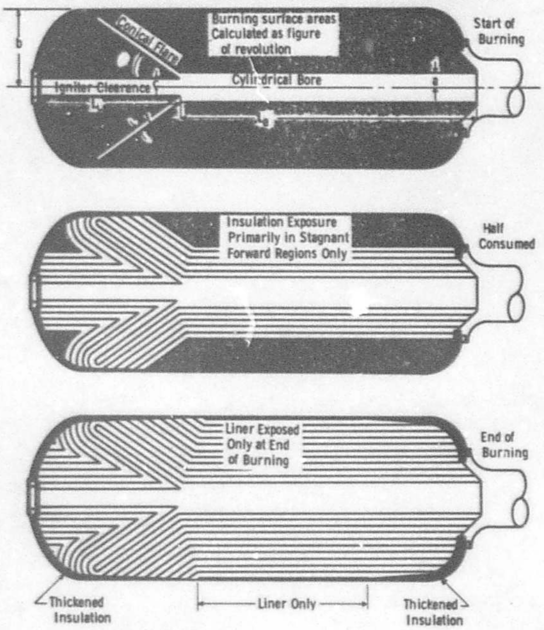

Figure 33

VERSATILITY OF THE CONOCYL CHARGE CONFIGURATION

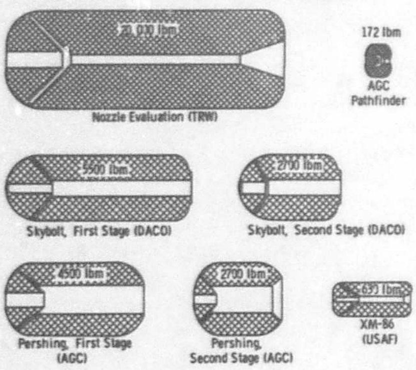

Figure 34

RODMAN INTERNAL-EXTERNAL BURNING SEVEN PERFORATION GRAIN

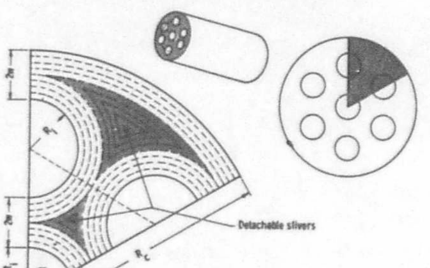

$R_c = 3 R_i + 4w$

$U = 2\pi \left[7 (R_i + y) + (R_c - y) \right] \quad (o < y < w)$

$\frac{d(U/U_o)}{d(y/w)} = \frac{(R_c - 3 R_i)}{4(7 R_i + R_c)} \left(\frac{dU}{dy} \right) = \frac{3}{2} \left(\frac{R_c - 3 R_i}{R_c + 7 R_i} \right)$

Figure 35

CRUCIFORM AND TRIFORM EXTERNAL-BURNING GRAINS

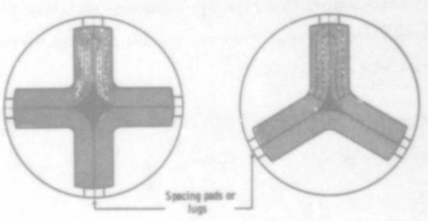

Figure 36

When the JATO was developed, first using an end-burning asphalt-$KClO_4$ composition (Figure 37) and later as an internal-burning cone-ended composite propellant (Figure 38), it was of course cartridge loaded. It was intended that the chambers be reusable, like guns.[7]

THE JATO END-BURNING SOLID ROCKET

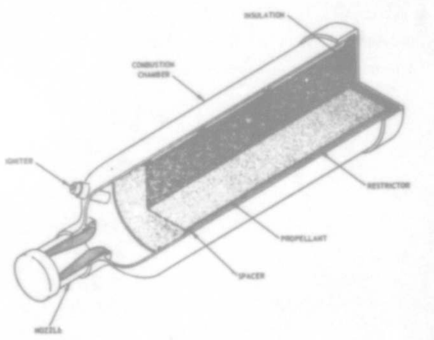

Figure 37

THE CARTRIDGE-LOADED CONE-ENDED JATO MOTOR

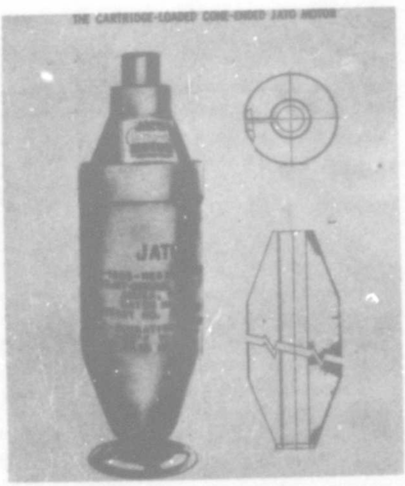

Figure 38

Boosters were next logically developed, using a single or double concentric internal-external burning cylindrical tube, held in place by steel spiders or traps which, as heat sinks, endured the 1 to 5 seconds of direct flame impingement. However, Figure 39 shows schematically that a thermoplastic propellant, heated between compression supports will flow

FAILURE OF TRAP SUPPORT IN CYCLING OF THERMOPLASTIC GRAIN

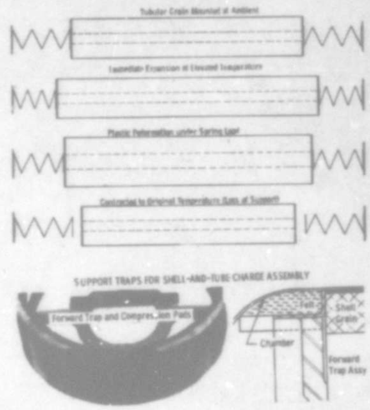

Figure 39

to decrease its effective length, and then when subsequently cooled to original or low temperatures will be too short to remain supported between the springs. The internal-external burning tube does have a constant total burning surface area. Neutrality is also obtainable from an internal-burning shell with a concentric external-burning rod, and this shell gives protection to the chamber wall. A shell and tube charge on the other hand is slightly progressive, and thus can absorb an "erosive-burning peak" without a pressure excess. However, this results in a saddle-shaped performance curve, since the first derivative of the burning surface area, although positive, is necessarily constant. That is, the cylindrical charges have no degrees of freedom for an erosive Zone I, neutral Zone II, and terminally-regressive Zone III burning, as has been shown characteristic of the star-perforated grain. Multi-perforated grains have also been developed to achieve one-piece assembly in lieu of the support problems of the equivalent-web multitubular charge. However, Figure 40 shows the stress concentration arising from differential thermal constriction when suddenly cooling the annular multiperforated grain. This design was therefore abandoned.[27,28] Likewise Figure 41 shows that in slotting the tubular charge for cylindrical stress relief, not only is chamber protection required under the slot, but that any mounting of rigid fiberglas restriction on the support ends or excess slot faces will create difficult problems in temperature cycling. Consequently partial restriction as a ballistic device is virtually obsolete, and every effort is made to develop case-bonded charge shapes that give the necessary ballistic burning surface area sequence from all initial surfaces without auxillary support devices.

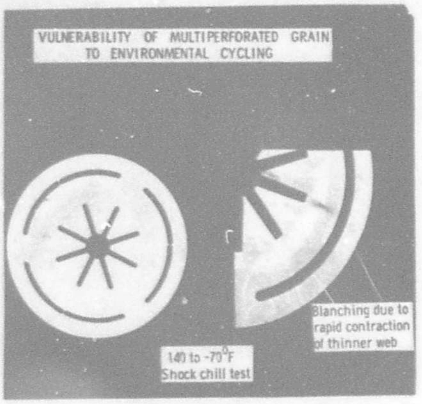

Figure 40

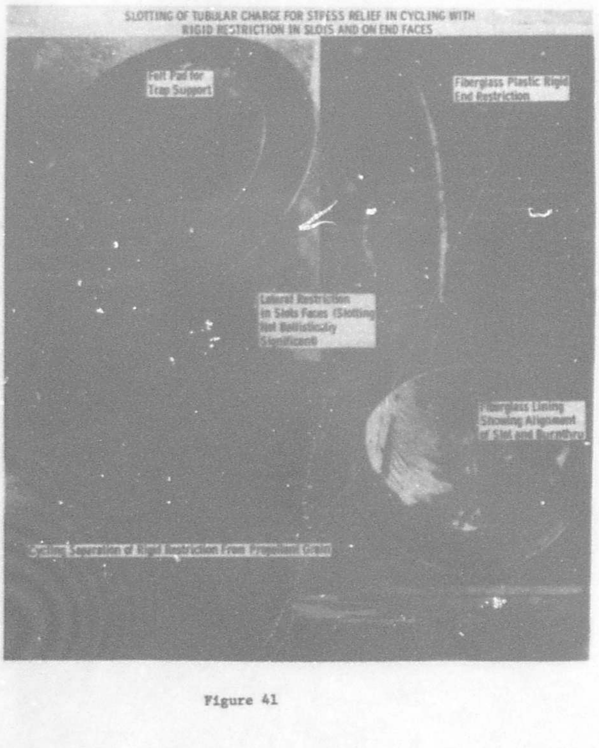

Figure 41

G. Development of Case-Bonded Grains

The rigid cartridge loading propellants were therefore replaced in the 1950's by case-bonded polyurethane and rubber base propellants, cast directly into the chamber and adhering to the chamber wall for support. Since there was no external-burning surface to balance the inherent progressivity of the inner bore, it was necessary to convolute or slot the inner surface to secure neutrality in high length-to-diameter ratio grains, or to use bipropellant or three-dimensional axial-burning effects in short length-to-diameter ratio or nearly spherical chambers to approximate a constant burning surface area. The consequent development of star-wagonwheel-dendrite sectorially deployed, internal-burning, two-dimensional configurations in web less than one-half of the chamber radius, or slot-conocyl-finocyl-end burner in web greater than one-half of the radius, and the consequent generalization in the "four laws" of grain design: first derivative, second derivative, exposure integral, and support vector have been discussed.

H. The Anchor and Dogbone Perforations

One grain configuration which has not been mentioned and which is more noteworthy for its position as a morphological reference than actual use in motors is the anchor-perforated charge.[77] The anchor-perforated grain can be thought of as a shell and tube charge, in which an isthmus or bridge of propellant connects the tube to the shell. This forms the annularly multiperforated charge shown in the previous section, which may then be cut between attachments to avoid the stress concentrations of differential pressurization and thermal cycling. The result has the appearance of an anchor-perforation (Figure 42) and in one sense may be thought of as the ultimate development of the secant fillet under the stress reinforcement theory.

Unfortunately, the large mass of the anchor arms or tines is subject to shear failure at the attachment bridge, and the design has seldom been used in practice. An unfortunate characteristic of the anchor configuration is also the presence of a detachable sliver, resulting from the meeting of burning fronts from lateral webs before all inwardly-supported propellant has been consumed. This breakup produces an irregularity in the performance curve and is generally undesirable.

FORMATION AND REMOVAL OF DETACHABLE SLIVER IN THE ANCHOR-PERFORATED GRAIN DESIGN

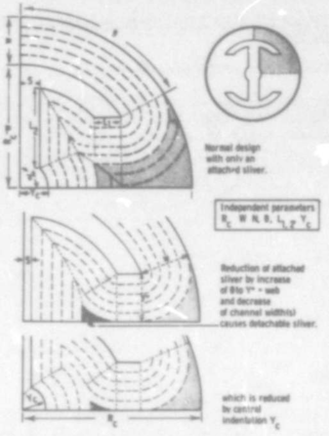

Figure 42

Another interesting grain is the "dogbone" perforation (Figure 43). This design can be approximated in a wagonwheel

BALLISTIC ANALYSIS OF THE DOGBONE-PERFORATED CONFIGURATION IN SYMMETRY OF THREE

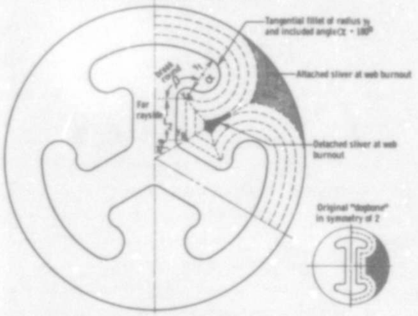

Figure 43

parametric computing system, with the stipulation that the tangential fillet (α) becomes 180°, the near rayside vanishes, and the breakround angle (β) becomes related to 90°+ ϕ. It is noted, however, that the higher-order dogbone design contains a small detachable fillet, which is not present in a true wagonwheel design. It is therefore suspected that this design is derived in part from the anchor-perforated grain in which the length of the tines has diminished to the endrounds only (Figure 44).* This exercise suggests that other designs, whether in two or three dimensions, analyzed functionally as above, and optimized analytically or graphically to the same objectives of performance expressed in the grain

GENERATION OF GENERALIZED ANCHOR-PERFORATION TO MAXIMIZE SECANT FILLET ANGLE WITHOUT LOADING LOSS

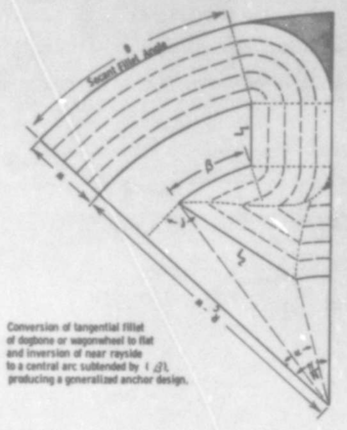

Figure 44

design laws stated above, will be found morphologically to be part of a taxonomic continuum and thus recognizable as to probable utility and functional characteristics.[5]

I. Generalized Grain Design - The Vector Surface Displacement Method

The two-dimensional parametric design of the star, wagonwheel, and dendrite perforated system, or the figure of revolution of the analytical conocyl, permit explicit expression for both ballistic and structural definition. However, to obtain additional burning surface area in the forward section, for additional degrees of freedom than obtainable from the simple flared surface of the conocyl, fins or slots are employed whose radius would exceed the aft opening of the monocoque chamber, thus requiring insertion of a collapsible core composed of expendable material such as styrofoam (Figure 45). In additon to the specific three-dimensional finocyl computer program, a generalized vector surface displacement method is developed that is capable of evaluation, even if not synthesizing, almost any system of fundamental geometrical elements: pyramids, cylinders, and spherical sections. These are evaluated by a

* The relationships of various grain design types, as discussed here, may be reviewed in the animated film Aerojet Production 484, "Two-Dimensional Grain Design," prepared for the Air Force under contract AF 04(611)-6358 (16 mm, color, sound, 18 min). This film shows the morphological transformation between various grain design types and the control of degrees of freedom for satisfying a performance curve.

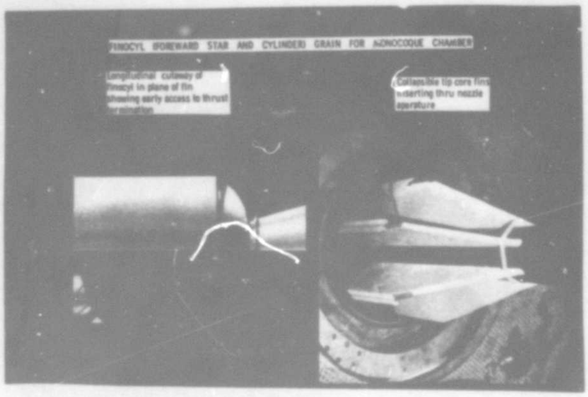

Figure 45

numerical analysis vector surface displacement (burning surface is actually the differential of propellant volume with respect to distance burnt). The method permits evaluation of performance for generalized forms not represented by codified parametric shapes, but lacks the capability for automatic variation in design iteration which was used in optimizing the explicit parametric systems. The following section presents the development of the three-dimensional vector displacement method and compares the utility of the generalized and the parametric grain design systems for ballistic/structural optimization.

V. Coordinate Systems for Ballistic/Structural Optimization of Propellant Grains

A. Evolution of Structural Over Ballistic Concern in Grain Design

In the 3 year AFRPL program conducted at Thiokol/Elkton to advance the state-of-the-art of grain design, a significant shift in emphasis occurred. Initially the project set out to develop computerized analyses for six selected typical grain designs: Broad point star, sharp pointed star, HH (wagonwheel), slotted circularly-perforated, two-dimensional bipropellant, and bipropellant cone and cylinder.[86] It was established that casting cores in use can generally be defined by a minimum symmetrical unit (sector) composed of not more than 50 straight line and circular arc segments.

Five types of intercepts were recognized: Acute point intersection, straight line segment, convex arc segment, and concave arc segment[87] as shown in Figure 46. This is a general statement of the parametric computer programs for generalized two-dimensional cross-sections.

Looking at the head effects, where a grain design cross-section intercepts the curvature of the chamber head closure, the conventional axial integration introduces an appreciable error when the rate of curvature of the head is large and the length-to-diameter ratio of the chamber is of the order of 2:1 or less, as in many ballistic missile and space motors. The alternative of direct Pappus theorem solution, although ac-

FIVE TYPES OF LINE INTERCEPTS IN GRAIN DESIGN CROSS SECTIONS

a. Point Intersection ($\theta < \pi$)

Two line segments intersecting at angle $\theta_1 < \pi$ produce an arc with radius Δd and center (A) with arc defined by:

$$(x - h_3)^2 + (y - k_3)^2 = (\Delta d)^2$$

b. Point Intersection ($\theta > \pi$)

Two line segments intersecting at angle $\theta_2 > \pi$, when $\theta > \pi$, cause the point of intersection to move along the bisecting line of the angle as Δd increases, and no new surface is generated. Line segments CD and DE diminish until they disappear from the calculation.

c. Straight Line Segment

A straight line segment, AB, whose equation is $y = mx + b$ produces a surface at Δd described by the equation

$$y = mx + (b + \frac{\Delta d}{\cos \Gamma})$$

d. Convex Arc Segment

A convex arc, BC, whose equation is

$$(x - h)^2 + (y - k)^2 = r^2$$

produces a surface at Δd described by the equation

$$(x - h)^2 + (y - k)^2 = (r + \Delta d)^2$$

e. Concave Arc Segment

A concave arc, EF, whose equation is

$$(x - h_1)^2 + (y - k_1)^2 = r_1^2$$

produces a surface at Δd described by the equation

$$(x - h_1)^2 + (y - k_1)^2 = (r_1 - \Delta d)^2$$

for $\Delta d < r$. At $\Delta d = r$, this arc becomes a point intersection and is dropped from the program.

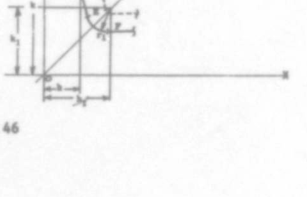

Figure 46

complished for spherical grain designs, and figure of revolution conocyls, would be formidable for each grain design cross-section and elliptic head contour.[88] A three-dimensional milling or vector displacement approach was adopted as the only universally effective method of head-end grain effects analysis.[89] This is based on differentiating the volume element between two successive projections of the normal burning surface, to obtain mean surface area at a time in burning, as shown in Figure 47. This has the advantage that it also yields the moments and products of intertia, the center of mass, and the total mass rate of change. Designated the Moore Method[90,91] it employs small elements of propellant bounded by normals to the inner propellant surface. The analysis then traces the planar regression of the prisms formed by coincident sets of bounding planes in the direction of normals to the burning surface until intersection or prior consumption by another burning front. This is similar to the familiar two-dimensional graphical construction of burning front contours. In extreme cases, for evaluation of final designs, a series of three-dimensional models of the position of the burning surface may be constructed, as shown in Figures 48 and 49.

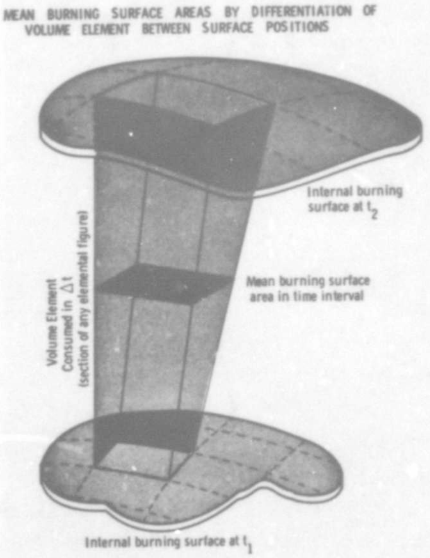

Figure 47

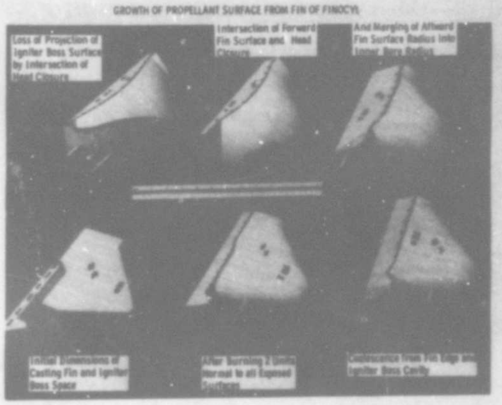

Figure 48

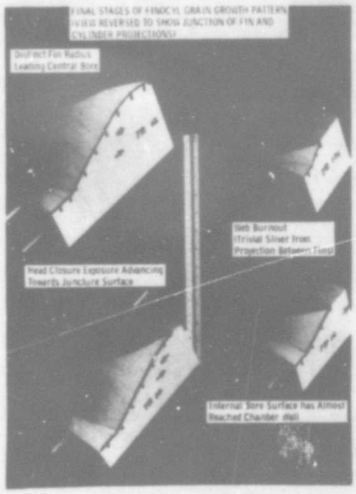

Figure 49

Having been freed of any restriction to classically defined grain configurations for which parametric analytical solutions are available, the method can be applied to grains containing non-uniform burning rates, resulting from standing temperature gradients, multi-propellant fabrication or polarized filament burning.[92] Subsequent studies under that program have been directed to the development of finite element structural analysis and experimental photo-stress techniques.[93]

The vector displacement method has been made operational by Peterson, et al, of Hercules/Bacchus.[51] This method requires only that the grain be described in terms of four basic input figures: a cylinder, a frustrum of a right circular cone, a right triangular prism, or a sphere (Figure 50). Elements can be defined as either propellant or void to produce exceedingly complex configurations, as the finocyl of Figure 51 shown in elemental partition in Figure 52. To simulate burning, each figure expands or contracts as appropriate until it intersects and is overcome by or super-

BASIC FIGURES FOR THREE-DIMENSIONAL GENERALIZED GRAIN DESIGN METHOD

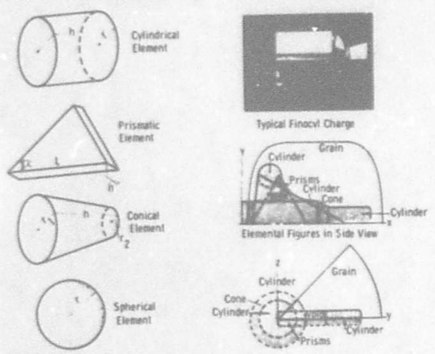

Figure 50

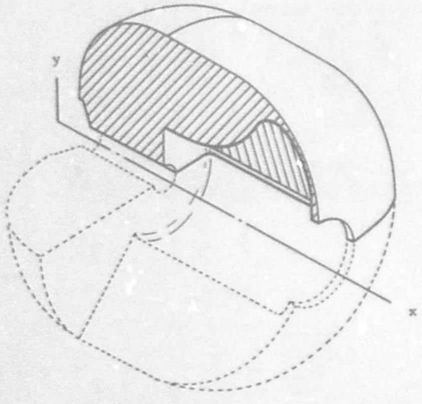

Longitudinal Section of Bore and Fin in Finocyl Propellant Charge
Figure 51

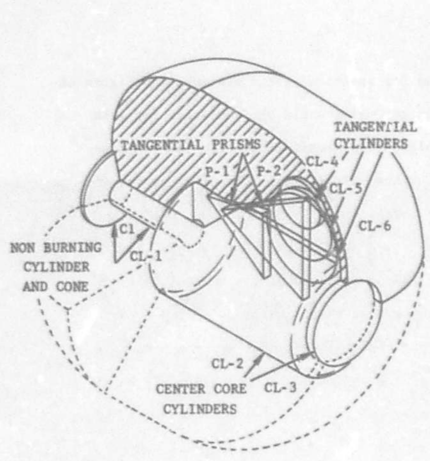

Simulation of Grain Void by Using Elemental Geometrical Figures
Figure 52

cedes another figure, and the record of such surfaces is integrated to give the mass flow generation at any time. The method obviates formidable graphical or modeling approaches to the evaluation of three-dimensional charge configurations. The entire grain is considered as a three-dimensional whole, as is necessary for structural analysis, rather than a series of two-dimensional cross-sections. It is thus not necessary that the configuration be a figure of revolution, although this simplifies the input and would bring the problem back under the province of the theorem of Pappus. Although the method is applicable to grains of any web thickness, it will generally be used for relatively thick-webbed grains (web 0.6 of the radius or greater) in relatively short length-to-diameter ratios, where two-dimensional solutions with mere end-effects corrections would be inadequate. For frequently used configurations, a parametric style pre-load can be devised to expedite the generalized coordinate evaluation.

From this generalized point of view, it is instructive to re-examine the conventional approach to the parametric two-dimensional designs. It will be seen that there were fortuitously developed two different sequences in examining the traditional star-perforated cross-section.

B. Degrees of Freedom and Construction Sequence in the Thiokol and Aerojet Maximum Parametric Two-Dimensional Grain

Figure 53 defines the Thiokol and Aerojet systems of parametric definition of the universal two-dimensional grain cross-section previously described in Figure 8, 15 and 20-22 for Aerojet and Figure 23 for Thiokol. However Aerojet does not have analytical provision for the sliver-minimizing "broken-back" feature seen in the latter. Alternating the long and short protrusions forms the forked wagonwheel (Boeing/

COMPARISON OF DENDRITE PARAMETRIC SYSTEMS

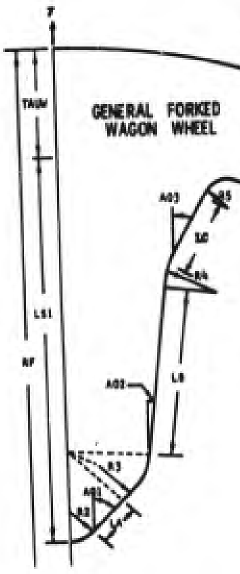

Boeing/Thiokol (20 variable input) (azimuth system)		Aerojet (17 variable input) (functional system)
NO (3), RF (4), TAUW (5)	Symmetry number, Charge radius, Web thickness	N, R_c, w
--	Secant fillet angle	ϕ_1, ϕ_2 *
R5 (16), R6 (17)*	Tangential fillet radius	y_{a_1}, y_{a_2}
--	Tangential fillet angle	α_1, α_2
L_C, L_D (implicit)	Near rayside length	L_1, L_2
A03 (8), A04 (9)	Near rayside azimuth	--
L_B (21)	Inside break length	Not available in Aerojet Configuration
R4 (15)	Inside break radius	
A02 (7)	Inside break azimuth	
R3 (14), R7 (18)	Breakround radius	y_{b_1}, y_{b_2}
LA (20), LE (22)	Far rayside length	Implicit
A01 (6), A05 (10)	Far rayside azimuth	--
--	Breakround angle	β_1, β_2
R2 (13), R8 (19)	Outside round radius	y_{r_1}, y_{r_2}
LS1 (11), LS2 (12)	Height of protrusion	--

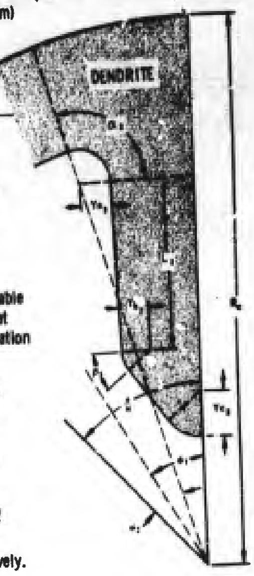

* All dual values refer to major and minor protrusion respectively. Parentheses indicate computer order of input.

Figure 53

Thiokol)* or the generalized dendrite (Aerojet). This includes the minor protrusion created by a normal wagonwheel, except that in the Thiokol design a "broken-back wagonwheel" has been used for the major protrusion while in the Aerojet design a normal wagonwheel is used. The "broken-back" feature accounts for the 20 variables input in the Boeing/Thiokol design compared to 17 cited for the Aerojet design. The central column shows the comparison of the variables in the two systems.

1. The first three variables (symmetry number, charge radius, and web thickness) are single valued and common to both design systems. For all remaining variables, except for the three associated with the Thiokol "broken-back" feature, there are two values, referring to the major and minor protrusions respectively (sub 1 and sub 2 in the Aerojet nomenclature; no direct association in the Thiokol symbols).

2. From this point the comparison is superficially different in that Thiokol designates explicitly the height of the protrusion and then begins a traverse along the rayside towards the case-bonded web; whereas Aerojet designates explicitly a secant fillet angle ϕ, and then proceeds to construct a traverse towards the extremity of the protrusion. There is also the difference that Thiokol uses the azimuth angle with respect to the protrusion bisector to define the direction of the next linear segment, whereas the Aerojet construction cites the actual angle of bending between each successive set of line segments.

Thus *for the comparison of parameters, they should be read from bottom-to-top for the Thiokol construction sequence, whereas they should be read from top-to-bottom for the Aerojet plotting method.* The first dual variable (height of major/minor protrusion - Thiokol) has no Aerojet analogy, while the last variable (secant fillet angle ϕ - Aerojet) has no Thiokol analogy. Furthermore, after constructing the outside round radius in either system, the far rayside length will be explicitely input by Thiokol, whereas it will be implicit to the Aerojet method. Conversely near the end of the table, it will be noted that the near rayside length (Aerojet) is a mandatory input, while in the Thiokol system this quantity is considered an implicit quantity. It is thus seen that there is a direct parallel between the systems, except that one method locates the extremity of the protrusion initially and constructs towards the web with the last rayside (near the web) implicit, while the other procedure commences at the

* Citation of Aerojet or Thiokol refers to references 76 and 81 respectively. The latter, although a Boeing report, is based on the Thiokol analysis system.

web and constructs towards the extremity with the last rayside (near the extremity) implicit.

Along the rayside the radii of junctures are expressed in parallel fashion, while the angles are parallel in occurrence but different in reference. The Thiokol system uses an azimuth angle measured with respect to the permanent protrusion bisector axis, whereas the Aerojet method takes the actual angle of intersection between adjacent linear segments.

It is not the purpose here to discuss which is the "better system: protrusion-to-web or web-to-protrusion sequence and azimuthal or included angle reference, since either system can be programmed for accurate convergence in digital computers and will be easiest to use by those to whom it is familiar. The comparison made in this manner is intended to assure that the degrees of freedom in the parametric expression are equal (allowing for the extra broken-back in the Thiokol design). This has been shown to be exactly satisfied by offset of explicit for implicit variables or vice versa in the parameter list.

C. <u>Control Zones Versus Functional Zones for Interpretation of Performance</u>

Regardless of the input system used, it will be immediately necessary for the computer to calculate a number of "control values" or "plane constants." These are shown in Figure 54 to consist primarily of the Cartesian coordinates of the center of all fillets and outside rounds, from which the progressive (from fillets) or regressive (from outside rounds) circular arc segments will emanate. This defines the growth or shortening of adjacent linear segments. Figure 55 shows how the configuration is broken into control zones, within which a single analytical function defines the behavior of the burning periphery segment. Figure 56 defines the specific construction of the reference segment (LA) in the far rayside. The functional significance of the control zones is indicated in Figure 57. It is intuitively obvious that regardless of the parametric sequence by which the initial configuration was defined with the option of one or the other of several explicit/implicit sets, the Cartesian coordinates of the radial centers and the corresponding functional zone boundaries will be the same. These may have formally different analytical expressions depending on the choice of evaluation sequence in transcendental expression of the coordinate

CARTESIAN COORDINATES AND RADII OF CENTERS OF ALL FILLETS AND ROUNDS

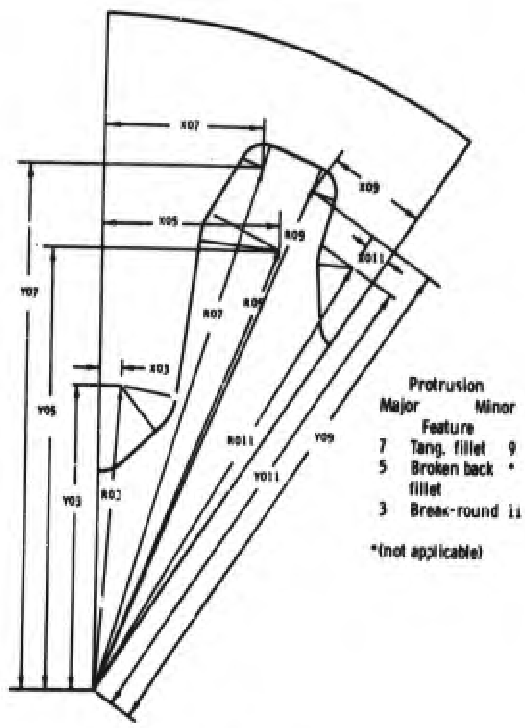

Figure 54

INCLUDED ANGLES AND DEFINING CHORDS FOR ALL FILLETS AND ROUNDS

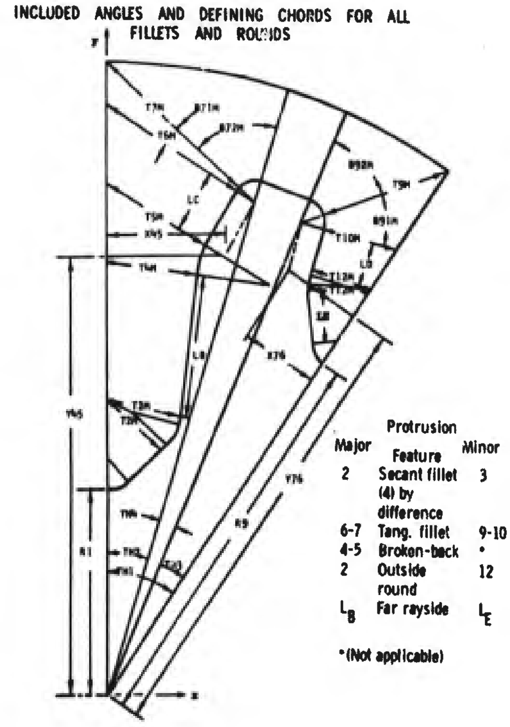

Figure 55

values, but theoretically they would all be convertible to a common system.

DEFINITION OF REFERENCE SEGMENT (LA) IN FAR RAYSIDE BY PROJECTION OF BREAK ANGLE

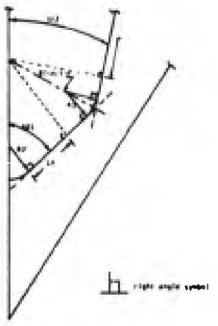

Figure 56

FUNCTIONAL ZONES FOR BURNING ANALYSIS OF GENERAL FURKED WAGON WHEEL GRAIN CONFIGURATION

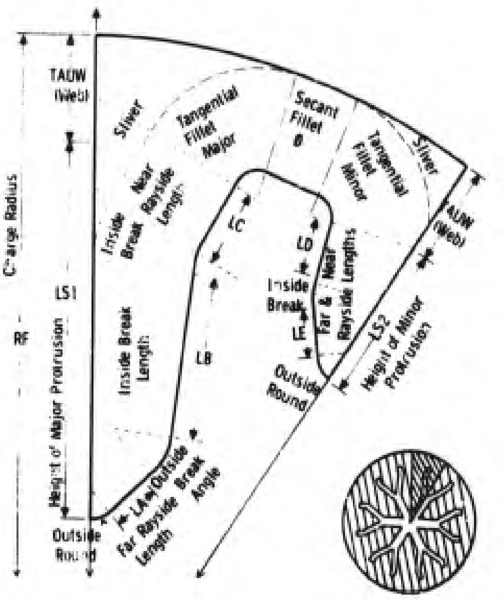

Figure 57

The actual computer time of the control parameter evaluation for the input check in either system is so small that it would be conceivable to program a self-checking input system whereby the parametric input of the system was converted to the common Cartesian definitions, and then the analogous parametric boundary description was output for the other option This would be a total check on the validity and reasonableness of the input assignment, and remove permanently any sense of uniqueness between systems. The modest effort required for this purpose is recommended.

This would have the added benefit of tending to develop a common descriptive nomenclature free of any conflict of the "official minimum inputs" which now tends to hold the systems at bay.

D. Degeneracy From Maximum Parametric to Simpler Designs

Certain quantities are subject to nominal assignments in preliminary design, and in fact to degeneracy to simpler design forms. Thus when the second set values are omitted (all subscript 2 values set to zero), the Thiokol forked wagonwheel becomes only a simple broken-back wagonwheel, or if the broken-back feature is set to zero, then the design becomes identical to the Aerojet wagonwheel (resulting from zeroing-out all subscript 2 values from the dendrite). That is, by allowing the mid-rayside and mid-break parameters (A02, LB, A03 - Thiokol) to vanish, the original general forked wagonwheel becomes an ordinary wagonwheel (Figure 58). If the values associated with the "break" are further allowed to vanish, the design becomes simply a star-perforated design (Figure 59).

WAGON WHEEL CONFIGURATION INPUTS

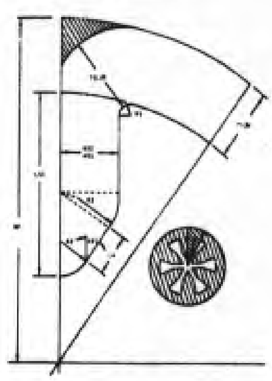

Figure 58

Finally by forcing all azimuth angles to be equal (Thiokol A01 = A02 = A03) and inputing only the tangential fillet radius (R5) and the outside round radius (R2) along the universal charge radius and web thickness, the Thiokol system can define a slotted cone design with input of the height of protrusion (LS1) and the insert of a circular bore with angle theta zero (TH "zero") as shown in Figure 60. This is analagous to the partially-slotted shell previously described for

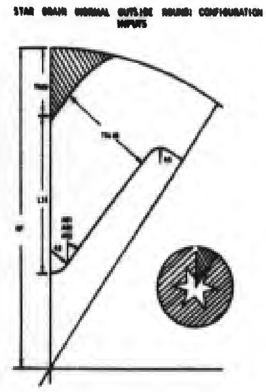

Figure 59

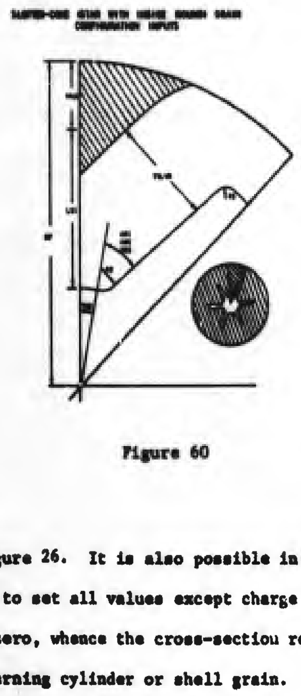

Figure 60

Aerojet in Figure 26. It is also possible in the generalized Thiokol input to set all values except charge radius and web thickness to zero, whence the cross-section reduces to simply an internal-burning cylinder or shell grain.

The principle factor for choice of calculating system, since the actual evaluation after determination of Cartesian control and functional zone lines is analytically equivalent, is convenience of assigning and revising input variables.

A key factor is height of protrusion. In tapered bore grains, designed to minimize the erosive burning by enlarging the port as the mass flow is incremented, it is convenient to assign a prescribed taper to the height of the grain. This is explicitly done in the Thiokol system, but must be implicitly arrived at by the several parameters making up the protrusion construction in the Aerojet system. This is only an illusionary convenience however, since the successive scalar parameters (lengths and radii) are absolute and not fractional to the protrusion height, and must be specifically programmed for taper whether beginning at a tapered height of protrusion (Thiokol) or at a web base to construct a protrusion (Aerojet). The relative ability to identify and manipulate control zones for generating the structural model and feedback of stress relieving revisions is thus the final criteria for coordinate system selection.

VI. CONCLUSION

Four principles describe the design of solid propellant grains: (1) The first derivative of the burning surface area with respect to distance burnt should be approximately zero (neutral burning) to assure maximum thrust coefficient commensurate with chamber strength. (2) The second derivative of burning surface area should be preferably negative, and certainly not positive, to allow a reduced initial surface area to be compensated by erosive-burning without exceeding the rated operating pressure, and yet to permit a terminal regressivity to minimize the peak acceleration imparted at web burnout. (3) The chamber interior surface should be protected by a layer of case-bonded propellant for as much of the area and as long a portion of the duration as practicable. Exposure in the forward stagnation region with ablative insulation may be tolerable if it simplifies the ballistics in the main and aft section of the chamber. (4) The propellant grain should obtain support from the chamber thruout the consumption of the grain, and should adjust to thermal and pressure environments with a minimum of stress concentrations resulting from boundaries between conflicting stress elements, as notches, case-propellant junctures, etc.

The star-wagonwheel-dendrite internally-perforated grain design system is fully described analytically with up to 20 parameters in the cross-section, and can be optimized for neutrality, progressivity or regressivity (first derivative) by control of symmetry number and fillet angles. It achieves second derivative control by the relation of the critical burning distance to the web, and the exhaustion times of the breakrounds and other features of the protrusion. It is essentially case-bonded and without exposure of the chamber wall except for end-effects. Support by the case is complete as long as the rayside does not diverge from the protrusion bisector inwardly (detachable sliver or slug).

The slotted cylinder charge has a discontinuous first derivative, with an inherently negative second derivative, making it ballistically desirable, but it employs exposure of the chamber wall to control the burning surface and is thus dependent on the quality and placement of insulation to preserve mass ratio. However, it does not have the sliver that a fully chamber-protecting star-wagonwheel-dendrite configuration would need. The slot configuration relieves the hoop stress in the propellant grain, but if concentrated only in the forward end to minimize ablation duty, results in a stress concentration at the juncture with the major cylindrical section

The dogbone and anchor grains are variations from the wagonwheel to minimize stress concentration between the case-bonded web and the protrusion but give technically inferior ballistics in return for the structural advantage. Since the ballistic sacrifices are quantitative, i.e., predictable in thrust-time performance curve and missile range, while the structural gains are qualitative, depending on mechanical properties of the propellant, the environmental exposure, photoelastic tests and correlations; these designs receive reluctant consideration by ballisticians.

Cartridge-loaded grains of the free-standing tube, shell-and-rod, or shell and-tube type do not offer a negative second derivative, have poor chamber protection and support, and receive logistic consideration for low weight fraction situations only.

In addition, free-standing grains require a high modulus propellant not compatible with case-bonding. Multi-perforated grains have a positive first derivative unless the external surface is burning, and yield a detached sliver.

Multipropellant grains based on the refraction of the burning front between propellants of differing burning rates satisfy all four principles of design within a two-dimensional cross-section including especially the negativity of second derivative, chamber protection without web, and fillets without sliver penalty, but are succeeded by monocoque grains on the basis of casting cost.

Monocoque grains are necessitated by the filament-wound chamber whose openings are too small for core withdrawal. The collapsible or consummable core technology thus required also makes it possible to locate slots and related ballistic features in the forward section while leaving a simple circular bore in the mid and aft section. Since end-effects predominate in such a configuration, the first derivative of the burning surface area is controlled primarily by the length-to-diameter ratio, the second derivative is suitably negative, the chamber is protected from propellant flame except in the suitable forward stagnation area, where insulation is strategically placed, and the circular-bore main section is relatively stress-free except for the juncture point with the forward ballistic detail.

These monocoque grains may be known as conocyl, finocyl, star-in-a-pocket, or winged slot. They are ultimate designs providing that the burning rate, duration and diameter permit the high web thickness (0.7 - 0.8 of the charge radius) characterizing the cylindrical main section. They are described parametrically in limited forms, but in general require a vector surface displacement type of ballistic calculation based on prism, cone and sphere representation, rather than an analytical calculation. This differs from the primarily two-dimensional, thinner web, star-wagonwheel-dendrite systems which are used in long length-to-diameter ratio chambers and where burning rate is not adequate for the thick-webbed cylindrical section. The "slots" in a finocyl or star-in-a-pocket configuration are usually diminuitive and so close together that they perform ballistically not as slots but as star cross-sections, so that the detail analysis of the finocyl continues to employ the star-wagonwheel-dendrite parametric logic in segments. A similar principle applies to the structural analysis, since a full three-dimensional treatment both longitudinal and cross-sectional exceeds the coordinate definition capacity of the structural analysis programs.

Finally coordinate system selection between azimuthal and vector displacement methods, although producing equivalent numerical results, differs in ease of recognizing control zones and performing a logical revision of parameters for maximum relief of stress concentration commensurate with maximum sacrifice of ballistic performance.

VII. Acknowledgements

Acknowledgement is made to M. G. Witcraft, T. L. Eriksson, and T. R. Threewit of Aerojet-General Corporation/Sacramento; A. R. Maykut of AMC/Redstone Arsenal, R. L. Thomas of RPL/Edwards Air Force Base, J. I. Shafer of JPL, C. H. Parr of Rohm & Haas, M. W. Stone of Spacecraft Corp., R. J. Vellacot of Thiokol/Redstone Div., B. R. Brinton of Thiokol/Wasatch Div., and J. L. Ergle of Hercules/Bacchus for assistance in identifying the design trends presented in this paper. Prof. F. R. Wagner of University of Utah and Dr. J. H. Wiegand of Aerojet gave council in relating the structural to the ballistic viewpoints. B. E. Graham, and L. G. Larduk in illustration; Mrs. P. Viret in manuscript review, and Mrs. S. Remington for typing are gratefully acknowledged.

VIII. References

1. Bacon, W. S., and Braun, J. V., "High Mass Ratio by the Use of Multiple Propellant Grains," Bull. of the 15th Meeting of the JANAF Solid Propellant Group, Vol. I, pp. 165-92, June 1959. (*0127, #0925)

2. Baldwin, M. G., and Gehlahus, P. H., "Very Fast Burning Solid Propellants," AIAA 3rd Propulsion Joint Specialist Conference, Washington, D. C., 17-21 July 1967. (#0086)

3. Bartley, C. E., and Mills, M. M., "Solid Propellant Rockets," in Jet Propulsion Engines, Ed. by O. E. Lancaster, Princeton University Press, 1959, p. 523-26.

4. Billheimer, J. S., "Case Bonded Grain Design for High Loading, Long Duration Solid Propellant Motor," Bull. of the 15th JANAF Solid Propellant Group " Vol. I, pp. 231-45, June 1959. (*0129, #0895)

5. Ibid., "Critique of a Series of Structurally-Oriented Grain Designs From a Ballistic Point of View," ICRPG Mechanical Behavior Working Group, 7th Meeting, Orlando 13-15 Nov, 1968.

6. Ibid., Optimization and Design Simulation in Solid Rocket Design," ICRPG/AIAA 3rd Solid Propulsion Conference, Atlantic City, June 4-6, 1968, AIAA Preprint 68-488.

7. Ibid., "Use of the Computer in Direct Grain Design for Erosive Burning, Sliver, Neutrality, and Tail-Off Considerations," Bull. of the 16th Meeting of the JANAF Solid Propellant Group, Vol. V, pp. 211-52 June 1960. (*0042, #0694)

8. Billheimer, J. S. and Wagner, F. R., "The Morphological Continuum in Solid Propellant Grain Design" 19th Congress of the International Astronautical Federation, New York, Oct. 13-19, 1968.

9. Billheimer, J. S., and Wiegand, J. H., "Integrated Solid Rocket Design Procedure Utilizing Computers," Bull. of the Interagency Solid Propulsion Meeting, Seattle, Vol. III, pp. 11-36, July 1963. (#0695)

10. Brisbane, E. B., and Becker, J. J., "Application of the Finite Element Method to Stress Analysis of Solid Propellant Rocket Grains," Vol. 1, (2nd Ed.), Rohm & Haas Co., Huntsville, Jan. 12, 1966, Contract DA-01-021 AMC-11536 (Z), 92 pp.

11. Britton, S. C., "Characterization of Solid Propellants as Structural Materials," Solid Rocket Structural Integrity Abstracts, Vol. 2, No. 4, Oct. 1965, pp. 1-71 (#0777)

+ Acknowledgement is made to two comprehensive bibliographies in grain design: (*XXXX) refers to citations in Thiokol Chemical Corp., Elkton, "A Research Study to Advance the State-of the Art of Solid Propellant Grain Design; Bibliography and Abstracts report," an attachment to Quarterly Progress Report No. 5, TCC-E E-181-60 (Addend. Conf.), Contract AF 33(616)-6530, by E. C. Cohen (28 October 1960). (#XXXX) refers to citations in Wagner, F. R., "Bibliography on Internal Ballistics and Grain Design of Solid Propellant Rocket Motors," Univ. of Utah, UTEC-ME-67-080, Contract NAS3-11179 (November 1967).

11a. Carey, D. F., "Development of a Ripcord Slot-Forming Rocket Motor Mandrel (u), paper presented at the ICRPG/AIAA Solid Propulsion Conference held at Washington, D. C., July 1966.

12. Chaiken, R. F., and Anderson, W. H., "The Role of Binder in Composite Propellant Combustion," Solid Rocket Research, Vol. 1 of ARS Progress in Astronautics and Rocketry Series, M. Summerfield (Editor), Academic Press, New York, 1960, pp. 227-49. (#0189)

13. Corner, J., Theory of the Interior Ballistics of Guns, John Wiley, 1950, Ch. 2, p. 38.

14. Coverdale, J. S., Matteo, M. A., and Witcraft, G. M., "Computer Program for Estimation of Rocket Motor Performance," Bulletin of the 15th Meeting JANAF Solid Propellant Group, Vol. 1, 16-18 June 1959, pp. 117-142. (#0458)

15. Crooks, J. R., "Skybolt Propulsion System," Bull. of the 18th Meeting of the JANAF-ARPA-NASA Solid Propellant Group, Vol. 1, pp. 113-23, 5-7 June 1962. (#1044)

16. Dehority, G. L., Bradley, H. H., Jr., and Price, E. W., "Flow of Gas in Tapered Channel with Mass Addition," U. S. Naval Ordnance Test Station, China Lake, California, Report No. NAVWEPS 8606, NOTS TP 3626, Sep. 1964 (AD-608 091). (#0459)

17. Dekker, A. O., and Manfred, R. K., "Development of Fast-Burning Propellants," Bulletin of the 20th Interagency Solid Propulsion Meeting, Vol. II, July 1964, pp. 65-82.

18. Dolgonas, Gene, and Gardner, N. C., "Effects of Environment on Rocket Motor Operation," ARS Preprint 2305-62.

19. Dudley, D. P., Veit, P. W., and Billheimer, J. S., "The Man-Computer Link in Solid-Propellant Rocket Preliminary Design and Optimization," ICRPG/AIAA 3rd Solid Propulsion Conference, Atlantic City, June 4-6, 1968, AIAA preprint 68-489.

20. Durelli, A. J., "Experimental Strain and Stress Analysis of Solid Propellant Rocket Motors," Catholic University of America, Report No. 6, Mar. 1965. (AD-615 038). (#0782)

21. Epstein, L. I., "The Design of Cylindrical Propellant Grains," Jet Propulsion Vol. 26, No. 9, pp. 757-59, Sep. 1956. (*0123, #0897)

22. Flanigan, D., "Mechanism of Burn Rate Tailoring - Theory and Practice," ICRPG/AIAA 2nd Solid Propulsion Conference, Anaheim, California, 6-8 June 1967. (#0095)

23. Fleming, E. R., Bacon, W. S., and Andrepont, W. C., "Design Approaches to Ultra High Performance Motors," Bulletin of the 16th Meeting JANAF Solid Propellant Group, Vol. II, 14-16 June 1960, pp. 23-36. (#0697)

24. Fletcher, E. A., and Hiroki, T., "Gas Evolution from Solid Propellants During Pressure Decays," AIAA Journal, Vol. 4, No. 12, Dec. 1966, pp. 2222-24. (#0514)

25. Fitzgerald, J. E., "Propellant Grain Structural Integrity Problems: Engineering Status," Solid Rocket Structural Integrity Abstracts, Vol. 2, No. 3, July 1965, pp. 2-44.

26. Fourney, M. E., and Parmerter, R. R., "Parametric Study of Rocket Grain Configurations by Photoelastic Analysis," Mathematical Science Corp., Seattle, Report No. 65-29-12, AFRPL-TR-66-52 (Mar. 66), Contract AF 04(611)-10529, 113 pp. (#0807)

27. Geckler, R. D., Noland, R. L., Roberts, E. R., and Rogers, W. L., "Internal Burning Grains and Related Components for Solid-Propellant Rocket Motors," Aerojet Report 445 (Final), 23 June 1950, 252 pp.

28. Gordon, L J., "Effect of Propellant Density on Vehicle Performance," Bulletin of the 15th Meeting JANAF Solid Propellant Group, Vol. VII, 16-18 June 1959, pp. 171-82. (#0728)

29. Gorny, L. J., "A Generalized Approach to Rapid Evaluation of Solid Propellant Grain Geometrics," ARS Preprint 2316-62. (#0886)

30. Green, L., Jr., "Erosive Burning of Some Composite Solid Propellants," Jet Propulsion, Vol. 24, No. 1, Jan.-Feb. 1954 pp. 9-15 (0366)

31 Gualillo, S. P., and Daigle, D., "Evaluation of Solid Propellant Rocket Motor Nozzles and Cases," Thiokol Chemical Corp., Report No. 38-66, Sept. 1966 (AD-489 127). (#0742)

32. Gualillo, S. P., and Dale, W. I., Jr., "Development of a Manufacturing Process and Associated Equipment to Improve Internal Core Forming in Solid Propellant Rocket Motors," Thiokol Chemical Corp., Report No. U-66-15A, Nov. 1965-Feb. 1966, (AD-481 020); Report No. U-66-30A, Feb.-May 1966 (AD-485 608). (#0754)

33. Hayes, T. J., Elements of Ordnance, John Wiley and Sons, N. Y. 1958, p. 11.

34. Hermance, C. E., "A Model of Composite Propellant Combustion Including Surface Heterogeneity and Heat Generation, " AIAA Journal, Vol. 4, No. 9, Sept. 1966, pp. 1929-1937.

35. Hilton, H. H., "A Summary of Linear Viscoelastic Stress Analysis," Solid Rocket Structural Integrity Abstracts, Vol. 2, No. 2, Apr. 1965, pp. 1-19.

36. Jackson, F., "Star Center Burning Surfaces," Canadian Armament Research and Development Report No. CARDE TM 312/60, Dec. 1960 (#0899).

37. Kaskey, B., Grain Design Handbook, Report 3413, Rocket Development Laboratory, Ordnance Missile Laboratory, Redstone Arsenal, 8 June 1956.

37a. Larimer, M. H. and Zeman, S."Development of Lightweight Inert Foam Mandrels for Ejection during Ignition of Solid Propellant Rocket Motors (u)," ICRPG/AIAA Solid Propulsion Conference, Washington, D. C., July 1966.

38. Lenoir, J. M. and Robillard, G., "A Mathematical Method to Predict the Effects of Erosive Burning in Solid-Propellant Rockets," Sixth Symposium on Combustion, Reinhold Publishing Corp., N. Y., 1957, pp. 663-67. (#0373)

39. Lumpkin, H. K., Mathematical Approach to Solid Propellant Grain Design, Army Rocket and Guided Missile Agency, Ordnance Missile Laboratories Division, ARGMA TN 1G5N, 21 Dec. 1959.

40. Majoros, J. and Sarlat, I. M., "Solid Booster Thrust Decay Control for Stage Separation," ICRPG/AIAA Solid Propulsion Conference, Washington D. C., July 1966. (#0515)

41. Manfred, R. K., Wilkes, B. F., and Brown, J. M., "Design and Development of Solid-Rocket Combustible Mandrels," Aerojet-General Corp., Sacramento, Report No. 0630-81Q-2 and 0630-81Q-3 (16 May - 15 Nov. 1962). (#0758)

42. Mellette, R. V., "The Automated Viscoelastic Grain Structural Analysis Program," ICRPG Mechanical Behavior Working Group, 6th Meeting, Pasadena, 5-6 Dec. 1967, pp. 73-202.

42a. Miller, R. A., and Vetter, R., "Investigations of Plastic and Foamed Mandrels," Bulletin of the 18th Meeting JANAF-ARPA-NASA Solid Propellant Group, Vol. III, 5-7 June 1962, pp. 83-96.

43. Muraour, Henri, and Aunis, Gabriel, "Combustion Laws of Colloidal Powders: A Survey of French Research Between World War I and World War II," Memorial des Poudres, Vol. XXXV, pp. 287-301, Paris, 1953; Translated by R. F. Brinkley for the Solid Propellant Information Agency.

44. Nicholson, A. H., and Wilsten, D. B., "Derivation of the Surface Integral and Neutrality Control Function for the Axially Tapered Internal-Burning Star Solid Propellant Charge," Aerojet-General Report No. 1785/89-2, Appendix A, 15 Nov. 1956.

45. O'Neill, R. W., et. al., "Development of a Manufacturing Process and Associated Equipment to Improve Internal Core Forming in Solid Propellant Rocket Motors," Thiokol Chemical Corp. Report No. U-386-65, Dec. 1965 (AD-476 837). (#0760)

46. Ordahl, D. D., and Williams, M. L., "Preliminary Photoelastic Design Data for Stresses in Rocket Grains," Jet Propulsion, June 1957. (*0016, #0805)

47. Pacanowsky, E. J., Pruder, G. D., and Waysack, E. A., "High Burning Rate Propellants," ICRPG/AIAA Solid Propulsion Conference, Washington, D. C., July 1966. (#0102)

48. Parr, C. H., "Problems on Ballistic/Structural Integration of Propellant Optimization," ICRPG/AIAA 3rd Solid Propulsion Conference, Atlantic City, 4-6 June 1968, AIAA Preprint 68-491.

49. Parr, C. H., "The Application of Numerical Methods to the Solution of Structural Integrity Problems of Solid Propellant Rockets," Solid Rocket Structural Integrity Abstracts, Vol. 1, No. 2, Oct. 1964, pp. 2-31.

50. Ibid., "The Application of Numerical Methods to the Solution of Structural Integrity Problems of Solid Propellant Rockets II," Solid Rocket Structural Integrity Abstracts, Vol. 4, No. 1, Jan. 1967, pp. 1-12.

51. Peterson, E. G., Nielsen, C. L., Johnson, W. C., Cook, K. S., and Barron, J. G., "Generalized Coordinate Grain Design and Internal Ballistics Evaluation Program," ICRPG/AIAA 3rd Solid Propulsion Conference, Atlantic City, June 4-6, 1968; AIAA Preprint 68-490, 7 pp.

52. Piasecki, L., and Robillard, G., "Generalized Design Equations for an Internal Burning Star-Configuration Solid Propellant Charge and Method of Calculating Pressure Time and Thrust Relationship," Jet Propulsion Laboratory, Memorandum No. 20-135, Sept. 18, 1956. (*0021, #0900)

53. Podell, H. L., "The Practical Application of a Bi-Propellant Grain System in Large Solid Rocket Engines," Bull. of the 16th Meeting of the JANAF Solid Propellant Group, Vol. II, June 1960. (*0038, #0922)

54. Power, A. M., "Research and Development for Advancing the State-of-the-Art of Segmented Solid Propellant Rocketry," Grand Central Rocket Co., Report No. GCR-P-0061, QPR 3, May 1961 (AD-365 219). (#0703)

55. Power, A. M., and Sweek, R. F., "Research and Development for Advancing the State-of-the-Art of Segmented Solid Propellant Rocketry," Grand Central Rocket Co., Report No. P-0020-61, QPR 2, Nov. 1960-Feb. 1961. (#0704)

56. Price, E. W., "Charge Geometry and Ballistic Parameters for Solid-Propellant Rocket Motors," Jet Propulsion, Vol. 24, No. 1, Jan.-Feb. 1954. (#0891)

57. Price, E. W., and Mills, J. K., "Internal Ballistics Theory for Rocket Motors with Solid Propellants having a Relatively General Class of Burning Characteristics," U. S. Naval Ordnance Test Station, Report No. NAVORD 2080, NOTS 815, 13 Jan. 1954 (AD-28 914). (#0471)

57a. Reed, W. W., "Non-Combustible Mandrels in the Skybolt, Large Solid Rocket,Genie and No. 3-KS-1000 Programs," Aerojet-General Corp., June 1962 (AD-329 878).

58. Rice, M. L., Roberts, W. C., and VandeVrede, R. G., "Application of End-Burning Grain Design to Sounding Rockets," Bulletin of the 15th Meeting JANAF Solid Propellant Group, Vol. 1, 16-18 June 1959, p. 247. (#0901)

58a. Robillard, G., "Propulsion Development for the Anti-aircraft Missile Loki," Jet Propulsion Laboratory, Progress Report 20-297, 20 April 1956.

59. Rogers, K. H., "Mathematical Design of a Sliverless Rocket Engine," ARS Solid Propellant Rocket Conference, Salt Lake City, Feb. 1-3, 1961, ARS Preprint 1616-61.

60. Rossini, R. A., Billheimer, J. S., and Threewit, T. R., "Configuration Efficiency: a New Measure of Ballistic Quality for Grain Design," ARS Solid Propellant Rocket Conference, Salt Lake City, Feb. 1-3, 1961; ARS Journal, Dec. 1961, pp. 1761-66.

61. Rossini, R. A., and Threewit, T. R., "An Automatic Design-Selection and Optimization Program for Solid-Rocket Systems," Bulletin of the Interagency Solid Propulsion Meeting, Vol III, July 1963, pp. 37-60, CPIA Publication No. 18. (#0702)

62. Schaafsma, W., Webster, R. O., and Keathley, A. C., "Segmented, Conical Rocket Motors," Bulletin of the 16th Meeting JANAF Solid Propellant Group, Vol. II, 14-16 June 1960, pp. 51-60. (#0705)

63. Selzer, H., "The Temperature Profile Beneath the Burning Surface of a Composite Ammonium Perchlorate Propellant," 11 Symposium (International) on Combustion, University of California, Berkeley, 14-20 Aug. 1966. (#0240)

64. Shafer, J. I., "Solid Rocket Propulsion," Chapter 16 in Space Technology, Ed. by Howard S. Seifert, John Wiley and Sons, N. Y., 1959, pp. 16-04 to 16-09.

65. Steins, J. A., Stang, P. L., and Summerfield, M., "The Burning Mechanism of Ammonium Perchlorate-based Composite Solid Propellants," AIAA 4th Propulsion Joint Specialist Conference, Cleveland, June 10-14, 1968; AIAA Preprint 68-658, 23 pp.

66. Stone, M. W., "A Practical Mathematical Approach to Grain Design," ARS Semi-Annual Meeting, San Francisco, 10-13 June 1957, Paper No. 445-57; Jet Propulsion, Vol. 28, No. 4, April 1958. (#0906)

67. Ibid., "Modified Wagon Wheel Grain Design: $W_1>W_2=W_3$, $W_1=W_2>W_3$, $W_1=W_3>W_2$," Rohm and Haas Co., Report No. S-36, Oct. 1962. (#0904)

68. Ibid., "The Modified Wagon Wheel Grain Design, $W_1>W_2>W_3$," Rohm and Haas Co., Report No. S-30, May 1961. (#0905)

69. Ibid., "Slotted Tube Grain Design and Some Practical Modifications and Use by Grain Designers," Rohm and Haas Co. Report S-27, 23 Dec. 1960; Am. Roc. Soc., Jan. 1960, 1055-60. (*0111, #0907)

70. Vandenkerckhove, J. A., "Internal Burning Star and Wagon-Wheel Designs for Solid Propellant Grains," Universite Libre des Bruxelles, USAF-ARDC Contract S61(052)58-13, 1958.

71. Ibid., "Recent Advances in Solid Propellant Grain Design," ARS Journal, Vol. 29, No. 7, July 1959, pp. 483-91. (#0893)

72. Vellacott, R. J., "A Computer Program for Solid Propellant Rocket Motor Design and Ballistic Analysis," ARS Preprint 2315-62 (1962).

73. Ibid., "Design Study of Solid Propellant Configurations," Thiokol Chemical Corp., Redstone Div., Huntsville, Final Report 28-61, U-A-61,28A, 399 pp. (28 July 1961). (#0911)

74. Ibid., "Solid Propellant Configuration Analysis for Digital Computer Solution," Thiokol Chemical Corp., Report No. U-A-60-40A (Special Report), 25 Oct. 1960. (#0912)

75. Vogel J. M., "A Quasi Morphological Approach to the Geometry of Charges for Solid Propellant Rockets," Jet Propulsion, Vol. 26, No. 2, Feb. 1956.

76. Whetstone, A. E., Threewit, T. R., and Billheimer, J. S., "Basic Grain Design and the 564 Interior Ballistics Computer Program," Aerojet-General Corp., Sacramento, STM-143, 10 June 1961, Contract DA-04-200-506-ORD-1120, 142+ pp. (#0915)

77. Whetstone, A. E., Threewit, T. R., and Rossini, R. A., "Intermediate Grain Design and the ACP-564B Interior Ballistics Computer Program," Aerojet-General Corp., Sacramento, STM-148, 20 Feb. 1962, Contract AF 04(611)-6358, 72+ pp. (#0914)

78. Wiegand, J. H., "Overall Considerations for Solid Rocket Grain Design," Air Force Rocket Propulsion Laboratory Seminar Program, 1966, AFRPL-TR-67-30, Jan. 1967, pp. 186-202 (AD-815 174). (#0708)

79. Williams, M. L., "Structural Analysis of Viscoelastic Materials," Chapter 9 of Solid Rocket Technology, John Wiley and Sons, Inc., New York, 1968, (#0829)

80. Aerojet-General Corporation, Azusa, "Investigation of Internal Burning Grain Configuration," PR No. 5-985/710, 985/711, 3 June 1959. (*0105)

81. Boeing Company, Seattle, "Solid Propellant Rocket Motor Internal Ballistics Computer Program," Report No. RK-TR-67-7, Sept. 1967, Contract DA-01-021-AMC-15557(Z), 256 pp.

82. Chemical Propulsion Information Agency, Silver Spring, Md., CPIA/M1 Rocket Motor Manual, Vol. 2, Motors of Current Interest, Contract NOw 62-0604-c., Sept. 1967, Conf.

83. Hercules Powder Co., Chemical Propulsion Div., Bacchus, "Minuteman Stage III, Weapon System 133-A (U)," QPR MCS-51 (Apr.-June 1960), Conf.

83a. Jet Propulsion Lab., "Combined Bimonthly Summary," No. 30, Apr.-June 1952, 20 July 1952, pp. 18-19.

83b. Ibid., No. 33, Oct.-Dec. 1952, 20 Jan. 1953, pp. 26-27.

84. Rocketdyne/McGregor, "Solid Propellant Extended Environmental Capability Evaluation Program," (U), Quarterly Report 1, July to Sept. 1966, AFRPL-TR-66-284 (AF 04(611)-11418), Conf.

85. Thiokol Chemical Corporation, Elkton Division, "A Program for Experimental Research and Testing of Unconventional Solid Propellant Grain Design," Report No. E-22-61, Feb. 1961 (AD-323 498). (#0923)

86. Ibid., Elkton Division, "A Research Study to Advance the State-of-the-Art of Solid Propellant Grain Design," QPR 4, Feb.-May 1960, Contract AF 33(616)-6530, Report E 132-60.

87. Ibid., QPR 5, May-Aug. 1960, Report E 181-60.

88. Ibid., QPR 6, Mar.-June 1961, Report E 99-61.

89. Ibid., QPR 7, June-Sept. 1961, Report E 156-61.

90. Ibid., QPR 8, Sept.Dec. 1961, Report E 11-62.

91. Ibid., Annual Summary Report, Mar. 1961-Mar. 1962, Report E 70-62.

92. Ibid., Summary Report, 15 Oct. 1963, Report E 92-63, RTD-TDR-63-1049.

93. Ibid., Final Report, 1 Jan. 1964-31 Dec. 1964, Report E 32-65, AFRPL-TR-65-129, 26 July 1965.

94. Thiokol Chemical Corporation, Redstone Division, "Pershing Propulsion System Development Program (U)," Progress Reports C-A-62-101A, -116A, -142A (21 Nov. 1961-20 Feb. 1962). Conf. (#1020)

95. Thiokol Chemical Corporation, Wasatch Div., "Minuteman Development of Large, High Performance Solid Propellant Rocket Engines (U)." QPR No. 1, AF 33(600)-36514, 24 Feb.-31 May 1958. Conf. (*0030)

96. Solid Rocket Structural Integrity Abstracts, Ed. by F. R. Wagner, Structural Integrity Information Center, University of Utah, for the Air Force Rocket Propulsion Laboratory.

GLOSSARY

Action Time - The time at which thrust is no longer considered significant to the mission, as "10% action time" when the thrust has decayed to 10% of its average value up to burn time. (Illustration below)

Anchor (Anchor-Perforated) Grain Design - An internal-burning singly-connected grain configuration formed by a bridge of propellant connected to the case-bonded web and supporting two annular sections of internal-external burning grain, known as arms or tines of the anchor, and forming a perforation resembling an anchor-shaped flow space. May be generalized in higher symmetry numbers. Has a unique negative second derivative for a singly-connected, single propellant, fully chamber-protecting grain design.

Bipropellant Sliverless Grain - The bipropellant sliverless charge employs the refraction of the line of burning passing through an interface between propellants of differing burning rates, so oriented that after refracting, the line of burning will be normal to the chamber wall. If, in addition, the initial surface is so related to the burning rate ratio that all these lines of burning are exhausted at the same time, then a sliverless, internal-burning (bipropellant) grain will be achieved. The design may be executed in 2, 3, and 4 symmetry for progressive, neutral, and regressive performance, respectively.

Breakround - The outside round occurring at a break defining the near and far rayside of a protrusion in an internal-burning grain design. The break is the characteristic of a wagonwheel design that makes it distinctive from a star.

Cartridge-Loaded Charge - Propellant grain(s) separately cast and inserted in the chamber with detachable aft

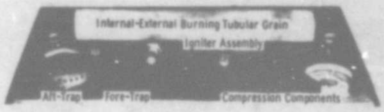

closures. Supported by compression traps or spacer lugs. Requires a high modulus propellant not suitable for wide temperature range, and subjects chamber wall to direct flame of propellant gases (see Case-Bonded Charge).

Case-Bonded Propellant Charge - Propellant cast directly into the rocket chamber, separated only by a bonding liner, and deriving structural support from the chamber and giving thermal protection to the chamber. Sacrificial insulation of the chamber required only under slots and at intersection with end closures where web will be prematurely exhausted (see Slotted Grain).

Configuration Efficiency - A measure of the impulse recoverable from a given performance curve compared to that which would be obtainable if the same quantity of propellant could be converted to thrust at a pressure corresponding to the maximum chamber pressure experienced at any time during that curve and to which the chamber wall has presumably been designed in the objective of impulse-to-weight ratio maximization. The integration of the actual performance curve for configuration efficiency may be terminated at any time, such as web, 10% action time, etc. in accordance with mission significance. Configuration efficiency measures the joint effect of sliver and deviation from neutrality under actual conditions of thrust loss in a nozzle as a function of altitude or back pressure. Used in evaluating progressive, neutral, and regressive grain designs. (Illustration below)

Conocyl Grain Design - An axisymmetric charge formed by a circularly perforated internal-burning cylinder mated with a conical element in the forward portion of the chamber to form a flared or funnel-shaped flow space, termed conocyl for cone-in-cylinder.

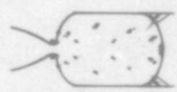

Critical Burning Distance - Distance from the initial surface along the boundary between the tangential fillet and the protrusion to the far sector boundary (see Tangential Fillet).

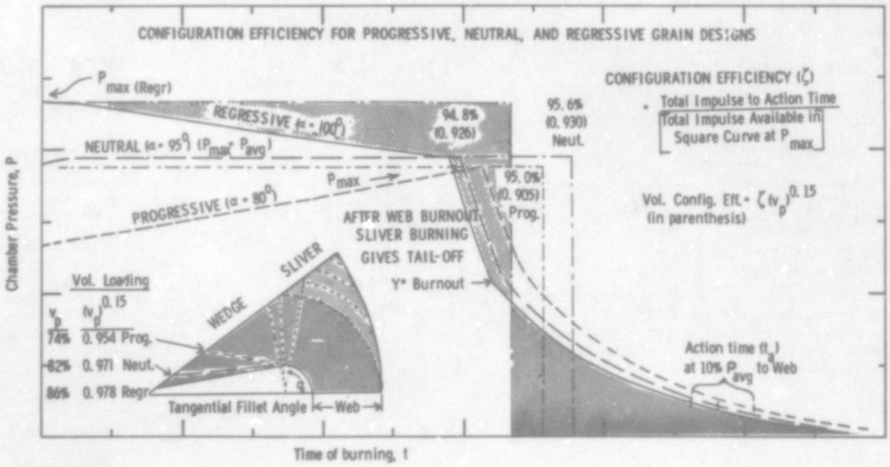

PRA/SA AFRPL dtd 3 Feb. 1969

Delta-Angle - An azimuthal definition of the coordinates of an intersection of two periphery elements, used primarily in the description of the extremity of the propellant arms in an anchor-perforated grain.

Dendrite (Dendritic-Perforated) Grain Design - An internal-burning case-bonded grain design composed of alternate long and short protrusions so arranged in a sector that the flow space appears to branch looking outward from the center toward the web. (It may contain the star and/or wagonwheel protrusion.)

Dogbone Configuration - A grain configuration in which the perforation is composed of a shank and enlarged termini suggestive of a dogbone, and including in a generalized sense, this type of terminus even though in a symmetry greater than two. Contains generally an elliptical fillet bounded by tangential fillets of essentially 180° magnitude.

End Effects - Calculation of the effect of axial burning on the ends of the grain to shorten the burning surface by interruption of radial burning by the contoured head closures, as a modification of the semi-infinite or 2-dimensional cross-section concept of grain design.

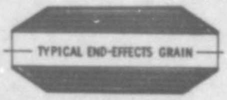

Exposure Integral - The integral of chamber interior surface area exposed to propellant flame by withdrawal of case-bonded propellant web, integrated with respect to time, to simulate the amount of sacrificial insulation that would be required to maintain the actual chamber wall unaffected by flame. (See Slotted Grain-Ballistic)

Far Sector Boundary - The sector boundary most removed from the reference axis, and thus the bisector of the maximum propellant protrusion.

Feasibility Parameter (Propellant Charge) - A parameter obtained by dividing thrust (F) by the duration (t) squared, which correlates with the interior design factors: burning rate, pressure, length-to-diameter ratio, and reduced web thickness in dimensional analysis independent of the size of the rocket - a measure scaling rocket motors of similar interior design.

Fillet Radius Ratio - The ratio of the inside radius of the web (a) to the local radius of the (tangential) fillet (ρ or y_f), as a measure of intensity of an attachment fillet in stress concentration effect.

Finocyl Grain Design - A three-dimensional configuration obtained by cutting slots or fins in the flare surface of a conocyl, to obtain a regressive element less dependent on length-to-diameter ratio of the chamber. Known also as "winged slot" or "star-in-a-pocket".

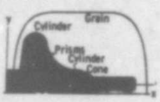

Flat - A boundary of a grain cross-section that is bounded on both sides by segments whose directrix lies on the solid side of the burning surface, so that the projection of the flat decreases in length as it burns.

Hexa-Star Grain Design - A star-perforated grain design in symmetry of six, which represents the regressive side of the neutrality threshold for ideal star-perforated grains (sector half-angle = 1 radian) without end-effects. Actually with moderate filleting, the hexa-star is usually the neutral-burning condition and resort to the hepta-star and higher symmetry numbers is made for regressive-burning grains.

Impulse-Density Exponent - The exponent (α) in the expression $I_s\rho^{\alpha}$ which expresses the density (ρ) weighted value of specific impulse (I_s) in comparing burnt velocity of fixed volume and open volume motor designs with propellants of varying density. Used by analog also for the loading factor (v_p) weighted value of configuration efficiency (ζ) in the expression $\zeta(v_p)^{\alpha}$ for comparing velocity increments of motors with configuration efficiency and loading factor.

Inside Round or Fillet - A circular arc forming a portion of the free boundary of a grain design such that the directrix lies on the gas side of that boundary. This feature increases in length proportional to the fractional increase in its radius as it burns, subject to curtailment by interception of burning fronts whose directrices cross the locus of this intercept.

Melon-Slice Grain Design - A spherical internal-burning propellant charge composed of star perforated

cross-sections inserted in a continuous spherical web, so that the actual height of protrusions is a maximum at the equator and diminishes towards the poles, producing the effect of a "melon-slice" when a protrusion is examined in longitudinal section.

Monocoque Chamber - Rocket case composed of a single continuous structural shell, as in filament wound chamber, and distinguished from cylindrical case employing separate end closures. Usually requires a collapsible or expendable core whose dimensions exceed the minimal opening allowed for nozzle attachment.

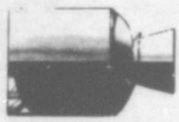

Morphological Transformation - A topological concept of propellant charge grain design wherein a given volume of propellant (usually expressed as a cross-sectional area) is manipulated so as to maintain a continuously changing initial surface area and mean thickness of burning path (web thickness) while conserving total volume, with the exception of "sliver" elements generated by burning points intersecting so as to separate portions of the charge from support or to remain attached to the chamber wall when the principal burning front is exhausted. Practically this is a means of arranging configurations in a geometrically logical order, whereby omissions of designs and relatedness of nomenclature can be examined, and the functions of geometrical elements recognized for optimum selection of the charge (see Web Spectrum).

Multi-Annular - A propellant charge composed of opposite concentric radial burning surfaces, as a set of concentric tubular charges, and thus having more than one web thickness on a radius. Exempt from the generalization of web thickness as a fraction of charge radius, except as a measure of the number of annular elements. Related morphologically to the anchor-perforated grain as a transitional case to the case-bonded internal-burning design.

Multi-Perforated - A grain configuration containing more than one internal perforation, and thus not singly connected in free surface. Can only be progressive in burning surface area when externally restricted until web between perforations is burnt through. Used as a free-standing grain with internal-external burning of seven equally spaced circular perforations for the Rodman artillery grain.

Negative Wedge Angle - A structural designation for a star-perforated grain design in which the sides of adjacent protrusions form a negative angle looking outward from the center of the charge (this design usually contains only a tangential fillet but in any case, the sum of the secant and tangential fillet angles must be less than 90°).

Neutrality - Constant burning surface area, pressure or thrust with respect to distance burnt or time, as a neutral performance curve, distinguished from progressive (increasing with time) or regressive (decreasing with time) (see Configuration Efficiency).

Outside Round - A circular arc forming a portion of the free boundary of a grain design such that the directrix lies on the solid side of that boundary. This feature decreases in length as it burns and vanishes when the burning distance equals its initial radius. The converse of an inside round or fillet which increases in surface area as it burns.

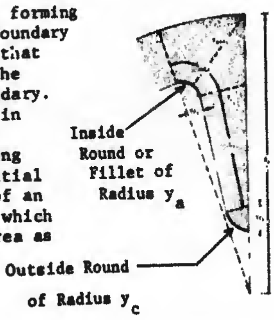

Penta-Star Grain Design - A star-perforated grain design in symmetry of five, which represents the progressive side of the neutrality threshold for ideal star-perforated grains (sector half-angle = 1 radian) without end-effects. Actually penta-star and lower symmetry number grain designs are usually combined with significant regressive end-effects to secure overall neutrality of total burning surface area.

Port Area - The fraction of a charge cross-section represented by flow space (compliment of the Volumetric Loading Factor).

Positive Wedge Angle - A structural designation for a star-perforated grain design in which the sides of adjacent protrusions form a positive angle looking outward from the center of the charge (this design must contain a secant fillet as defined in the ballistic nomenclature and the sum of the secant and tangent fillet angles must exceed 90°).

Rayside - The linear segment of a protrusion in a case-bonded grain (e.g. star-perforated) immediately adjacent to the attachment fillet, the normal to which at this point defines the critical burning distance (y_*). For the wagonwheel design, two raysides must be distinguished, the "near" adjacent to the tangential fillet and case-bonded web, and the "far" separating the break-round and the outside round.

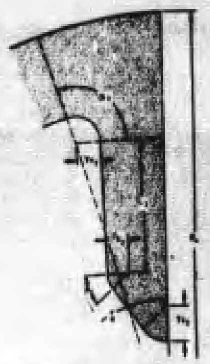

Rayside Clearance - Nearest approach of the boundary of a protrusion to the reference axis or web bisector, and thus defining the minimum structural web of the casting core, or to the adjacent protrusion in a dendrite. Significant also in radial equalization of chamber pressure in highly convoluted bores.

Reduced Web Thickness - The ratio of web thickness to charge radius in correlating grain configuration independent of size.

Reference Axis - The radius or sector boundary bisecting the web at the nearest approach to the chamber wall.

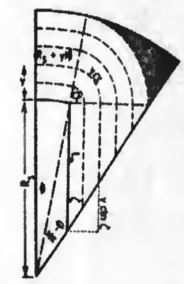

Rod - An external-burning free-standing propellant element of constant outer radius, necessarily regressive-burning when standing alone.

Secant Fillet - An inside round in the free surface of a grain-design whose center of curvature is congruent with that of the outer boundary of the charge.

Second Derivative (Ballistic Performance Curve) - The second derivative of the burning surface area with respect

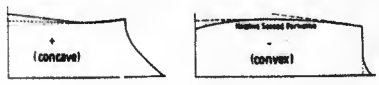

to distance burnt, which is zero for peripheries composed of tangential inside rounds (fillets) and linear segments (see Tail-off), positive for outside rounds or flats (concave curve), and negative for non-tangential inside rounds (convex curve) such as cusped boundaries or non-concentric intersections with the chamber wall.

Shell - An internal-burning case-bonded propellant element of constant inner radius, necessarily progressive burning when standing alone.

Shell-and-Rod Charge - Combination of an internal-burning shell grain and an external burning rod grain to give neutrality to the total charge design.

Sliver - A segment of propellant remaining unburnt when the chamber wall becomes exposed to direct propellant flame in a case-bonded grain. As attached sliver, it will be consumed at decreasing pressure (i.e., forming tailoff), which is not a complete loss but reduces the overall configuration efficiency. Detached sliver is physically lost from the chamber and detracts from usable propellant and can cause ballistic irregularity.

Slotted Grain - Structurally, a grain design having sides of adjacent protrusions parallel so as to form a slot cut from the inner bore surface towards the case-bonded web. The sum of the secant and tangent fillets is specifically 90°.

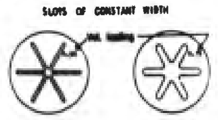

Ballistically, the parallel condition is an immaterial case of the star-perforated grain (ballistic continuity between positive and negative wedge angles), and the significant condition for slotting is whether the critical burning distance terminates on the far sector boundary or on the charge circumference (i.e., uses exhaustion of the protrusion or exposure of the chamber wall as the neutrality control device).

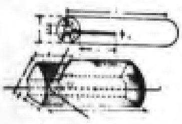

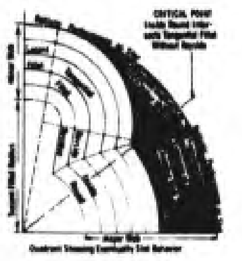

Star (Star-Perforated) Grain Design - An internal-burning case-bonded grain design composed of identical protrusions where the side of the protrusion is unbroken from the attachment fillet at the case-bonded web to the commencement of rounding or flat at the extremity of the protrusion.

Star-Wagonwheel-Dendrite - A system of parametric definition of grain designs for ballistic analysis, wherein the mathematical model of the dendritic-perforated grain contains that of the wagonwheel and star as special cases.

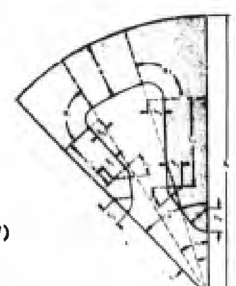

Independent Parameters (17)

R_c W $y_{a_{1,2}}$ $y_{b_{1,2}}$ $y_{c_{1,2}}$

$L_{1,2}$ N $\alpha_{1,2}$ $\beta_{1,2}$ $\phi_{1,2}$

Stress Concentration Factor - A factor obtained from photoelastic specimen tests versus finite difference stress network calculations which multiplies the stress which would exist in a circular bore grain design of the same web thickness, and thus accounts for the contribution of reinforcing elements resulting from protrusion or convolution on the propellant inner surface.

Tangential Fillet - An inside round in the free surface of a grain design that meets the adjacent boundaries tangentially, and thus projects a straight line through its center as the boundaries jointly regress. (Serves to connect the case-bonded web to the protrusion, whose equivalent of web is measured by y_*.)

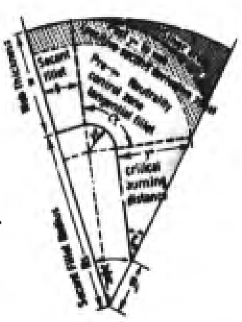

Tail-off - A rapid decline of chamber pressure or thrust occurring in a performance curve when the principal burning fronts have been exhausted. Commences at web burnout time and represents the rapid decrease in surface area associated with sliver consumption, magnified by the decrease in thrust coefficient and elongation of time - corresponding to decreasing pressure, modified by the discharge of chamber capacitance.

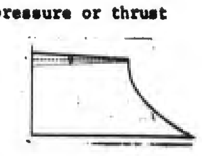

Tapered Star Configuration - Uses overly progressive aft configuration, neutral midships, and elongated highly regressive fore section to achieve overall neutrality of burning surface area with the port space increasing with mass flow to minimize erosive-burning. For web > y_*, compensation by end effects required to avoid terminal progressivity of cross-section.

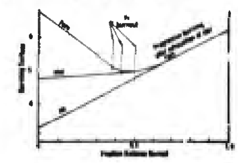

Tubular Charge - A free-standing internal-external burning grain having a neutral burning surface area.

Volumetric Loading Factor - The fraction of a charge cross-sectional area represented by propellant (used in weighted configuration efficiency).

Wagonwheel (Wagonwheel-Perforated) Grain Design - An internal-burning case-bonded grain design composed of identical protrusions where the side of the protrusion is broken to approach parallelity between adjacent protrusions in the innermost segment, and displays a positive wedge angle for the segment nearest the web, giving a spoke and hub appearance to the flow space.

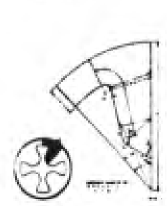

Web - Literally membrane or covering, structurally the thickness between opposite surfaces, as in a beam. For ballistics, the depth of the burning path from initial ignition surface to primary exhaustion of burning front or an inert surface such as chamber. Thus associated with burn time in data reduction for average burning rate under motor conditions. Originating from multiperforated grains, (actually, a double web in the ballistic sense) and now applied singly to externally-restricted star-perforated grains (see Tangential Fillet).

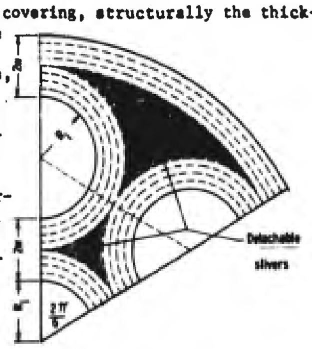

Web Burn Time - The time required to burn through the propellant web - generally the time for first exposure of the chamber wall in a star-wagonwheel-dendrite type internal-burning grain design.

Web Spectrum - A morphological sequence of internal-burning grain designs of increasing relative web thickness, in the sequence dendrite-wagonwheel-star-perforated (1/6, 1/5, 1/4 of the charge radius); thick-web star, bipropellant sliverless (0.5-0.7 rel. web); slotted cylinder and conocyl (0.75-0.90 rel. web). Configuration efficiency and volumetric loading factor increase systematically 0.91-0.98 and 0.60-0.90 respectively, in this order, while neutrality is independent of length-to-diameter ratio for relative web less than 0.5 radius, is typically 3:1 for the thick-web-star and bipropellant, and becomes controlling at about 2:1 for the slotted cylinder and conocyl.

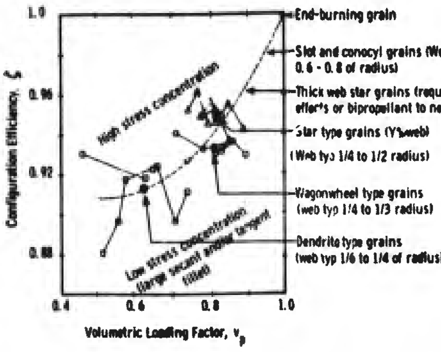

Web Thickness - The least distance from a point on the initial ignition surface of the propellant grain to the chamber wall, or to intercept another burning front causing a major decrease in burning surface area (see Tangential Fillet).

y_* **= Web Locus** - The grain design condition where the critical burning distance is made equal to the web thickness so that chamber wall exposure commences at the same instant that lateral burning of the protrusion is exhausted, so that there is neither post-y_* positive change of the second derivative, or web < y_* excessive-sliver generation (theoretical condition of minimum sliver for maximum configuration efficiency at sea level). See Tapered Star for web > y_*. When y_* > web, sliver is excessive as shown below.

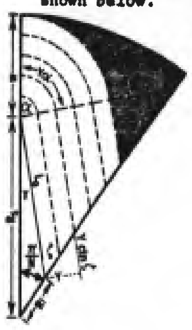

BASIC STAR-PERFORATED GRAIN DESIGN

Note $Rs = Ri \cos \frac{\pi}{N} + Lo \cos \gamma$

while $Ri \sin \frac{\pi}{N} = Lo \sin \gamma$,

So $Rs = Lo (\sin \gamma \ctn \frac{\pi}{N} + \cos \gamma)$

defines the initial rayside length Lo.

"Burning" the surface a normal distance Y, forms a circular arc of length Yα and shortens the rayside by Y ctn ζ.

Thus the periphery $U = Lo + Y\alpha - Y \ctn \zeta$

where $\gamma = \frac{\pi}{2} - \alpha$ and $\zeta = \frac{\pi}{N} + \gamma = \frac{\pi}{N} + \frac{\pi}{2} - \alpha$

THE RELATIVE WEB SPECTRUM AND ATTRIBUTES OF NEUTRAL-BURNING GRAIN DESIGNS

Dendrite	Wagonwheel	Star	Bipropellant	Slotted-cylinder
Dendrite	Voiture-roue	Etoile	Deux poudres	Montaise-cylindre
Древовидный	Вагонное колесо	Звездообразный	Двух горящих	Щелевой заряд

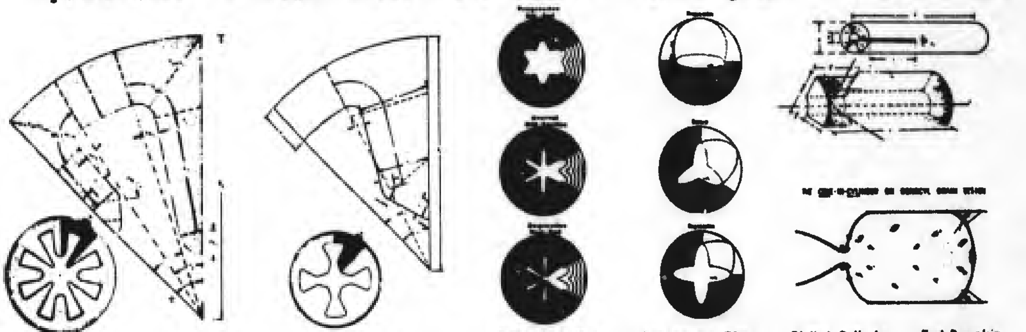

Configuration	Dendrite (forked wagonwheel)	Wagonwheel	Ideal Star (Web ≤ y_*)	Thick Web Star (Web > y_*)	Bipropellant Star (refractive interface)	Slotted Cylinder and Conocyl	End-Burning (cigarette)
Relative Web (web/radius)	$\frac{1}{8} - \frac{1}{6}$	$\frac{1}{5} - \frac{1}{4}$	0.3-0.4	0.45-0.60	0.6-0.8	0.8-0.9	2 L/D
Gross Volume Loading	0.60	0.70	0.75	0.85	0.90	0.95	1.00
Sliver at Web Burnout	2%	3%	5%	4%	None	None	None
Configuration Efficiency	90%	92%	93%	95%	96%	98%	100%
Maximum L/D for Neutrality	Unlimited	5:1-8:1	4:1-5:1	3:1-4:1	3:1-4:1	2:1-3:1	
Shape of Performance Curve (Sign of Second Derivative)	0* (linear)	0* (linear)	0* (linear)	+ (concave)	- (convex)	- (convex)	0 (Constant cross-sectional area)
Exposure Index	none to web	none to web	none to web	none to web	none to burnout	Sacrificial Insulation controls burning surface area.	Exposure proportional to fraction burnt.

* Based on Zone 2 ($y_r \le y \le y_*$) burning with web not exceeding y_*.

CALENDAR OF CONFERENCES AND SHORT COURSES

DATE	PLACE	EVENT	INFORMATION
Apr. 6-9	Washington, D. C.	ASME Metals Engineering	ASME 345 East 47th Street New York, N. Y. 10017
Apr. 8-9	St. Louis, Missouri	4th Annual Symposium on High Performance Composites	Monsanto Company 800 N. Lindbergh Blvd. St. Louis, Missouri 63116
Apr. 8-11	Philadelphia, Pa.	Acoustical Society of America Spring Meeting	Dr. Mary L. Harbold Temple University Philadelphia, Pennsylvania 19122
Apr. 14-16	New Orleans, La.	ASME/AIAA 10th Structures, Structural Dynamics and Materials Conference	A. H. Hausrath, General Chairman Bldg. 520, Room 144, TRW Systems P. O. Box 1310, Norton AFB San Bernardino, California 92402
Apr. 16-17	New Orleans, La.	AIAA Structural Dynamics and Aeroelastic Specialists Conference	H. Norman Abramson, Director Department of Mechanical Sciences Southwest Research Institute 8500 Culebra Road San Antonio, Texas 78206
Apr. 28-30	Cincinnati, Ohio	AIAA 4th Aerodynamic Testing Conference	Elmer G. Johnson, General Chairman Aerospace Research Laboratories WPAFB
Apr. 28-May 1	Washington, D. C.	American Physical Society Meeting	Dr. W. W. Havens, Jr., APS Hdq. Pupin Physics Laboratories Columbia University New York, N. Y. 10017
Apr. 29-May 1	Los Angeles, Calif.	Rubber Chemistry Division Meeting, American Chemical Society, Spring Meeting	American Chemical Society 1155 16th Avenue N. W. Washington, D. C. 20036
Apr. 29-May 2	Los Angeles, Calif.	Society of Aerospace Materials and Process Engineers 15th National Symposium and Exhib.	A. F. Feldbush, SAMPE Hdq. P. O. Box 613 Azusa, California
May 5-9	Chicago, Illinois	Society of Plastics Engineers 27th Annual Technical Conference	Director, Member Activities 65 Prospect Street Stanford, Conn.
May 5-9	Detroit, Michigan	Polymer Conference Series, *Fundamentals of Polymer Science*	Professor Irving N. Einhorn, Conf. Chairman Polymer Institute, University of Detroit 4001 West McNichols Road Detroit, Michigan 48221
May 6-9	Philadelphia, Pa.	SESA Spring Meeting	Dr. B. E. Rossi, Exec. Sec. 21 Bridge Square Westport, Connecticut 06880
May 7-9	Venice, ITALY	2nd International Conference of Space Engineering	Cdr. G. A. Partel Conference Organizer Centro Studi Trasporti Missilistici Via Squarcialupo, 19-A 00162 Rome, ITALY
May 12-16	Detroit, Michigan	Polymer Conference Series, *Optical Methods of Polymer Characterization*	Professor Irving N. Einhorn, Conf. Chairman Polymer Institute, University of Detroit 4001 West McNichols Road Detroit, Michigan 48221
May 13-16	Philadelphia, Pa.	SESA Spring Meeting	Society for Experimental Stress Analysis 21 Bridge Square, Westport, Conn. 06880
May 19-23	Detroit, Michigan	Polymer Conference Series, *Mechanical and Thermodynamic Properties of Crystalline Polymers*	Professor Irving N. Einhorn, Conf. Chairman Polymer Institute, University of Detroit 4001 West McNichols Road Detroit, Michigan 48221
May 19-30	Los Angeles, Calif.	Aerospace Vehicle Systems Engineering (Short Course)	UCLA Engineering and Physical Sciences Extension University Extension P. O. Box 24902 Los Angeles, California 90024

May 19-30	Ann Arbor, Michigan	Engineering Summer Conferences, *Numerical Methods, Optimization Techniques, and Simulation for Engineers*	James O. Wilkes, Co-Chairman Chrysler Center The University of Michigan Ann Arbor, Michigan 48105
May 19-30	Ann Arbor, Michigan	Engineering Summer Conferences, *Applications of Computers in Engineering*	Maurice J. Sinnott, Co-Chairman Chrysler Center The University of Michigan Ann Arbor, Michigan 48105
May 20-22	Chicago, Illinois	Interagency Chemical Rocket Propulsion Group, 4th Solid Propulsion Conference	CPIA, Johns Hopkins University Applied Physics Lab 8621 Georgia Avenue Silver Spring, Maryland
May 21-23	Seattle, Washington	AIAA 2nd Advanced Marine Vehicles and Propulsion Meeting and Technical Display	AIAA Meeting Manager 1290 6th Avenue New York, N. Y. 10019
May 22-23	Santa Clara, Calif.	4th Aerospace Mechanisms Symposium	Dr. George G. Herzl, Symposium Chairman Orgn. 51-10, Bldg, 201 Lockheed Missiles and Space Co. 3251 Hanover Street Palo Alto, California 94304
June 2-6	Detroit, Michigan	Polymer Conference Series, *Adhesion*	Professor Irving N. Einhorn, Conf. Chairman Polymer Institute, University of Detroit 4001 West McNichols Road Detroit, Michigan 48221
June 2-13	Ann Arbor, Michigan	Engineering Summer Conferences, *Instrumentation for Mechanical Analysis*	Francis Fisher, Chairman Chrysler Center The University of Michigan Ann Arbor, Michigan 48105
June 4-6	Denver, Colorado	Modern Photoelastic Stress Analysis (Short Course)	Photoelastic, Inc. 67 Lincoln Highway Malvern, Penna. 19355
June 9-13	Colorado Springs, Colo.	AIAA 6th Propulsion Joint Specialist Conference	AIAA Meeting Manager 1290 6th Avenue New York, N. Y. 10019
June 9-13	Andover, N. H.	Gordon Research Conference, *Polymer Physics*	Alexander M Cruickshank, Director Gordon Research Conference Pastore Chemical Laboratory University of Rhode Island Kingston, R. I. 02881
June 9-13	Detroit, Michigan	Polymer Conference Series, *Recent Advances in Polymerization Catalysis*	Professor Irving N. Einhorn, Conf. Chairman Polymer Institute, University of Detroit 4001 West McNichols Road Detroit, Michigan 48221
June 9-20	Ann Arbor, Michigan	Engineering Summer Conferences *Computer Graphics for Designers*	Bert Herzog, Chairman Chrysler Center The University of Michigan Ann Arbor, Michigan 48105
June 15-19	Cambridge, Mass.	6th U. S. National Congress for Applied Mechanics	Prof. Howard W. Emmons 6th U.S. National Congress for Appl. Mech. Pierce Hall, Harvard University Cambridge, Massachusetts 02138
June 16-17	London, ENGLAND	Plastics Institute, *Polymers in High Performance Applications*	Plastics Institute 11 Hobart Place London, S. W. 1, ENGLAND
June 16-18	Chicago, Illinois	ASME Applied Mechanics Conf.	American Society of Mechanical Engineers 345 E. 47th Street New York, N. Y. 10017
June 16-18	Evanston, Illinois	ASME Summer Annual Meeting	American Society of Mechanical Engineers 345 E. 47th Street New York, N. Y. 10017
June 16-20	Colorado Springs, Colo.	AIAA 5th Propulsion Joint Specialists Conference	AIAA, 1290 6th Avenue New York, N. Y. 10019
June 16-20	Detroit, Michigan	Polymer Conference Series, *Flammability Characteristics of Polymeric Materials*	Prof. Irving N. Einhorn, Conf. Chairman Polymer Institute, University of Detroit 4001 West McNichols Road Detroit, Michigan 48221

June 16-27	Ann Arbor, Michigan	Engineering Summer Conferences, *Numerical Analysis*	Cleve B. Moler, Co-Chairman Chrysler Center The University of Michigan Ann Arbor, Michigan 48105
June 16-27	Los Angeles, Calif.	Vibrations Theory and Applications to Engineering Cases (Short Course)	P. O. Box 24902 Engineering & Physical Sciences Extension University Extension UCLA Los Angeles, California 90024
June 18-20	Rochester, New York	American Physical Society	Dr. W. W. Havens, Jr. 335 East 45th Street New York, N. Y. 10017
June 22-25	New York, N. Y.	ASME Summer Annual Meeting	A. B. Conlin, Jr., ASME Hdq. 345 East 45th Street New York, N. Y. 10017
June 22-27	Atlantic City, N. J.	ASTM 72nd Annual National Meeting	T. A. Marshall, Jr., ASTM Hdq. 1916 Race Street Philadelphia, Pennsylvania
June 22-29	Weimar, GERMANY	5th International Congress on the Application of Mathematics in Engineering	Prof. H. Matzke, Director Weimar College of Arch. and Bldg. Karl-Marx-Platz 2 53 Weimar, GERMANY (Dem. Rep.)
June 23-25	Toronto, CANADA	7th International Shock Tube Symposium	Prof. I. I. Glass, Institute for Aerospace Studies University of Toronto Toronto 5, CANADA
June 23-27	Detroit, Michigan	Polymer Conference Series, *Organic Coatings Technology*	Prof. Irving N. Einhorn, Conf. Chairman Polymer Institute, University of Detroit 4001 West McNichols Road Detroit, Michigan 48221
June 30-July 4	New London, N. H.	Gordon Research Conference, *Polymers*	Alexander M. Cruickshank, Director Gordon Research Conference Pastore Chemical Laboratory University of Rhode Island Kingston, R. I. 02881
July 7-18	Ann Arbor, Michigan	Engineering Summer Conferences, *Probability and Random Processes for Engineers and Scientists*	Ralph L. Disney, Chairman Chrysler Center The University of Michigan Ann Arbor, Michigan 48105
July 7-18	Ann Arbor, Michigan	Engineering Summer Conferences, *Design and Analysis of Engineering Experiments*	Charles Lipson, Chairman Chrysler Center The University of Michigan Ann Arbor, Michigan 48105
July 21-25	Meriden, N. H.	Gordon Research Conference, *Chemistry at Interfaces*	Alexander M. Cruickshank, Director Gordon Research Conference Pastore Chemical Laboratory University of Rhode Island Kingston, R. I. 02881
July 21-Aug. 1	Ann Arbor, Michigan	Engineering Summer Conferences, *Fundamentals and Applications of Optical Data Processing and Holography*	E. N. Leith, Co-Chairman Chrysler Center The University of Michigan Ann Arbor, Michigan 48105
July 28-Aug. 1	Ann Arbor, Michigan	Engineering Summer Conferences, *Application of Computers to Automated Design*	Paul Reinhard, Chairman Chrysler Center The University of Michigan Ann Arbor, Michigan 48105
July 28-Aug. 1	New London, N. H.	Gordon Research Conference, *Elastomers*	Alexander M. Cruickshank, Director Gordon Research Conference Pastore Chemical Laboratory University of Rhode Island Kingston, R. I. 02881
Aug. 4-8	Ann Arbor, Michigan	Engineering Summer Conferences, *Written Communication for Engineers, Scientists, and Technical Writers*	W. Earl Britton, Chairman Chrysler Center The University of Michigan Ann Arbor, Michigan 48105
Aug. 4-15	Ann Arbor, Michigan	Engineering Summer Conferences, *Simulation of Mechanical Systems*	Joseph E. Shigley, Co-Chairman Chrysler Center The University of Michigan Ann Arbor, Michigan 48105

Aug. 18-20	Ames, Iowa	11th Midwestern Mechanics Conference	H. J. Weiss, Conference Chairman Department of Engineering Mechanics Iowa State University Ames, Iowa 50010
Aug. 18-22	New Hampton, N. H.	Gordon Research Conference, *Chemistry and Physics of Cellular Materials*	Alexander M. Cruickshank, Director Gordon Research Conference Pastore Chemical Laboratory University of Rhode Island Kingston, R. I. 02881
Aug. 18-22	Tilton, N. H.	Gordon Research Conference, *Thin Films*	Alexander M. Cruickshank, Director Gordon Research Conference Pastore Chemical Laboratory University of Rhode Island Kingston, R. I. 02881
Aug. 24-31	Mexico City, MEXICO	7th International Conference on Soil Mechanics and Foundation Engineering	Institution of Civil Engineers Great George Street London, S. W. 1, ENGLAND
Aug. 25-29	Eugene, Oregon	50th Summer Meeting of Mathematical Association of America (Joint Mtg. with Amer. Math. Soc.)	H. M. Gehman, MAA Hdq. SUNY, University of Buffalo Buffalo, N. Y. 14214
Aug. 25-29	New Hampton, N. H.	Gordon Research Conference *Science of Adhesion*	Alexander M. Cruickshank, Director Gordon Research Conference Pastore Chemical Laboratory University of Rhode Island Kingston, R. I. 02881
Aug.	Alburquerque, N. M.	Applied Mechanics Western Conference	A. B. Conlin, Jr., ASME Hdq. 345 E. 47th Street New York, N. Y. 10017
Sept. 1-3	Prague, CZECH.	5th Microsymposium on Cyclopolymerization and Cyclopolymers	O. Wichterle, Head of Institute Institute of Macromolecular Chemistry Czechoslovak Academy of Sciences Prague 6 - Petriny, CZECHOSLOVAKIA
Sept. 1-4	Prague, CZECH.	4th Microsymposium on Rheology of Polymer Solids and Concentrated Solutions	O. Wichterle, Head of Institute Instute of Macromolecular Chemistry Czechoslovak Academy of Sciences Prague 6 - Petriny, CZECHOSLOVAKIA
Sept. 8-10	Grenoble, FRANCE	National Scientific Research Center, International Colloquium on Physical Properties of Solids under Pressure	D. Block, Maitre de Conferences Faculte des Sciences, University of Grenoble 7, Pl. Bir-Hakeim, Grenoble, FRANCE
Sept. 8-11	Prague, CZECH.	6th Microsymposium on Light Scattering in Polymer Science	O. Wichterle, Head of Institute Institute of Macromolecular Chemistry Czechoslovak Academy of Sciences Prague 6 - Petriny, CZECHOSLOVAKIA
Oct. 6-10	Los Angeles, Calif.	National Aeronautic and Space Engineering and Manufacturing Meeting	W. I. Marble, SAE Hdq. 485 Lexington Avenue New York, N. Y. 10017
Oct. 13-16	Philadelphia, Pa.	ASM Materials Engineering Exposition and Congress	American Society for Metals Metals Park, Ohio 44073
Oct. 14-17	Houston, Texas	SESA Fall Meeting	The Society for Experimental Stress Analysis, 21 Bridge Square Westport, Connecticut 06880
Oct. 14-17	Detroit, Michigan	28th Annual Meeting of the Society for Nondestructive Testing	American Society for Nondestructive Testing, 914 Chicago Avenue Evanston, Illinois 60202
Oct. 20-24	Anaheim, Calif.	AIAA 6th Annual Meeting and Technical Display	AIAA 1290 Sixth Avenue New York, N. Y. 14214
Nov. 16-21	Los Angeles, Calif.	ASME Winter Annual Meeting and Energy Systems Exposition	A. B. Conlin, Jr., ASME Hdq. 345 E. 47th Street New York, N. Y. 14214
Nov. 18-20	China Lake, Calif.	JANAF Mechanical Behavior Working Group, 1st Meeting	Mr. Tony San Miguel, Program Chairman Naval Weapons Center China Lake, California 93555 714-375-1411 Ext. 72425

Dec. 1-3	Monterey, Calif.	AIAA Strategic Offensive/Defensive Missile Systems Meeting	AIAA Meeting Manager 1290 6th Avenue New York, N. Y. 10019
Dec. 7-12	Cincinnati, Ohio	American Society for Testing and Materials, Winter Meeting	Henry H. Hamilton, Public Relations Dir. 1916 Race Street Philadelphia, Pa. 19103
1970			
May 12-15	Huntsville, Alabama	Society for Experimental Stress Analysis, Spring Meeting	Society for Experimental Stress Analysis 21 Bridge Square Westport, Connecticut 06880
June 21-26	Toronto, CANADA	American Society for Testing and Materials, 73rd Annual Meeting	Henry H. Hamilton, Public Relations Dir. 1916 Race Street Philadelphia, Pa. 19103

ENGINEERING THERMODYNAMICS, by Munir R. El-Saden, D. Van Nostrand Company, Inc., Princeton, New Jersey, 1965, 216 pp.

In this text, the author has attempted to reduce the treatment of thermodynamics based on Jayne's formalism of information theory, as presented by M. Tribus in his book "Thermostatics and Thermodynamics," D. Van Nostrand Company, Inc., 1961 to the level of an introductory course for undergraduate engineering students with no previous training in thermodynamics. The first five chapters present the basic information theory approach with application of the resulting mathematical formalism to the determination of the properties of an ideal gas and a discussion of the principle of the increase of entropy. The remaining five chapters present a very abbreviated treatment of elementary engineering thermodynamics.

The major difficulty with this text, in the opinion of this reviewer, is stated by the author himself in his introduction to his treatment of macroscopic thermodynamics, quoting page 96, "New advances in engineering require the insights which the statistical treatment afford. The student should note that in the working out of many, if not most, engineering problems, the macroscopic laws will be found to be most efficient, especially if the microscopic foundations are used as a guide to the intuition." From this point on, the author relies almost exclusively upon macroscopic concepts, as is usually required in engineering thermodynamic analysis. Here lies the basic point; the macroscopic approach to thermodynamics is most efficient for systems analysis, while the microscopic approach yields property analysis. The author attempts to bridge the gap, but falls short because of difficulties with the concepts of temperature and heat.

It is the opinion of the reviewer, having taught introductory thermodynamics from both the classical and the statistical approaches, that the most effective way to present thermodynamics to the student, is to provide first a thorough treatment of classical thermodynamics, with the student gaining an ability for systems analysis, followed by a treatment of the statistical approach in depth. The approach presented in this text is just the reverse, presenting first the abstract concepts of probability theory, followed by an elementary treatment of engineering thermodynamics. Such an approach seems to be inefficient from a pedagogical standpoint.

Contents:

1. Propability, Uncertainty, and Entropy
2. The Statistical Formalism
3. The Ideal Gas
4. The General System
5. The Principle of Increase of Entropy
6. The Laws of Thermodynamics
7. The First Law and the Closed System
8. The Second Law and the Closed System
9. The Open System
10. Fundamentals of Energy Conversion and Refrigeration

Appendix

A. Data For Computations
B. Some Definite Integrals
C. Definite Integrals and the Error Function

L. K. Isaacson

* * * *

RECENT PROGRESS IN APPLIED MECHANICS: THE FOLKE ODQVIST VOLUME, edited by Bertram Broberg, Jan Hult & Frithiof Niordson, Almqvist & Wiksell, Stockholm, John Wiley & Sons, New York, London, Sydney, 1967, 586 pp.

This volume on Applied Mechanics was prepared as a tribute to Folke K. G. Odqvist when he retired from his professorship at the Royal Institute of Technology in Stockholm. The contents include a short biography and bibliography of professor Odqvist and contributions of forty-five of his colleagues from twelve countries:

Barenblatt, G. I., Kozyrev, Yu. I., Malinin, N. I., Pavlov, D. Ya., Shesterikov, S. A., "On the Thermal Vibrocreep of Polymers."

Berndt, S. B., "The Vorticity Jump Across a Gasdynamic Discontinuity as Influenced by Extraneous Forces."

Besseling, J. F., "Thermodynamic Interpretation of the Concept of Ideal Creep and Plasticity."

Bishop, R. E. D., Gladwell, G. M. L., "The Spacing of Natural Frequencies and Critical Speeds of Coupled Systems."

Bland, D. R., "Lagrange's Equations for Finite Elasticity."

Broberg, K. B., "Discussion of Fracture from the Energy Point of View."

Carlsson, A. J., "A Simple Method for Measurement of Crack Propagation Velocities."

Carlson, R. L., "Structural Instability Induced by Creep."

Dorn, J. E., Mitchell, J. B., "Mechanisms of Creep in Ordered Alloys."

Drucker, D. C., "On Time-Independent Plasticity and Metals Under Combined Stress at Elevated Temperature."

Edstam, U., Hult, J., " Design Charts for Stationary Creep."

Hill, R., "On the Classical Constitutive Relations for Elastic/Plastic Solids."

Hoff, N., Ross, B., "A New Solution of the Buckling Problem of Thin Circular Cylindrical Shells Heated Along an Axial Strip."

Hohenemser, K., "Recent Work on the Energy Transfer Across Moving Gaseous Interfaces."

Johnson, A. E., "Some Progress in Creep Mechanics."

Kachanov, L. M., "On the Theory of Creep Rupture."

Koiter, W. T., "Post-Buckling Analysis of a Simple Two-Bar Frame."

Laasonen, P., "On Stresses in a Thin-Webbed Profile Induced by a Point Load."

Neuber, H., "Stress and Strain Concentration at Non-Linear Elastic and Plastic Deformation."

Niordson, F. I., "A Method for Solving Inverse Eigenvalue Problems."

Olszak, W., Perzyna, P., "General Constitutive Equations for Elastic/Viscoplastic Materials."

Parkus, H., "On the Lifetime of Viscoelastic Structures in a Random Temperature Field."

Persson, A., "A Complex Variable Study of Shrink Fits."

Phillips, C. E., "Recent Advances in Time-Independent Plasticity at the National Engineering Laboratory."

Piechnik, S., "Creep of a Solid Circular Bar Under Bending and Torsion."

Prager, W., "Variation Principles of Linear Elasto-Statics for Discontinuous Displacements, Strains and Stresses."

Reiner, M., "Examination of Strain-Tensors."

Reissner, E., Wan, F. Y. M., "On Stress Strain Relations of the Linear Theory of Shells."

Shu, L. S., Onat, E. T., "Finite Deformations of an Extensible Plastic Arch."

Sjöström, S., "Experimental Methods Used at Scania-Vabis for Fatigue Life Determination of Vehicle Components."

Steneroth, E., "The Longitudinal Strength of Ships."

Ziegler, H., McVean, D., "On the Notion of an Elastic Solid."

Zyczkowski, M., "General Solution for the Linear Creep Buckling of Heavy Bars."

W. L. Hufferd

* * * *

MILITARY AND CIVILIAN PYROTECHNICS, by Herbert Ellern, Chemical Publishing Company, Inc., New York, 1968, 464 pp., $15.00.

This is an enlarged version of the book entitled Modern Pyrotechnics which was originally published in 1961. It is a primer and a collection of up-to-date information on pyrotechnics and their uses. This version has been enlarged to include commercial aspects as well as the well-known military applications. A competent technical discourse in which Dr. Ellern discusses the reasons why as well as the "how to do it."

The book is primarily organized by applications, which include flame and glow production, light production, heat production, production of chemicals, etc. He then discusses the basic characteristics of materials which affect their useage in pyrotechnic devices. Next, specific materials including carbon, sulfur, boron, aluminum, etc., are examined. The book then ends with a summary of formulations and a discussion of the language of pyrotechnics. For those desiring further information a bibliography of over 700 references is included.

Contents:

I. General Outline
II. Primary Flame and Glow
III. Light
IV. Aerosols (Smoke and Dispersed Agents)
V. Kinetic Energy
VI. Noise
VII. Heat Production per se
VIII. Chemical Production
IX. Basic Behavior and Properties of Materials
X. Specific Materials
XI. A Formulary of Pyrotechnics
XII. The Language of Pyrotechnics
XIII. Aftermath; Afterthoughts

F. R. Wagner

* * * *

PYROTECHNICS, 2nd Edition, by George W. Weingart, Chemical Publishing Co., Inc., New York, 1947, 244 pp., $8.50.

A dated but interesting discourse on the precursor to solid propellant rockets, namely fireworks. Treating the topic as a craft, the author discusses the ingredients, methods of manufacture, and the design of fireworks including large displays for exhibitions. He ends on some notes of historical interest, namely the use of pyrotechnics in warfare and industry. Although of primary interest to the novice fireworks manufacturer this book does give some interesting insight into the origin and history of solid rocketry.

Contents: Introduction
Ingredients
Manipulation
Products of Manufacture and Formulae
Exhibition Fireworks
Miscellaneous

F. R. Wagner

* * * *

PROBABILISTIC APPROACHES TO DESIGN, by Edward B. Haugen, John Wiley & Sons, Inc., New York, 1968, 323 pp., $13.95.

This book takes on the very difficult and thankless task of showing how statistical or probabilistic calculations can be used in engineering design, a function which this reviewer is grateful to see someone take the lead. Although primarily concerned with structural reliability and the abolishment of the safety factor and margin of safety, the author develops the basic tools necessary to expand into other applications.

The book is divided into two major sections. The first section is devoted to development of the foundations of probabilistic analysis and the second part to applications. The portion of the book devoted to fundamentals is excellent and worthwhile in itself. Almost all conceivable distributions are considered. It includes both the law of propagation of error although it is called the "method of partial derivatives" and Monte Carlo techniques. It also includes a section on numerical integration.

The portion devoted to applications is heavily weighted towards structural problems and reads like an elementary text in strength of materials, i.e., simple beams - concentrated loading, cantilever beams, column design, combined torsion and bending, etc. This is not really surprising since this is the easiest and most logical application to begin with. There is a chapter devoted to electromechanical devices.

In general the book is considered excellent. It is somewhat lengthy for the person who is already acquainted with statistical techniques but is not verbose, and is probably well suited to the uninitiated.

Contents: Chapter 1. Introduction
Part I - Foundation
Chapter 2. Mathematical Considerations
Chapter 3. Algebra of Normal Functions
Chapter 4. Determination of Reliability
Chapter 5. Numerical Methods
Chapter 6. Monte Carlo Methods
Part II - Applications
Chapter 7. Mechanical Elements
Chapter 8. Elements in Tension
Chapter 9. Simple Beams: Concentrated Loading
Chapter 10. Simple Beams: Distributed Loads
Chapter 11. Cantilever Beams
Chapter 12. Column Design
Chapter 13. Torsion and Combined Torsion and Bending
Chapter 14. Statistical Study of Distortion
Chapter 15. Electromechanical Devices

F. R. Wagner

* * * *

COMPOSITE MATERIALS WORKSHOP, edited by S. W. Tsai, J. C. Halpin, and N. J. Pagano, Technomic Publishing Co., Inc., Stamford, Conn., 1968, 360 pp., $22.50.

This is a compilation of most of the papers presented at the advanced session of the summer workshop: Physical Aspects of Composite Materials, held at Washington University, St. Louis, Mo., 13-21 July 1967. This workshop was sponsored by the ONR-ARPA Association of Monsanto and Washington University.

The papers in this book range from basic fundamentals and theoretical developments to the design data for the practical applications of composite materials. An excellent coverage of the field. Two excellent papers which fall into the fundamentals category are "Introduction to Viscoelasticity" by J. C. Halpin and "Stress Analysis of Viscoelastic Composite Materials" by R. A. Schapery. Both of these papers introduce their materials in a manner that can be followed by the beginning engineer yet also provide significant depth. Halpin addresses the question of what is viscoelastic behavior and how do you describe it while Schapery discusses predicting the stress and strains in viscoelastic bodies. In a related paper, "Fracture Mechanics of Anisotropic Plates," E. M. Wu investigates the effect of anisotropicity upon fracture characteristics. In so doing, he uses the fracture mechanics approach of investigating what the magnitude of the stresses in strains in the vicinity of a crack or defect. The material is assumed to be a continuum in the rest of the body.

The volume ends with two relatively practical papers. The first one is by M. E. Waddoups and is entitleo "Characterization and Design of Composite Materials." In this paper Mr. Waddoups presents the methods and data for achieving a composite material with a specific set of properties. In the final paper, "Structural Synthesis" by L. A. Schmit, the author presents the methodology for designing a structure to a set of criteria. It is an excellent discussion of structural optimization.

Contents:

F. R. Wagner

* * * *

SPACE SYSTEMS TECHNOLOGY, edited by Regis D. Heitchue, Jr., Reinhold Book Corp., New York, 1968, 300 pp.

This book is a very comprehensive yet practical treatise prepared by members of Advance Systems and Technology, Missile and Space Systems Division, Douglas Aircraft Company. It is truely written for the systems engineer. The contributors have been very successful in avoiding the long mathematical developments which too often bog down the reader yet provide the results required by the systems. The text is concise and fast moving while the book is replete with descriptions of present systems, typical performance data and compilations of material and component properties which are useful to systems designers.

Although those steeped in intellectualism may argue that this book lacks sophistication, this reviewer feels that is what gives the book its charm. It is a lucid straightforward presentation which even the novice should be able to understand and should only upset those dedicated to the philoeophy that things must be complicated to be worthwhile.

Contents:

F. R. Wagner

ABSTRACTS

1.0 Mechanical Characterization

5522 Murakami, K. et al: "Viscoelastic Properties of Random, Block and Blended Polymers," Fifth International Congress on Rheology, Kyoto, Japan, 1968.

This paper deals with the results of observation about the viscoelastic properties of the various kinds of polymers which are random copolymer, block copolymer and blended polymer containing two kinds of monomer units. The behavior of the mechanical properties of these polymers is observed under the given condition such that the ratio of the weights of two homopolymers is constant.

In this paper, styrene, methyl acrylate, isoprene and butadiene were used as monomer species. Viscoelastic parameters observed here are η_t (steady-state tensile viscosity), J_e (steady-state compliance), τ_m (maximum relaxation time obtained by Procedure X) and E_m (maximum modulus).

The results that J_e depends upon molecular weight, slightly, and remarkably upon molecular weight distribution were obtained from our previous papers, and these were supported by the data of Leaderman and Ninomiya. In addition to J_e, other parameters such as η_t, τ_m, etc. are also affected by molecular weight and its distribution. Then the viscoelastic behaviors of the various polymers were observed and compared with each other by a variation of composition when molecular weight and its distribution remain to be a constant. The values of τ_m of block copolymers were generally larger than those of other polymers under the above conditions. This reason will be based upon the specific mechanism of entanglement among polar chain groups in the block copolymers.

Electron and phase photomicrographs indicate that the state of fine structures of block polymers is roughly between those of random and blended polymers. On the other hand, the curve of rigid modulus against temperature shows the same tendency above described for block, random and blended polymers.

Other results for these polymers will be described and discussed.

1.1 Uniaxial Linear Characterization

5523 Mercier, J.; Howell, J.; Silva, G. Da.: "Exact and Intrinsic Derivation of the Strain Rates in a Continuous Medium," Séanc. Acad. Sci., Paris, No. 266A, 1968, pp. 1266-68, (in French).

By use of intrinsic co-moving coordinates, authors derive the linear relationship $\dot{\gamma}_{ij}=\frac{1}{2}(v_{j/i} + v_{i/j})$ between the strain rate tensor and the covariant derivatives of the components of the vector velocity field. The derivation implies no simplifying assumption about the velocity field, and does not require the fixed and the co-moving coordinate systems to coincide at the time the derivation is taken.

5524 Tsai, S. W.; Halpin, J. C.: "Polymer-Polymer Composites," Fifth International Congress on Rheology, Kyoto, Japan, 1968.

It is becoming common practice, in polymer mechanics, to develop polymeric solids which consist of two or more thermodynamically distinguishable phases. The classical treatment of particular composite leads to a development for the effective elastic moduli in terms of the moduli and volume fractions of the constituent materials. Additional refinements in theory invoke the additional variables of reinforcement and phase geometries. While these solutions are specific, with respect to the variables assumed, they can be reduced to a unified formulation which is applicable not only to particular systems, but also to fiber reinforced materials. Since polymer-polymer composites (block copolymers, blends, etc.) are generally intermediate between the reinforcement and phase geometries associated with either particulate or fiber reinforced systems, one must employ a treatment of composite response in which a variable phase geometry can be introduced into the theory. In this manner a casual relationship is established between the volume fractions, moduli, and morphology of constituents and the overall composite response. This analysis shall be demonstrated for two phase polymeric systems and then extended to the multiphase problem. In addition the viscoelastic response of the polymer-polymer composite shall be outlined with specific emphasis being placed upon the time-temperature reduction relationship. It is shown that the elasticity treatments of inclusion problems by Kerner, Hashin, Hill, Hermans, and others, are special cases of the unified formula.

SEE ABSTRACT 5590

1.1.1 Elastic Characterization

5525 Wallis, F. R.: "Stress Analysis of Incompressible Solids of Revolution by Point Matching," Journal of Spacecraft, Vol. 6, No. 1, 1968.

The analysis applies to any solid of revolution composed of an incompressible homogeneous isotropic elastic material under conditions of small strain. The axial component of the body force must be constant radially, and the radial component must be constant axially. Any axisymmetric boundary conditions that are consistent with incompressibility may be applied, provided that at least one value of a direct stress is given. The boundary points are fitted by least squares, with an optional subset matched exactly.

5526 Wheeler, Lewis T.: "Some Results in the Linear Dynamical Theory of Anisotropic Elastic Solids," California Institute of Technology, Division of Engineering and Applied Science, Pasadena, Calif., Nov., 1968.

This paper aims at generalizations to anisotropic homogeneous elastic solids of some of the results contained in a recent comprehensive study of various topics in the linearized dynamical theory of homogeneous and isotropic elastic media. All of the theorems proved encompass unbounded domains. Specifically, the prolonged quiescence of the far elastodynamic field in an initially quiescent anisotropic body is established. In addition, a uniqueness theorem and a reciprocal identity are proven which are applicable to infinite anisotropic solids, in the absence of artificial regularity requirements at infinity.

5527 Carroll, M. M.: "Finite Deformations of Incompressible Simple Solids II. Transversely Isotropic Solids," Quart. Journ. Mech. and Applied Math., Vol. 21, Pt. 3, 1968.

Four families of inhomogeneous finite deformations are known to be controllable for homogeneous, transversely isotropic, elastic solids, i.e., to be possible in every such material in the absence of body forces. These deformations are shown to be controllable also for homogeneous, transversely isotropic, simple solids. The corresponding stresses are expressed in terms of material functionals which characterize the response to homogeneous plane deformations, whose fundamental plane contains, or is normal to, the symmetry direction of the material.

5528 Perkins, Richard W., Jr.: "A General Theory of Plane Elastostatic Dislocation Problems for Anisotropic Media," Journal of the Franklin Institute, Vol. 286, No. 1, July 1968.

The general solution to the dislocation problem is considered for anisotropic media which have a plane of elastic symmetry for the plane strain and anti-plane strain deformation cases. The displacement discontinuity function is assumed to satisfy a Hölder condition for all points along the dislocation cut. It is shown that the general dislocation problem can be identified with the Hilbert problem, and can effectively be reduced in the customary boundary value problems of plane or antiplane elasticity. The general properties of the solution functions are discussed. The case of a set of Volterra dislocations is given as an illustrative example.

5529 Edmonds, D. V.; Beevers, C. J.: "The Effect of Inclusions on the Stress Distribution in Solids," Journal of Materials Science, Vol. 3, Sept. 1968, pp. 457-463.

Examination of the effect of a hard inclusion on local magnification of an applied stress. The stress distribution existing in and around hard inclusions in solids subjected to a uniaxially applied stress is investigated both by a photoelasticity technique and by a theoretical analysis due to Eshelby (1957). It is stated that the local constraint of the matrix by hard inclusions during tensile loading can produce severe stress concentrations, which depend on the elastic modulus, shape, and orientation of the inclusions.

5530 Beatty, Millard F.: "Stability of the Undistorted States of an Isotropic Elastic Body," International Journal of Non-Linear Mechanics, Vol. 3, September 1968, pp. 337-349.

Incremental stability criteria appropriate for compressible and incompressible, general isotropic elastic solids are used to study the stability of all undistorted states of an arbitrary body subject to dead loads corresponding to a uniform hydrostatic stress. General conditions sufficient for stability of all such hydrostatic stress states are derived. The results indicate a geometrical dependence for the apparent shear and bulk moduli. The relation of the main results to uniqueness theorems in the theory of small deformations superimposed on large, to broad plausibility restrictions imposed on the elasticities so as to assure physically reasonable material behavior, and to the propagation of elastic waves is also outlined; these relations constitute only specific application of certain general theorems already in the literature. Finally, it is shown that the principal results coincide with estimates that may be gotten by aid of Holden's (1964) inequality.

5531 Diatlovitskii, L. I.; Lemberg, E. D.: "Plane Problem with Central Symmetry for an Incremental Body with a Variable Modulus of Elasticity," Prikladnaia Mekhanika, Vol. 4, August 1968, pp. 74-84, (in Russian).

Investigation of the stressed state of a solid whose modulus of elasticity is a function of the coordinates. During the application of the load the boundaries of the region change - i.e., the body becomes incremental. In view of the complexity of the problem for real structures, the study is begun with a body of very simple shape. The solution is obtained in closed form and can be used not only to judge the nature of the stressed state of the body studied, but also to estimate the accuracy of approximate methods of solving more complex problems for bodies whose configurations and moduli of elasticity are altered when they are immersed, such as is the case with hydraulic structures.

5532 Haythornthwaite, R. M.: "Analysis of Complex Stress States in Classical Plasticity," Developments in Mechanics, Vol. 3, Midwestern Mechanics Conference, 9th, University of Wisconsin, Madison, Wis., August 16-18, 1965, Proceedings, Part I, Solid Mechanics and Materials, ed. Huang, T. C. and Johnson, M. W., Jr., 1967, pp. 41-52.

Study of stress distributions in bodies undergoing plastic deformation. This deformation may be highly dependent on the precise form of the yield criterion. Treating the tube subject to combined axial force and internal pressure as an example, it is shown that significant error can be introduced by assuming uniformity of stress even in relatively thin tubes. Rational interpretation of failure loads is possible only when exact solutions are available, and several of these are discussed.

5533 Hartmann, Christian: "Equilibrium Problem of an Elastic Medium with Stress Couples in Linearized Theory," Académie des Sciences (Paris), Comptes Rendus, Série A - Sciences Mathématiques, Vol. 267, No. 17, Oct. 21, 1968, (in French).

Extension of a method of solving equilibrium problems in plane elasticity, by representing a biharmonic function with the aid of two analytical functions, to media with stress couples. The solution of a Type II problem is demonstrated for the case of a disk.

1.1.1 Elastic Characterization (contd.)

5534 Shen, M. K.: "Note on the Static Criterium of Elastic Stability," Zeitschrift fuer Angewandte Mathematik und Mechanik, Vol. 48, July 1968, pp. 356-57.

Evaluation of the von Mises version (1923) of the static criterion of elastic stability of a conservative system ($\delta^2 \Pi = 0$, where Π is the potential energy of the system and δ is a special variation). By confining the study to structures for which the critical load is known a priori to be nonzero, it is demonstrated that both the von Mises and the Pflüger (1964) expressions of the static criterion of the elastic stability of a conservative system may be employed for the stability study of properly designed structures.

5535 Eimer, Cz.: "The Boundary Effect in Elastic Multiphase Bodies," Archiwum Mechaniki Stosowanej, Vol. 20, No. 1, 1968, pp. 87-93.

Discussion of the solution to problems of elasticity for a body with finite dimensions, and made of multiphase materials. It is suggested that the solution is similar to the solution of the corresponding problem for a macroscopically nonhomogeneous elastic body. Equations are given for expressing the elastic tensor as a function of position.

5536 Willis, J. R.: "The Stress Field Around An Elliptical Crack in an Anisotropic Elastic Medium," International Journal of Engineering Science, Vol. 6, No. 5, June 1968, pp. 253-263.

Development of a mathematical method for finding the stress field surrounding a flat elliptical crack in an infinite elastic medium, which is subjected to general loading at infinity. The Fourier transform method which was used by Willis (1967) to solve Boussinesq's problem is used. Detailed results are presented when the stress at infinity is a linear function of the coordinates.

1.1.2 Constant Strain Rate Characterization

5537 Kydoniefs, A. D.: "The Finite Deformation of an Almost Homogeneous Elastic Solid," Akademia Athenon, Praktika, Vol. 42, Pt. 2, 1967, pp. 331-348.

Description of a perturbation and approximation method for solving problems in the theory of finite deformations. The method uses the perturbation of the strain-energy function $W(I_i)$, where I_i are the strain invariants to be defined. The effect on the deformation of the inhomogeneous perturbation term $\varepsilon W'(I_i, \theta_i)$, where I_i and θ_i are the strain invariants and the convected coordinates, respectively, and ε is a constant number small compared with unity, is considered. The general theory is given and is applied to the case where the original deformation is a uniform extension. As an example, a solution is given for a problem in which the specified deformation is a uniform extension and the undeformed body is an incompressible right circular cylinder.

SEE ABSTRACT 5729

1.1.3 Creep Compliance Characterization

5538 Barenblatt, G. I. et al.: "Vibrational Creep of Polymer Materials," Journal of Applied Mechanics and Technical Physics, No. 5, September-October 1965, pp.44-48.

In the mechanics of deformed solids it is usually assumed that superposing small amplitude vibrations on a static load has no effect on the over-all characteristics of a material under strain. This hypothesis is reflected in the fact that the existing equations of state for the case of static loads with superposed small vibrations give deformation characteristics which differ little from the corresponding parameters of deformation processes taking place in the absence of excitations. At the same time, substantial changes in the deformation characteristics of a number of materials are observed under certain conditions after the application of alternating stresses of small amplitude. Reports on studies of creep of metals, elastomers, and concrete have been published, in which the fatigue curves obtained with small vibrations superposed on static loads lie above curves obtained for static loads corresponding to the maximum pulsating load level. Attempts have been made to explain this effect from the standpoint of the molecular-kinetic and phenomenological theories. Certain theoretical considerations and experimental data, discussed in this article, show that superposing a small dynamic component on a static load leads to an increase in the rate of creep of several polymer materials. This effect, which is due mainly to an increase in the polymer temperature as a result of dissipation of vibrational energy, differs from the 'vibration effect' observed on elastomers by Slonimskii and Alekseev, in which the temperature rise due to the heat generated by vibrations plays no substantial part.

5539 Namestnikov, V. S.: "Creep Beyond The Elastic Limit," Inzhenernyi Zhurnal - Mekhanika Tverdogo Tela, May-June 1968, pp. 173-176, (in Russian)

Extension of previous work (Namestnikov, 1964), in which creep was found to have a pronounced effect on the instantaneous loading curve and a pronounced deviation was seen in the behavior of a material under variable loading beyond the elastic limit from the predictions of strain-hardening theory. Analytical relations are derived which describe the behavior of a material beyond the elastic limit in a manner which agrees well with experimental results.

5540 Tagai, H.; Zisner, T.: "High Temperature Creep of Polycrystalline Magnesia. 1. Effect of Simultaneous Grain Growth," J. Am. Ceram. Soc., Vol. 51, No. 6, 1968, pp. 301-310.

The creep of pure magnesia (99.9+ % MgO) was tested in transverse bending at temperature from 1200 to 1500°C, strain rates near 10^{-2}% /hr and grain sizes from 4 to 50 microns. In most cases grain growth during the test affected the apparent behaviour more than all the other variables combined. An analytical graphical method was used to separate the grain growth from other effects and to obtain more meaningful creep data. Creep occurred primarily by a viscous mechanism (Nabarro-Herringtype, cation-lattice-diffusion controlling) with a minor amount of plastic creep dislocation climb. The agreement with previous creep data was good.

5541 Zisner, T.; Tagai, H.: "High Temperature Creep of Polycrystalline Magnesia. II. Effects of Additives," J. Am. Ceram. Soc., Vol. 51, No. 6, 1968, pp. 310-314.

The creep of magnesia doped with 0.035 to 2.26 cation per cent of nine other oxides and three binary mixtures thereof, and of three seawater products (about 96, 98 and 99.5% MgO) was evaluated in transverse bending at 1200 to 1500°C, with strain rates of about 10^{-2}%/hr and average grain sizes 5-50 microns. The results obtained were compared with those for pure magnesia. Most additives accentuated the plastic (diffusion controlled) nature of the creep process, presumably by pinning dislocations and/or slowing grain growth. In most cases the rate determining diffusing species seemed to be the cation, Mg, but in two cases it was suspected that oxygen boundary diffusion was controlling. Porosities above about 10 per cent appear to increase the temperature dependence of creep, probably by introducing boundary sliding. The agreement of the creep data with those of other diffusion controlled processes (electrical conductivity, sintering and grain growth) is demonstrated.

5542 Ajroldi, G. Garbuglio, C.; Pezzin, G.: "Dynamic-Mechanical and Creep Measurements. A Comparison of Approximate Conversion Methods," Journal of Polymer Science, Part B, Vol. 6, 1968, pp. 119-121.

The validity of approximation methods proposed by McLeod and by Hopkins and Hamming to correlate stress relaxation modulus and creep compliance, has been tested by experimental examination of plasticised PVC, evaluating the results by means of a computer. It is concluded that the approximation methods can be applied with confidence.

5543 Listvinskii, G. Kh.: "Determination of the Time to Failure During Creep," Heat Resistance of Materials and Structural Components, ed. by G. S. Pisarenko, 1967, pp. 193-197, (in Russian).

Determination of the time to failure during creep on the basis of a phenomenological approach which associates failure with the variation in the mechanical properties of the body during creep, as well as with the variation of stresses in the body during the deformation process. This approach makes it possible to consider both ductile and brittle failure from the same viewpoint.

5544 Marriott, D. L.: "Approximate Analysis of Transient Creep Deformation," Journal of Strain Analysis, Vol. 3, October 1968, pp. 288-296.

A method has been proposed which approximates transient creep behavior by the superposition of elastic and steady-state creep deformation. The paper discusses the errors incurred by this method and shows that they are small. Equations are derived which enable corrections to be calculated with moderate accuracy for an important group of creep theories. Some numerical examples are included for comparison.

5545 Marriott, D. L.: "Approximate Estimation of Strain-Hardening Creep Deformation," Journal of Strain Analysis, Vol. 3, October 1968, pp. 297-303.

It is demonstrated that creep deformations of a structure based on strain-hardening behavior are bounded by time-hardening and total-strain solutions. The bounds are not exact, but it is shown that any error is small compared with the difference between the exact solution and the approximate solution when the superposition method is used. As this difference is itself small compared with overall deflections, the error due to assuming the strain-hardening solution to be bounded is negligible. It is also shown that strain hardening is asymptotic to the total-strain solution as time increases. A relatively rapid method is suggested for the approximate calculation of deflections, based on an approximate method devised previously for total-strain theory. Numerical examples verify that total-strain theory is a better approximation to strain hardening than is time hardening, especially for large times.

SEE ABSTRACT 5721

1.1.4 Relaxation Modulus Characterization

5546 Becker, G. W.: "Mechanical Relaxation Behavior in High Polymers. I. Area of Small Deformation," Kunststoff-Rundsch., Vol. 15, No. 8, August 1968, pp. 377-387, (in German).

A discussion is given of mechanical relaxation in high polymers in general as related to their molecular structure and of the region in small deformation in particular. Measurements are made of the dependence of elasticity modulus on time, solidification temperature and frequency. Examples are given using polyisobutylene, polyvinyl chloride, polymethylmethacrylate, polyvinyl acetate, polystyrene, polyvinylcarbozole and polyimides.

5547 Yoshioka, N.; Obata, Y.; Kawai, H.: "Theoretical Approaches to the Mechanical Relaxation Mechanisms in Semi Crystalline Polymers," J. Macromol. Sci., Vol. B.1, 1967, pp. 567-585.

The non-crystalline and crystalline relaxation mechanisms are interpreted in terms of the theories both of Bueche and Montroll.

5548 Yannas, I. V.; Tobolsky, A. V.: "Stress Relaxation of Anhydrous Gelatin Rubbers," J. Appl. Polym. Sci., Vol. 12, 1968, pp. 1-8.

Materials tested have rubbery behaviour in the temperature range -40° to +40°C, with gelating weight fraction 0.1-0.4. Stress relaxation moduli are measured and shear viscosities deduced.

5549 Takayanagi, M.; Kawasaki, N.: "Mechanical Relaxation of Poly-4-Methyl-Pentene-1 at Cryogenic Temperatures," J. Macromol. Sci., Vol. 81, 1967, pp. 741-758.

Both bulb crystallized material and single crystal mats were examined using a Vibron visco-elastometer at temperatures down to -160°C. The absorption peaks recorded were interpreted in terms of molecular structure.

5550 Slonimsky, G. L.: "Laws of Mechanical Relaxation Processes in Polymers," J. Polym. Sci., Part C, Vol. 16, 1967, pp. 1667-1672.

Certain distinctive characteristics of relaxation processes in polymers due to a chain structure of macromolecules and super molecular structure of a polymeric body call for a new approach to their quantitative description. A mathematical method of description of relaxation processes based on the use of fractional integral operators is proposed.

SEE ABSTRACTS 5621, 5652

1.1.5 Time-Temperature Shift Function Characterization

5551 Soffer, L. M.; Molho, R.: "Mechanical Properties of Epoxy Resins and Glass-Epoxy Composites at Cryogenic Temperatures," J. Macromol. Sci., Vol. 81, 1967.

Tensile properties, notch toughness, impact strength, thermal expansion and thermal shock resistance were measured for four resins at temperatures of 75, -320 and -423°F.

5552 Armeniades, C. D.; Kuriyama, I.; Roe, J. M.; Baer, E.: "Mechanical Behaviour of Poly(ethylene terephthalate) at Cryogenic Temperatures," J. Macromol. Sci. (Phys.) Vol. 81, 1967, pp. 777-791.

Experiments were performed, using a freely oscillating torsion pendulum and an Instron tester, in the temperature range 4-300°K. Relaxation peaks, elastic modulus, and toughness, were measured and are discussed.

5553 Valanis, K. C.: "Unified Theory of Thermomechanical Behavior of Viscoelastic Materials," Mechanical Behavior of Materials under Dynamic Loads; Proceedings of a Symposium, San Antonio, Texas, September 6-8, 1967, ed. U. S. Lindholm, Springer Verlag, New York, pp. 343-364.

Derivation and proof of a general theorem and its corollary which establish the existence of a viscoelastic potential from which the stress tensor and the entropy density are derivable. The theorem presents the constitutive equations of a viscoelastic material with an initial elastic response and in the presence of large deformations (small deformations for the corollary) and time-varying, spatially inhomogeneous thermal field. A theory is developed and applied with the object of developing explicit forms of constitutive equations of viscoelastic materials for two cases: (1) nonisothermal small deformation, and (2) isothermal large deformation.

5554 Murthy, P. N.; Patel, T. S.: "A Study of the Creep Rupture Parameters," Indian Journal of Technology, Vol. 6, No. 4, April 1968.

The reasons for the superior extrapolative ability of the Manson-Haferd (M-H) creep rupture parameter compared to the other two parameters (Larson-Miller and Dorn parameters), observed by K. M. Goldhoff have been investigated. It is shown that the superior performance of the M-H parameter in enabling relatively accurate predictions of the long-term rupture characteristics of metals on the basis of short-term creep data is due to the implied dependence of the activation energy(Δ H) on stress and temperature, and by assuming a suitable polynomial expression for Δ H, the M-H parameter can be derived from the general creep deformation equation.

5555 Brinson, Halbert F.: "Mechanical and Optical Viscoelastic Characterization of Hysol 4290," Experimental Mechanics, December 1968, pp. 561-566.

(See Abstract 5249).

SEE ABSTRACT 5593

1.1.6 General Time-Dependent Characterization

5556 Somov, A. I.; Chernyi, O. V.: "Stressed State and Mechanical Properties of Composite Materials," Heat Resistance of Materials and Structural Components, ed. G. S. Pisarenko, 1967, pp. 76-85, (in Russian).

Discussion of the generalized results and conclusions of numerous recent studies dealing with the production and properties of composite fibrous materials with metallic matrices. Conditions are analyzed under which these materials meet the requirements of modern technology when used in structural parts. The Young modulus, inclusion orientation, matrix deformation, and stress distribution at inclusions are considered. The behavior of such compositions under mechanical load and at high temperatures is investigated.

5557 Haydl, H. M.: "Stress Concentration in the Plastic Range," Strain, Vol. 4, July 1968, p. 29.

Calculation of the plastic stress concentration factor, when material at a discontinuity under high stresses loses elasticity and becomes plastic. The formula obtained is similar to that of Neuber (1961). The new relationship can be expressed as 'the square of the ratio of stress concentration factors is equal of the ratio of the secant moduli.' Future experimental work on stress concentrations in the plastic state may profit from this result.

5558 De Arantes E Oliveira, Eduardo R.: "Theoretical Foundations of the Finite Element Method," International Journal of Solids and Structures, Vol. 4, No. 10, October 1968, pp. 929-952.

The finite element method is nowadays the most general and one of the most powerful tools for the analysis of structures.

It is also a general mathematical technique and the main concern of the paper is to present it in this light. Functional Analysis is used as the ideal frame for a general abstract formulation.

The ability to predict convergence to the exact solution of a sequence of approximate solutions obtained from patterns of finite elements with decreasing size is fundamental in the application of the method.

In case conformity between elements is obtained, the finite element method is a particular case of Ritz's method, so that convergence can be ensured as far as completeness is achieved.

A general completeness criterion is justified in the paper. Such criterion requires that the field components and all their derivatives, of order not higher than the highest order of derivative entering into the energy density expression, can take up any constant value within the element.

It is finally proved that such criterion is also a general convergence criterion, i.e. a sufficient condition for convergence even if conformity is not achieved.

5559 Carroll, M. M.: "Finite Bending, Stretching, and Shearing of a Block of Orthotropic Incompressible Simple Solid," Journal of Applied Mechanics, September 1968, pp. 495-98.

It is shown that a finite deformation history, involving bending, stretchning, and shearing, can be supported in every incompressible orthotropic simple solid by the application of suitable surface tractions, if the bending axis is along a material symmetry direction. The corresponding stresses are expressed in terms of the material functionals which characterize the response to homogeneous plane deformations, and these material functionals are calculated explicitly in terms of the constitutive functionals of the material. The surface tractions which are required in order to effect bending and stretching of a rectangular block are also calculated.

5560 Green, W. A.; Rivlin, R. S.: "Simple Deformations of Materials with Memory," Acta Mechanica, Vol. 5, 1968, pp. 254-73.

Four classes of simple time-dependent deformations are examined for general incompressible viscoelastic solids and for incompressible rate independent materials with memory. These are: (i) rectilinear shear, (ii) simple torsion of a right-circular cylinder, (iii) helical shear of a cylindrical annulus contained between rigid coaxial cylinders, (iv) simple torsion of material contained between two rigid coaxial cones with common vertex. In each case the deformation of an element of material may be regarded as a superposition of a rigid rotation and a time-dependent simple shear with constant direction of shear and plane of shear. For the viscoelastic solids the state of stress in each class of deformations is shown to be determined to within an arbitrary hydrostatic pressure by the same three material functionals of a single argument function, the history of the amount of shear. For rate independent materials these three functionals become ordinary functions of the amount of shear at the instant under consideration.

5561 Leigh, D. C.: "Asymptotic Constitutive Approximations for Rapid Deformations of Viscoelastic Materials," Acta Mechanica, Vol. 5, 1968, pp. 274-288.

Asymptotic constitutive approximations for the rapid finite deformation of general viscoelastic materials are developed. The zero-order approximation is an elastic-type constitutive equation, although different from the elastic equation for the slow-deformation approximation. The higher-order terms are multiple integrals of the departure of the deformation history from the step-function history. The approximations are shown to be form-invariant to change of deformation measure. The approximations are specialized to isotropic solids and to fluids. As observed by Metzner, White and Denn and Pipkin, fluids undergoing rapid deformations exhibit a solid-like behavior.

5562 Olear, P. D.; Erdogan, F.: "Time-Temperature Dependent Brittle Fracture of Viscoelastic Solids," Journal of Applied Polymer Science, Vol.12, 1968, pp. 2563-2574.

The Griffith formulation is used to study fracture behavior of poly(methyl methacrylate) (PMMA) as a function of strain rate and temperature over the range $4.4 \times 10^{-5} \le \dot{\epsilon} \le 4.4 \times 10^{-2}$ in/in/sec and $25^{o}C<T<T_g$, T_g being the glass transition temperature. It is found that the transition from brittle to ductile failure occurs abruptly at a temperature T_f which is dependent on strain rate and is approximately the same as the glass transition temperature of the material. The Griffith brittle fracture criterion is found to apply below T_f for all strain rates. The brittle fracture behavior is shown to obey the time-temperature equivalence principle in the same way as the material's other viscoelastic properties, having the same shift function.

5563 Nowacki, W.: "On the Completeness of Stress Functions in Asymmetric Elasticity," Académie Polonaise des Sciences, Bulletin, Série des Sciences Techniques, Vol. 16, No. 7, 1968, pp. 546-555.

Development of a new simplified method for deriving formulas for the stress functions in the asymmetric theory of elasticity, without recourse to the laborious solutions of sixth-order determinants. A completeness theorem for the solutions is obtained with the aid of the stress functions ζ and η. Expressions relating the Stokes-Helmholtz potentials and the stress functions are proposed, together with relations for representing the displacements, rotations, and temperature in terms of the vector functions ϕ and ψ and the scalar θ. A system of wave equations in these functions is derived.

5564 Rosen, B. Walter: "The Strength and Stiffness of Fibrous Composites," Modern Composite Materials, ed. L. J. Broutman and R. H. Krock, 1967, pp. 106-119, 529, 530.

Discussion of recently developed methods for evaluating the relationship between properties of composites and properties of constitutents. Several problem areas which are critical to the understanding of the synthesis, design, and response of composite structures are examined. The use of the results of these studies to influence future composite development is emphasized. Attention is also directed to the contrast between the analytical results and those which have been popularly accepted in the absence of suitable analyses. Problems of average elastic stress-strain response and tensile strength are discussed. The average stress and strain in the composite, rather than the actual stress and strain distribution, are considered. This permits the representation of the actual composite which is inhomogeneous and isotropic by an equivalent idealized homogeneous anisotropic material.

5565 Krokosky, Edward: "Behavior of Time-Dependent Composite Materials," Modern Composite Materials, ed. L. J. Broutman and R. H. Krock, 1967, pp. 120-145, 530-532.

Study of the behavior of composite materials consisting of time-dependent binders coupled with fillers that are either time-dependent or time-independent. Basic viscoelastic theory and the fundamental parameters of a time-dependent characterization are examined. The work has applicability to solid rocket propellants and to fiber-reinforced plastics.

5566 Bickford, W. B.; Warren, W. E.: "The Propagation and Reflection of Elastic Waves in Anisotropic Hollow Spheres and Cylinders," Development in Theoretical and Applied Mechanics, Vol. 3, Proceedings, ed. W. A. Shaw, 1967, pp. 433-445.

The propagation and reflection of elastic stress waves in anisotropic hollow spheres and cylinders subjected to time-dependent surface pressures are investigated. The material is assumed to be transversally isotropic with respect to a direction of symmetry, and solutions to the displacement field equations are formally obtained using Laplace transforms. It is shown that if rational approximations are used to represent the modified Bessel functions which occur in the transformed expressions for stress and displacement, the inversion of these expressions for short times may be readily carried out. These short-time results are valid for times much longer than the customary short-time solutions obtained using asymptotic approximations, and are of considerable practical interest since the material internal damping can be expected to diminish the motion for increasing time. The physically interesting problem of a pressure suddenly applied to the inside surface of the sphere or cylinder is considered in detail. For the tangential stress at the inside surface, a comparison between the maximum dynamic stress and the corresponding static condition shows the customary dynamic factor of 2 to be low in varying degrees depending upon the particular elastic constants.

5567 Ohji, Kiyotsugu: "The Elastic Analogue in Creep Stress Analysis," JSME Bulletin, Vol. 11, August 1968, pp. 585-592.

Discussion of the applicability of the elastic analog for various combinations of boundary conditions and mechanical assumptions for creep behavior. It is concluded that when the boundary condition is independent of time, the elastic analog in the creep stress analysis is valid for the choice of either the time-hardening theory or the strain-hardening theory. When the boundary condition changes with time, the elastic analog is valid for the time-hardening theory. When the boundary condition varies with time and the material behavior is compatible with the strain-hardening theory, the elastic analog is valid only under the constraint that the stress-boundary values and/or the displacement boundary values change in the same way as the proportional loading.

5568 Moghe, S. R. et al.: "Mechanical Breakdown of Oriented Solids under Time Dependent Loads," Fifth International Congress on Rheology, Kyoto, Japan, 1968.

A theory describing the time dependent mechanical breakdown phenomena for homogeneous, oriented solids subjected to time dependent loads or stresses is formulated. The kinetic nature of the microscopic molecular behavior is taken into account. The analysis is based upon the mathematical model which consists of a system of randomly oriented linear elements, composed of molecular chains or domains. The solutions for the time required to fracture under repeated loading conditions are obtained. The influence of some parameters involved on the solution is discussed. Within a large range of various applied periodic tensile stresses the logarithm of time-to-break is found to be almost linearly related with the maximum amplitude of the applied stress. As this amplitude gets smaller and smaller the time required for fracture becomes greater and greater and approached to infinity for a certain small limiting value. Qualitatively the analytical results to represent closely the general fatigue behavior of a material. However, in order to correlate this behavior with actual data and to gain confidence in the validity of the formulation and solution, experiments have to be conducted for oriented media. Certain material parameters are obtained from fatigue tests of oriented nylon under different stress ratios. Results are compared and correlated.

5569 Ross, B. E.: "Adaptation of the Moiré Fringe Technique to Rheological Studies of Polymers," Fifth International Congress on Rheology, Kyoto, Japan, 1968.

A brief résumé of current techniques is presented. Present efforts to increase the accuracy and sensitivity of the method when applied to high modulus material are noted.

A specific example involving research related to the stress distribution around elastic and rigid inclusions in an elastic polymer matrix is included. Variations in stress distributions due to spacing of the inclusions and to relative moduli of inclusions and matrix are presented. The pertinent results of the specific investigation indicate that present methods of analysis yield conservative values for stress concentration factors.

The Moiré fringe technique is extended to the flow of polymers by imbedding grids in the polymer material and recording by motion picture camera the changing Moiré fringe patterns which are related to the velocity field. Methods of analysis of the data are presented. Techniques for the experimental implementation of the method are explained. An example of the two dimensional flow of a polymer through a die is shown.

1.2.1 Elastic Characterization

5570 Teodorescu, Petre: "Two-Dimensional Problems of Elasticity Theory. II - Two Zero Tangential Stresses," Accademic Nazionale dei Lincei, Atti, Rendiconti - Classe di Scienze Fisiche, Matematiche e Naturali, Vol. 44, Mar. 1968, (in French).

Investigation of a previously defined two-dimensional problem in the case of two zero tangential stresses. The stress and strain states are expressed by means of a biharmonic function F_0 and two harmonic functions F_1 and F_2 in two variables. Some particular interesting cases are considered, and questions connected with the investigated problem are discussed.

5571 Irobe, Makoto: "Method of Numerical Analysis for Three Dimensional Elastic Problems," Japan National Congress for Applied Mechanics, 16th, University of Tokyo, Japan, October 19-20, 1966, Proceedings, Central Scientific Publishers, 1968, pp. 1-7.

A numerical method for solving three-dimensional elastic problems is presented. Partial differential equations of equilibrium are transformed to three sets of system of ordinary differential equations, and the solution is derived by successive approximation. Numerical examples for a cubic problem of symmetry and for a cylindrical problem of axisymmetry are worked out in order to examine the rate of convergence and the accuracy of this method.

5572 Golecki, J.; Jeffrey, A.: "Two-Dimensional Dynamical Problems for Incompressible Isotropic Linear Elastic Solids with Time Dependent Moduli and Variable Density," Acta Mechanica, Vol. 5, No. 2, 1968, pp. 118-130.

The paper describes a new general method of solution of two-dimensional problems involving the dynamical behavior of incompressible linear elastic solids. As formulated, the solution takes account of density variation with both position and time and a shear modulus which is purely time dependent. Several simple applications are made to problems involving thick cylinders and an infinite plate containing a circular hole.

5573 Alblas, J. B.: "On the State of Stress in a Semi-Infinite Elastic Body with a Cylindrical Hole, I, II," Koninklijke Nederlandse Akademie van Wettenschappen, Proceedings, Series B - Physical Sciences, Vol. 71, No. 4, 1968, pp. 279-296.

Investigation of the problem of the three-dimensional stress concentration around a cylindrical hole in a semi-infinite body, uniaxially loaded at infinity. The solution is obtained in the form of an infinite integral with an integrand that may be algebraically expressed in terms of an auxiliary function which satisfies a Fredholm integral equation of the third kind. The results are obtained by applying integral transform techniques to the displacement equations of equilibrium over the region $(0, \infty) \times (1, \infty)$. The method may be extended to a larger class of boundary value problems for the same region of space.

1.2.3 General Time-Dependent Characterization

5574 Grubin, A. N.: "Criteria of Static Strength under Conditions of Triaxial Tension," Akademiia Navuk BSSR, Vestsi, Seryia Fizika-Tekhnichnykh Navuk, No. 2, 1968, pp. 5-12, (in Russian).

Analysis of the stress state arising as a result of tension on a cylindrical specimen with a small annular notch in a state of great plastic deformation. The problem is solved for an elliptical profile, which can easily be obtained from a rectilinear profile with a notch with a rounded base. This study is a supplement to an earlier analysis by the author (1968), based on a problem discussed by Neuber (1958).

1.3 Dynamic Characterization

5575 Shen, M. C.; Strong, J. D.; Matusik, F.J.: "The Effect of Hydrogen Bonds on the Dynamic Mechanical Properties of Glassy Polymethacrylates from 77°K," J. Macromol. Sc.(Phys.), Vol. 81, 1967, pp. 15-27.

Experiments were carried out over the temperature range from 77°K-Tg using a specially designed resonance-type acoustic spectrometer. The results are examined in terms of 'volume of action' and 'bond loosening' hypotheses.

5576 Hammond, R. J.; Work, J. L.: "Dynamic Mechanical Properties of Plasticized Poly (vinyl chloride) Linear Free Energy Relationships in the Poly(vinyl chloride)-ester System," Journal of Polymer Science, A1, Vol. 6, 1968, pp. 73-83.

A considerable number of quantitative attempts have been made to predict the properties of solutions containing polymers and polar solvents. Thermodynamic approaches have generally failed to accurately describe these systems. This can be ascribed to the difficulty in determining structural characteristics arising from the variety of secondary interaction present in these highly complex solutions. A linear free energy relationship has been used here to explore changes encountered in solutions of monofunctional esters in poly (vinylchloride) undergoing mechanical deformation. This treatment appears valid only for the rubbery region of the viscoelastic spectrum of this polymer. The data indicate that the observed changes are a function of corresponding changes in polymer intramolecular interactions.

5577 Sharma, M. G.; Lawrence, W. F. St.: "Investigation on the Dynamic Mechanical Behavior of a Filled Rubberlike Material," Fifth International Congress on Rheology, Kyoto, Japan, 1968.

This paper is concerned with a study on the dynamic mechanical behavior of a rubberlike material (Solithane 113) filled with finely divided aluminum spherical particles of prescribed volume concentrations at frequencies in the lower audiofrequency range, and at several temperatures above and below room temperature. The dynamic behavior of the material is studied by subjecting a specimen in the form of a rod to longitudinal vibrations and determining the resonant frequencies and the bandwidths of the mechanical resonance curve, corresponding to various modes of vibration.

From the dynamic mechanical data obtained at several temperatures and frequencies, reduced curves for the storage and loss moduli corresponding to a standard temperature are constructed for an extended frequency range by utilizing the time-temp, shift hypothesis. An examination of the dynamic data for various filler concentrations indicates that the viscoelastic transition region is shifted to lower frequencies with the increase in the volume fraction of the filler in the bulk material.

5578 Vinogradov, G. V. et al.: "Correlation of Static and Dynamic Mechanical Characteristics of Some Elastomers," Fifth International Congress on Rheology, Kyoto, Japan, 1968.

The correlation of dynamic characteristics and steady shear flow characteristics of noncured elastomers is discussed. Tests were performed with low-molecular polyisobutylene, butyl rubber and a plasticized specimen of the latter. The measurements were carried out at frequencies ω of from 5×10^{-2} to 5×10^{4} c/s and shear rates $\dot{\gamma}$ of from 10^{-3} to 10^{2} sec^{-1}, and at temperatures of from 20 to 140°C. If we accept that $\omega = \dot{\gamma}$, there exists an ambiguous correlation between the following functions: (1)dependences of the absolute complex shear modulus value $|G^*|$ and ω and of the shear stress on $\dot{\gamma}$; (2) dependences of the ratio of $|G^*|^2$ to the loss modulus on ω and of the difference of the normal stresses on $\dot{\gamma}$. On the other hand, the correlation between the frequency dependences of the dynamic modulus components and the dependence of the stress tensor components on $\dot{\gamma}$ can be discussed of if it is assumed that $\dot{\gamma} = \alpha\omega$ where α is a certain weak function of $\dot{\gamma}$, determined by the influence of deformation on the relaxation spectrum of polymer systems.

The results obtained are discussed proceeding from the ideas of the linear theory of viscoelasticity and the thixotropic theory of nonlinear viscoelasticity, in which it is assumed that during a flow at a shear rate $\dot{\gamma}$ the relaxation spectrum is 'cut off' up to the frequency $\dot{\gamma}/\alpha$.

5579 Kambe, H.; Kato, T.: "Dynamic Viscoelastic Properties of Dispersed Polymers," Fifth International Congress on Rheology, Kyoto, Japan, 1968.

Dynamic properties of amorphous polymers filled with particles, which are homogeneous in size and shape, are investigated. As a model of dispersed polymers, we use a polyepoxide resin dispersed with beads of emulsion-polymerized polyethylmethacrylate. Temperature dependence of tensile dynamic properties was measured using a rheometer made by Rion Co., Tokyo, with 25 c/sec from 30 to 150°C.

Polyethylmethacrylate (PEMA) beads were obtained by the emulsion polymerization. Beads were dispersed in water as a concentrated suspension. From optical investigations, the size of particles is 1 micron on the average and narrowly distributed. Glass transition temperature (T_g) is determined as 69-71°C with D.S.C. Sample films were prepared.

1.3.1 Dynamic Modulus Characterization

5580 Schimmerl, J.: "Determining Torsional Vibrations in an Inhomogeneous Linear Elastic Continuum," Ingenieur-Archiv, Vol. 36, No. 5, 1968, pp. 314-319, (in German).

An elastic isotropic inhomogeneous half-space is replaced by a uniaxial cylinder-symmetrical model showing equivalent behavior under torsional vibrations. This can be achieved by determining the corresponding moment of inertia $J(z)$ characterizing the dispersion-free model for prescribed shear modulus $G(z)$. Twist ϕ (z) and amplitude ψ (z) under torsional vibrations of a base-plate on an inhomogeneous half-space are calculated, and determination of soil parameters from experimental data is discussed.

1.4.1 Elastic Uniaxial Characterization

5581 Steel, T. R.: "Linearized Plane Strain of a Mixture of Two Elastic Solids. II., Proc. Camb. Phil. Soc., Vol. 64, 1968, p. 915.

In a recent paper, we derived the solutions to the equilibrium equations for linearized plane strain of an isotropic mixture of two elastic solids. The solutions were given in terms of four complex potential functions. Here we examine the properties of these solutions and evaluate the forces and couples across an arc in the mixture.

1.4.3 Viscoelastic Uniaxial Characterization

5582 DeHoff, Paul H.: "A Note on the Nonlinear Viscoelastic Behavior of Polymers," AIAA Journal, Vol. 6, May 1968, pp. 956-958.

Discussion of a type of nonlinear viscoelastic behavior of polymers which exists only under very special conditions and for limited strain levels. A possible justification for the validity of an empirical relation, patterned after the hereditary form of linear viscoelasticity and proposed by Leaderman to fit the longitudinal creep and recovery behavior of polyvinyl chloride, is obtained.

5583 Francis, E. C.; Carlton, C. H.: "Some Aspects of Nonlinear Mechanical Behavior of a Composite Propellant," Journal of Spacecraft, Vol. 6, No. 1, January 1969.

Effects of strain on Young's modulus E and Poisson's ratio v for a composite propellant (86% solids, 14% polymeric binder) are evaluated from constant-strain-rate dilatation tests at temperatures from -60° to 160°F. Linear and nonlinear viscoelastic response are separated, and the nonlinearities found are accounted for by extensive volume change at low temperatures and strain hardening at elevated temperature because of high solids loading. Data from stress-relaxation tests at four strain levels at -60° and 80°F confirm the nonlinearities measured in the constant-strain-rate tests. Dewetting and subsequent volume change at low temperatures cause approximately a 50% change in E and a decrease in v (Cauchy relation) from 0.50 to 0.27. The significance of these E and v variations is assessed by a finite-element computer analysis with typical grain designs subjected to cooldown and pressurization loading conditions. The results show that neglect of nonlinearities in propellant modulus and v would yield high (conservative) predictions of stress and strain during cool-down in a steel-case motor but low predictions of strain because of the pressurization in fiberglass motor. Fortunately, in the latter case, the pressure would tend to reinforce E and v and reduce their nonlinearities.

1.5 Chemical Structure and Its Relation to Mechanical Behavior

5584 Chompff, A. J.; Prins, W.: "Viscoelasticity of Networks Consisting of Crosslinked or Entangled Macromolecules.II. Verification of the Theory for Entanglement Networks," J. Chem. Phys., Vol. 48, 1968, pp. 235-243.

A refinement of an earlier theoretical study. Results are compared with experimental data obtained on a high molecular weight sample of poly-n-octyl methacrylate. Some discrepancy is noted but it is concluded that the fit between theoretical and experimental results might be better if the molecular-weight distribution were known for the particular polymer sample examined.

5585 Briscall, H.; Thomas, C. R.: "Cellular Structure and Physical Properties of Plastics," Br. Plast., Vol. 41, No. 7, 1968, pp. 79-84.

Certain physical properties of plastics are modified by the presence of cellular structure in a manner that is dependent on the relationships between the gaseous and solid phases. This article outlines the usual process of formation of cellular structure in plastics and discusses its effect on mechanical strength, thermal conductivity and vapour permeability.

5586 Van Hoorn, H.: "A Dynamic Mechanical Study of the Effect of Chemical Variations on the Internal Mobility of Linear Epoxy Resins (polyhydroxyethers)," Journ. of Appl. Polymer Science, Vol. 12, 1968, pp. 871-888.

A torsion pendulum at 0·1 Hz and a vibrating reed at 100Hz were used to study a range of polyhydroxyethers at temperatures from -180°C to Tg (85-170°C). The results were interpreted in terms of the molecular structure.

5587 Pezzin, G.; Zinelli, G.: "Influence of Molecular Weight on Some Properties of Poly(vinyl chloride)," Journal of Applied Polymer Science, Vol. 12, 1968, pp. 1119-1136.

Stress-strain,creep and recovery tests were performed. The creep results showed that a relatively stable network was present. Ultimate tensile properties depended strongly on molecular weight, due to increased stability of crosslinks with increasing chain length.

5588 Yau, W.; Stein, R. S.: "Optical Studies of the Stress-Induced Crystallization of Rubber," Journal of Polymer Science, Part A2, Vol. 6, 1968, pp. 1-30.

Low angle light scattering by films of stretched natural and synthetic rubbers was investigated. The dependence of scattering was studied as a function of light polarization direction, orientation direction, elongation temperature, degree of swelling, type of swelling liquid, and degree of crosslinking.

5589 Matsuoka, S. et al: "A Further Study of the Properties of Transcrystalline Regions in Polyethylene," Journal of Polymer Science, Part B, Vol. 6, 1968, pp. 87-91.

Dynamic Young's moduli have been measured in polythene crystalline lamellae grown on copper oxide surfaces. The moduli were observed to be higher than for bulk polyethylene at various temperatures. The increases in the moduli are attributed to an anisotropic structure. Absence of chemical changes was demonstrated by gel permeation chromatography.

5590 Valanis, K. C.: "Elastic Materials with Particle Interactions of Finite Range," presented at the 39th Annual Meeting, The Society of Rheology, Inc., January 13-15, 1969.

In this paper the effect of 'long range' particle interactions on the constitutive equation of an elastic material is considered. If the range is not 'too long' it is found that a symmetric stress tensor as well as a stress vector are necessary to describe the state of stress at a point in the material. If the deformation is small, the state of strain is described by the classical strain tensor and a 'strain vector' which is a contracted form of the second displacement gradient tensor. For an isotropic material the state of stress is related to the state of strain through three elastic constants instead of the two that occur in the classical theory of elasticity.

5591 Rotne, Jens: "Variational Treatment of Hydrodynamic Interaction in Polymers," presented at the 39th Annual Meeting, The Society of Rheology, Inc., January 13-15, 1969.

It has recently been pointed out by several authors that the Kirkwood-Riseman diffusion tensor normally used to treat hydrodynamic interaction in polymer molecules is not necessarily positive definite, an unphysical behavior which results from the neglect of short-range contributions to the interaction between chain segments. The problem can be reformulated as a minimization of the rate at which energy is dissipated by the motion of the suspending fluid, and in this way we have obtained an approximate diffusion tensor which (1) is positive definite for all configurations of the polymer molecule, (2) approaches the Kirkwood-Riseman diffusion tensor at large separations between the interacting segments, and (3) can be written as the true diffusion tensor plus a positive definite correction. The last feature can be used to obtain variational bound on relaxation times and sedimentation rates.

5592 Carreau, Pierre J.: "Rheological Equations from Molecular Network Theories," presented at the 39th Annual Meeting, The Society of Rheology, Inc., January 13-15, 1969.

Lodge's molecular network theories are quite successful in describing the linear viscoelastic behaviour of polymer solutions and melts, but cannot account for the rate-of-strain dependence of various material functions. By allowing the junction-creation rate and the probability of loss of junctions to depend on the second invariant of the rate-of-strain tensor, more realistic constitutive equations were obtained. The form of the equations is the same as for some previous models, but the memory function is new; two rheological models are proposed by assuming two different mechanisms for the effect of the rate of strain on the kinetics of the network.

5593 Van Fo Fy, G. A.: "Theory of Shrinkage Stresses in Oriented Glass-Reinforced Plastics, Polymer Mechanics, Vol. 1, No. 6, Nov-Dec 1965, pp. 36-40.

The problem of shrinkage stress distribution in glass-reinforced plastics is examined on the basis of an improved model under certain assumptions concerning the nature of the curing process. Cylindrical tubes of epoxy glass-reinforced plastic are investigated under stepped temperature conditions.

5594 DiMilo, A. J.; Mastrolia, E. J.; Quacchia, R. H.: "The Development and Evaluation of a Hydrocarbon Binder for High Energy Solid Propellants,' Aerojet-General Corp., Final Technical Report AFRPL-TR-68-236, Nov. 68.

Saturated, partially saturated, and unsaturated, hydroxy terminated, polybutadienes were characterized and evaluated as solid propellant ingredients. In two series, the prepolymers consisted of an unsaturated parent and prepolymers derived from the parent by hydrogenation to various satura-

1.5 Chemical Structure and Its Relation to Mechanical Behavior (contd.)

tion levels. Both saturated and unsaturated prepolymers were fractionated on a silica gel column by the Esso method. The unsaturated prepolymer differed from the saturated ones in not having non-functional units. It was postulated that the non-functional units derive from monofunctional ones during hydrogenation.

The causes of the poor low temperature mechanical properties of saturated binders and the corresponding propellants were investigated by dilatometry, pour point studies, microscopy, differential thermal analysis, and by mechanical properties studies. No evidence of crystallinity was obtained. The saturated prepolymers and binders showed two transitions by DTA while the unsaturated and partially saturated ones showed a single transition.

The poor low temperature mechanical behavior was the result of saturation which stiffens the prepolymer chain. The increased rigidity was caused by the rotational energy barriers.

5595 Tokita, N.; Scott, R.: "Rheological Properties and Molecular Structure of Elastomers: EPM, EPDM," Fifth International Congress on Rheology, Kyoto, Japan, 1968.

The relationship between stress relaxation behavior and molecular structure of EPM and EPDM polymers has been investigated. Theoretically, the maximum relaxation time, τ_m, determined from stress relaxation curves reflects certain basic rheological properties of bulk polymers; i.e. the viscosity and elastic memory. The factors which most influence the stress relaxation of polymers are the following:

EPM: 1) molecular weight and its distribution, 2) ethylene-propylene ratio.

EPDM: 1) molecular weight and its distribution, 2) ethylene-propylene ratio, 3) termonomer characteristics in polymerization kinetics.

5596 DeVries, K. L.; Williams, M. L.: "Effects of Strain Rate and Cyclic Loading on Primary Bond Rupture in Polymeric Materials," Fifth International Congress on Rheology, Kyoto, Japan, 1968.

Electron paramagnetic resonance provides a means of detecting the free radicals associated with bond rupture during mechanical damage in some polymers. As such it allows a direct measurement of the relative amounts of primary bond rupture during deformation. Experiments have been conducted on the accumulation of such damage and number of chains broken as functions of strain rate and cyclic load rate and amplitude during deformation in nylon and polyethylene. These results are compared with what might be expected on the basis of some theoretical models.

5597 Nishijima, Y.: "Molecular Motions in High Polymer Solids and Melts Studied by the Fluorescence Method," Fifth International Congress on Rheology, Kyoto, Japan, 1968.

The heterogeneity of molecular motions in polymer systems is manifested in the phenomena of multiple transitions. Fluorescence techniques of measuring the molecular motions in polymer systems have been developed utilizing the life-time of excitation of fluorescent molecules as the reference time scale. By this method, molecular motions of relaxation time ranging from 10^{-11} to 10^{-6} seconds can be observed.

It has been found that fluorescent aromatic compounds capable of internal rotation exhibit an enhancement of the fluorescence intensity with increasing restriction of the internal rotation. When such fluorescent molecules are dispersed in polymer solid, the intensity of the fluorescence emitted from the system varies with temperature. The variations of the intensity of fluorescence can be treated in terms of the relaxation time of the internal rotation of the fluorescent molecule. The change of the relaxation time in various polymer solids, including polystyrene, polyvinyl alcohol, polyvinyl acetate, polyacrylonitrile, polyamides and ethylene-propylene copolymers are studied at temperatures ranging from -50°C to 100°C. Multiple transitions are thus observed, and the variations in the relaxation time in those solids are discussed in terms of the local molecular motions of polymer chains.

5598 Williams, M. L.: "The Relation Between Mechanical Behavior and Chemical Parameters," Fifth International Congress on Rheology, Kyoto, Japan, 1968.

The mechanical behavior of a viscoelastic material, as represented for example by its relaxation modulus, depends upon its chemical composition. For the most part, qualitative associations have been developed. A more definitive relationship would be useful for proper utilization of viscoelastic materials in engineering design. As an illustration of how this improvement might be effected the relaxation modulus is described mathematically through parameters whose variation is then related to chemical parameters such as crosslink density and molecular weight. A simple example is included to illustrate how the engineering results can be directly related to the molecular parameters.

5599 Iwayanagi, S.; Nakane, H.: "The Relaxation and Phase Transition in Crystalline Polymers," Fifth International Congress on Rheology, Kyoto, Japan, 1968.

Two topics are discussed concerning the relaxation phenomena in crystalline polymers: (1) the grain-boundary relaxation and (2) the viscoelastic behavior in the neighborhood of the solid-phase transition temperature.

5600 Muenker, A. H.; Hudson, B. E.: "Functionality Determination of Binder Prepolymers," Esso Report No. GR-8-FBP-68, Esso Research and Engineering Company, Linden, N. J., September 1968.

This is the final report describing research aimed at the development of accurate and reasonably fast test procedures to determine the functionality and functionality distribution of prepolymers currently of interest to the Air Force. Research was carried out under Contract No. F04611-67-C-0012 during the period October 1, 1966 to September 30, 1968. The effect of solute concentration, solvent type and temperature on number average molecular weight measurements by VPO was studied for a series of binder prepolymers. It was concluded that molecular weight measurements of a given polymer in different solvents give identical molecular weights when extrapolated to infinite dilution, although measurements at finite concentrations in different solvents may give widely varying results. A number of micro-methods were developed which can accurately determine the equivalent weight of hydroxy- and carboxy-functional prepolymers on a 50 to 100 mg sample size. A method was also developed to determine the functionality distribution of binder prepolymers. The method is based on the adsorption of prepolymer on activated silica gel and subsequent selective desorption by stepwise elution using solvent mixtures of progressively greater elution power. The following eight prepolymers were studied on this program: OH-Telagen-S, COOH-Telagen-S, P-BEP, 3M's hydroxy-functional perfluoroalkylene oxide prepolymer, COOH-Polyisobutylene, Thiokol's CNR-Nitroso Terpolymer, COOH-Butarez and Sinclair's Poly B-D. Typical prepolymer samples contain from 0-7% nonfunctional polymer, and 16 to 33% monofunctional polymer.

5601 Krimm, S.: "Infrared Spectroscopy and Polymer Structure," Pure Appl. Chem., Vol. 16, Nos. 2/3, 1968, pp. 369-388.

Some facets of polymer structure that can be illuminated by means of detailed vibrational analysis are illustrated. These include the structure of the individual regular chain in the crystalline phase and features of the arrangement of chains in the crystal. It is also possible to determine the nature of the noncrystalline structures present in a polymer system. Examples are cited from experimental work on polyvinyl chloride and polyethylene.

1.5 Chemical Structure and Its Relation to Mechanical Behavior (contd.)

5602 Cowking, A. et al.: "A Study on the Orientation Effects in Polyethylene in the Light of Crystalline Texture, Part 3: On the Effect of Applied Stress on the Molecular and Textural Orientation," Journal of Materials Science, Vol. 3, No. 6, November 1968.

Special sample types established and characterised in Parts 1 and 2 were examined systematically under different modes of external deformation at constant temperatures. The structural changes recorded by means of wide- and low-angle X-ray patterns fully substantiated the bodily rotation of the otherwise unaltered crystallites in accordance with the interlamellar slip mechanism postulated in Part 1 and 2, both in tension and under two modes of compression. Dimensional changes, however, were significantly in excess of those expected from the rotation of crystallites, but were uniquely correlated with this relation in the different samples under different conditions of deformation. This point to a unique structural and mechanistic interrelation between the crystallites and more compliant amorphous regions. As the X-ray long periods were unaffected by the deformation, the more extensible material cannot be identical to that associated with the lamellar periodicity, a fact which points to a previously unsuspected superlamellar regularity in the texture. A simple structural suggestion is made.

5603 Yamamoto, Yoshiyuki: "An Intrinsic Theory of a Cosserat Continuum," International Journal of Solids and Structures, Vol. 4, No. 10, October 1968.

In this paper, a linear intrinsic theory is developed for a Cosserat continuum as a natural extension of the classical theory of elasticity. Introducing the stress functions, a decomposition theorem of Hilbert space for stress distribution is derived, and the properties of the so-called eigen stress is discussed.

2.4 Glass Transition Temperature

5604 Penwell, Richard C.; Porter, Roger S.: "Rheology of Polystyrene Near the Glass Transition," 39th Annual Meeting, The Society of Rheology, Inc., January 13-15, 1969.

Anomalous viscosity increases with shear can occur in tests made near the glass transition and vanish at higher temperatures. The anomalous viscosity behavior arises because the glass transition temperature is a reference temperature which can potentially shift with the application of the interdependent variables - pressure, frequency, shear rate, and shear stress. In our first studies, viscosity measurements have been made on a high and low molecular weight polystyrene of narrow distribution. Viscosity measurements as a function of shear have been made on these samples over a temperature range down to 120°C. Equivalent measurements have been made in both a steel capillary and a cone-and-plate geometry in order to distinguish effects due to pressure from those due to simple shear. Deviations from data reduction have been observed, thus far in only high-shear, high-pressure capillary data. Among alternate methods of explanation, the most general and satisfactory correlation developed to date involves a viscosity increase due to a reduction in sample volume at higher pressures which is the region of higher shear rates in capillary studies.

3.1 Photo-Elastic Characterization

5605 Tokuoka, T.: "A Mathematical Theory of Birefringence of Continuous Media," Fifth International Congress on Rheology, Kyoto, Japan, 1968.

The theoretical investigations with respect to the birefringent phenomena are shown from the point of view of the continuous media.

The polynomial approximations of the photo-constitutive equations and the birefringent effects in zeroth, first, second-order... are presented. In first-order the well-known 'stress optical law' holds for elastic and viscous material.

The simple extension and the pure homogeneous strain deformation of elastic media are analysed and the results coincide with the formulae deduced by Kuhn and Grün, and Treloar.

For some simple deformation of the plastic media, the birefringent effect is expressed as a linear combination of stress and strain, which coincide with the experimental results.

The Couette flows of viscous fluids, Rivlin-Ericksen viscoelastic fluids and Noll's simple fluids are analysed. The extinction angle of the first is 45° in spite of large shearing-rate while the angle of the second and third decreases monotonically as the shearing-rate attains high values.

4.0 Analytical Methods

5606 Simha, Robert; Utracki, Lechoslaw: "Corresponding State Relations for the Newtonian Viscosity of Polymer Solutions. II. Further Systems and Concentrated Solutions," J. Polym. Sci., Part A2, Vol. 5, 1967, pp. 853-874.

Previous papers have developed a procedure for the description of viscosity-concentration functions leading to master curves over a wide range of molecular weights. By examination of vinyl polymers and cellulose derivatives in good and in poor solvents the treatment is now extended to concentrated solutions.

5607 Keller, Evelyn F.; Keller, J. B.: "Statistical Mechanics of the Moment Stress Tensor," Physics Fluids, Vol. 9, 1966, pp. 3-7.

The moment stress tensor, Mijk, and the internal moment per unit volume, li, are obtained for an inhomogeneous fluid in terms of inter-particle forces and a two-particle distribution function. The usual elastic constants are recovered for the homogeneous case, and further elastic constants are derived to relate the change in couple stress, Mijk, to the strain in a displacement for the inhomogeneous material.

4.1 Linear Elastic Analysis

5608 Yogananda, C. V.: "On a Mixed Boundary Value Problem of a Cylindrical Hole in an Elastic Matrix," Indian Institute of Science, Journal, Vol. 50, April 1968, pp. 72-82.

Development of a formal solution, using the Love function, for the axisymmetric localized piston-type indentation problem of a cylindrical hole in an infinite elastic space. The problem is reduced to the solution of a pair of dual integral equations which are solved by a series method, using Legendre orthogonal polynomials.

5609 Flügge, W.; Kelkar, V. S.: "The Problem of an Elastic Circular Cylinder," International Journal of Solids and Structures, Vol. 4, April 1968, pp. 397-420.

Analysis of a homogeneous, isotropic and elastic circular cylinder subjected to prescribed forces of displacements at its surfaces. A general method of solution is presented which can be used to satisfy exactly arbitrary boundary conditions prescribed on the curved and flat surfaces of a hollow or solid cylinder of any length. Boundary conditions in displacements lead to the simplest presentation of the solution and are, therefore, used to demonstrate the method. It is considered sufficient to solve two fundamental problems and then to use linear superposition to solve any other specific problem. The first problem deals with satisfying arbitrary displacements on the curved surfaces of an infinitely long cylinder, while in the second problem arbitrary displacements on the flat end of a semiinfinite cylinder are satisfied with zero displacements maintained on its curved surfaces.

5610 Stumpf, H.: "Pointwise Bounds in the Theory of Elasticity. I, II," Académie Polonaise des Sciences, Bulletin, Série des Sciences Techniques, Vol. 16, No. 7, 1968, pp. 569-584, (in German).

Application of methods of functional analysis to the development of a method which, by appropriate selection of the singularities, makes it possible to establish upper and lower bounds for the static or geometric field values in two-dimensional and three-dimensional elasticity theory. The bounds are determined with the aid of Green's functions and by substituting comparative states (which satisfy only the geometric or only the static conditions) for the unknown elastic states, with subsequent assessment of the error introduced by this procedure.

5611 Bueckner, H. F.; Johnson, M. W., Jr.; Moore, R. H.: "The Calculation of Equilibrium States of Elastic Bodies by Newton's Method," Developments in Mechanics, Vol.3, 9th Midwestern Mechanics Conference, Uni. of Wisconsin, Madison, Wis., August 16-18, 1965, Proceedings, Part I - Solid Mechanics and Materials, ed. T. C. Huang and M. W. Johnson, Jr., 1967, pp. 201-213.

Consideration of the numerical calculation of equilibrium states of elastic bodies under large deformation, where the governing differential equations are nonlinear. Newton's iterative method is modified by a reparametrization scheme which makes it possible to obtain a global solution in problems where buckling occurs. The method is applied to the problem of the buckling of a shallow clamped spherical shell under uniform pressure.

5612 Ponter, A. R. S.: "Convexity Conditions and Energy Theorems for Time Dependent Materials," J. Mech. Phys. Solids, Vol. 16, 1968, pp. 283-288.

Global convexity conditions, corresponding to the convexity of strain energy and complementary energy of classical elasticity, are derived for history dependent time independent materials. Energy theorems, which provide generalizations of the elastic theorems, are discussed.

5613 Halpin, J. C.; Thomas, R. L.: "Ribbon Reinforcement of Composites," J. Composite Materials, Vol. 2, October 1968.

A clear demonstration of the potential of ribbon shaped reinforcements in composite materials applications is presented. From a micromechanics analysis, supported by experimental results, we find that ribbon reinforcement offers superior stiffness properties in the plane of the lamina. The macromechanics analysis introduces the concept of a hybrid composite in which the engineer may combine the outstanding strength properties of fibers with the superior stiffness properties offered by ribbon reinforcements. It is pointed out that the low strength observed for glass-ribbon composites is a consequence of fabrication procedures and does not correspond to the theoretical limiting strength of ribbon reinforcements.

5614 Knops, R. J.; Payne, L. E.: "Stability in Linear Elasticity," International Journal of Solids and Structures, Vol. 4, No. 12, December 1968, pp. 1233-1242.

Conditions are established ensuring the continuous dependence on the initial data of the equilibrium solution and certain other classes of solution to the elastodynamic initial boundary value problem. The method of proof depends upon logarithmic convexity arguments and is notable for the abscence of any definiteness condition on the elasticities. In some cases the conclusions reached differ from corresponding ones derived according to classical Lyapounov stability theory and examples are given to illustrate this difference.

5615 Stricklin, James A.: "Integration of Area Coordinates in Matrix Structural Analysis," AIAA Journal, Vol. 6, No. 10, October 1968.

5616 Huet, C.: "Representation of Complex Moduli and Compliances in Complex Arithmetic and Logarithmic Planes," Cahiers du Gpe. Francais de Rhéol., Vol. 1, 1967, pp. 237-258, (in French).

A theoretical paper treating linear visco-elastic bodies, but with a final section showing the theory applied to bitumens and elastomers. Terms are defined and a description is given of the Cole-Cole (arithmetic) and Black (logarithmic) complex planes. Numerous illustrated tables show how the representation may be applied to various model systems. Temperature effects are also considered.

5617 Canter, Nathan H.: "Viscoelasticity of a Butadiene-Styrene Block Copolymer," J. Polym. Sci., Part A2, Vol. 6, 1968, pp. 155-163.

Transitions in a butadiene-styrene block copolymer have been studied by differential thermal analysis and also by observing variations in the torsional modulus with temperature. The upper transition is broad but becomes sharper for samples which have been stress-relaxed at high elongation before torsional testing. The results suggest that chain segments in the copolymer aggregate in the solid state and that stretching of the bulk material enhances aggregation of the styrene chain segments.

5618 Halpin, J. C.: "Introduction to Viscoelasticity," Composite Materials Workshop: Proceedings of the Summer Workshop on the Physical Aspects of Composite Materials, Washington University, St. Louis, Mo., July 13-21, 1967, ed. S. W. Tsai, J. C. Halpin, N. J. Pagano, (Progress in Materials Science Series, Vol. 1), 1967, pp. 87-152.

Discussion of those phenomenological aspects of the mechanical properties of solids which are of general applicability for the study of composite systems. The framework of continuum mechanics is used to consider the forces on, and the changes of shape in a typical infinitesimal volume element of both an isotropic and an anisotropic body. A method of modifying the constitutive equations of elasticity theory to include time effects is discussed, and the resulting relationships between surface forces, surface displacements, and time for solids are derived. A discussion is given of the treatments available for the nonlinear behavior suitable for rigid composite materials. An approach is outlined which leads to a linear integral equation for the treatment of boundary-value problems for materials which are approximated by the constitutive equations.

5619 Tuijnman, C. A. F.; Kruyer, S.; Zwietering, Th. N.: "On the Calculation of Limiting Quantities of Linear Viscoelastic Materials from Dynamic Measurements," Fifth International Congress on Rheology, Kyoto, Japan, 1968.

It is well known that the retardation or relaxation behaviour of a viscoelastic material is strongly revealed by the frequency-dependence of the ratio of the steady-state output to the input amplitude for pure sinusoidal stimuli applied to the material. This ratio is a complex function of the real radial frequency ω and may be, e.g. the complex dielectric constant $\varepsilon^*(\omega)$ or the dynamic compliance. The behaviour of $\varepsilon^*(\omega)$ is reflected in the shape of the curves obtained when the real and imaginary parts of ε^*, denoted by $\varepsilon'(\omega)$ and $\varepsilon''(\omega)$ resp., are plotted versus log ω. Such curves give a more direct picture of a dispersion in the dynamic response than those obtained from complex plane plots. The latter plots are still widely used, especially because the extrapolations necessary for obtaining the limiting quantities $\varepsilon'(\omega = 0)$ and $\varepsilon'(\omega = \infty)$ are relatively easy to make. In many cases, however, the values of limiting quantities obtained in this way are rather inaccurate, which need not be the case when the function $\varepsilon''(\omega)$ itself is used as a starting point.

In this paper it is shown that analytical expressions can be found describing satisfactorily the $\varepsilon''(\omega)$ curves, even complicated ones, met with in practice. After substitution in the Kronig-Kramers integral equation and solving for $[\varepsilon'(\omega) - \varepsilon'(\infty)]$, this calculated function $[\varepsilon'(\omega)-\varepsilon'(\infty)]$ is compared with the experimental $\varepsilon'(\omega)$ curve.

5620 Bozhinov, G. M.: "Viscoelastic Behaviour of Complex Mechanical Systems," Fifth International Congress on Rheology, Kyoto, Japan, 1968.

The linear viscoelastic behaviour of certain classes of materials is considered using the simplest methods of theoretical rheology. The basic physical equation is represented by an n-order differential equation and a corresponding rheological model is assumed as a complex mechanical system formed by a terminal number of elements.

Both creep and relaxation phenomena are analyzed on the basis of the above mentioned equation. For some particular cases corresponding differential equations are solved.

Special attention is drawn towards some characteristics of model behaviour, which are result of the model structure itself as well as of the interrelation between the components of the mechanical system.

A method to define the initial terms is described and a second order differential equation is solved as an application.

5621 Gromov, V. G.: "Volterra Operator Algebra and its Application to Viscoelasticity Problems," Akademiia Nauk SSSR, Doklady, Vol. 182, Sept. 1, 1968, pp. 56-59, (in Russian).

Demonstration that the construction of a Volterra operator algebra for boundary-value problems involving linear viscoelasticity with a continuous relaxation time and continuous delay time spectra is not restricted to special forms of Volterra operators but is realizable for any initial resolvent operators. A theorem generalizing the Robotnov theorem (1948) concerning the multiplication of operators with fractionally exponential kernels is formulated and proved. Several theorems are derived from this theorem to facilitate the construction of a theory of anisotropic viscoelastic media. A class of resolvent operator functions which permit a simple realization of a Volterra algebra is indicated.

5622 Ting, T. C. T.: "A Mixed Boundary Value Problem in Viscoelasticity with Time-Dependent Boundary Regions," Stanford University, Department of Applied Mechanics, Technical Report No. 191, October 1968.

A correspondence principle of linear viscoelasticity theory for mixed boundary value problems with time-dependent boundary regions was studied by Graham in which the associated elastic solutions are required to satisfy certain restricted conditions. In this paper a generalized correspondence principle is given in which no restrictions are imposed on the associated elastic solutions. The results can be extended to thermo-rheologically simple viscoelastic media if the temperature field is either purely position-dependent or purely time-dependent.

5623 Sneddon, I. N.; Ejike, B. C. O.: "The Stress Intensity Factors for a Griffith Crack Whose Surfaces are Loaded Asymmetrically," North Carolina State University, Applied Mathematics Research Group, April 24, 1968.

Formulae for the calculation of the stress intensity factors at the tip of a Griffith crack and for the normal component of the surface displacement are derived for a crack whose surfaces are subjected to completely arbitrary surface tractions.

SEE ABSTRACTS 5560, 5590

4.3 Nonlinear Elastic Analysis

5624 Sherbourne, A. N.; Krishnasamy, S.: "Moment-Curvature Models under Reverse Cyclic Straining," Experimental Mechanics, January 1969, pp. 36-40.

The paper describes the development of M-ϕ models from stress-strain curves resulting from tests on axially loaded mild-steel specimens subjected to cyclic alternating plastic strains. These 'push-pull' tests lead to the formulation of a power law which can be used to predict the nonlinear response of sections in bending under similar ambient conditions. These predictions are compared with experiments on beams subjected to pure bending involving strain control. The resulting load-deflection curves, derived directly from experimental M-ϕ models and indirectly from theoretical M-ϕ models arising from stress-strain data, are themselves compared with similar experimental data in the case of cantilever beams under tip loads.

4.4 Nonlinear Viscoelastic Analysis

5625 Distéfano, J. N.; Sackman, J. L.: "On the Stability of an Initially Imperfect Nonlinearly Viscoelastic Column," International Journal of Solids and Structures, Vol. 4, No. 3, March 1968, pp. 341-354.

The stability of an initially imperfect, simply-supported, H-section beam-column, subjected to an axial compressive load, is investigated. The material of the column is taken to behave as a general nonlinear viscoelastic solid with a constitutive relation represented by a Volterra-Fréchet functional polynomial. Conditions sufficient to assure instantaneous, short term and long term stability are established. It is shown that a complete knowledge of the material creep functions is not required in order to determine stability conditions. A program of experiments to characterize the material for stability studies is presented.

5626 Ting, E. C.: "Nonlinear Viscoelastic Stress Analysis with Small Dilatational Changes," Stanford University, Department of Applied Mechanics, Technical Report No. 189, September 1968.

A derivation is given of the nonlinear stress constitutive equation for viscoelastic materials with small dilatational changes. This particular derivation results in a form for the constitutive equations which is suitable for application in solving boundary value problems. The resulting equations are applied to obtain the quasi-static solution for a pressurized viscoelastic hollow cylinder bonded to an elastic casing. The inner boundary of the cylinder is assumed to be ablating and hence time-dependent. The problem is solved for linear and nonlinear, both incompressible and compressible, materials. For linear problems, both analytical and numerical solutions are obtained. For nonlinear problems, numerical solutions are evaluated by using finite difference techniques and assuming particular forms of kernel functions in the constitutive equation. The linear and nonlinear results are compared. The effects due to the material nonlinearity and compressibility are discussed.

5627 Eargle, George Marvin: "A Nonlinear Integro-Differential Equation Associated with a Class of Wedge Problems," North Carolina State University, Applied Mathematics Research Group, May 1968.

The Mellin integral transform is used to investigate the displacement near the vertex of an infinite, isotropic, elastic wedge in a state of plane stress under mixed boundary conditions. Normal stresses are prescribed near the vertex and normal displacements are assumed to be zero elsewhere along the boundary.

A nonlinear integro-differential equation is derived in which the unknown function is related to the desired displacement. This and a related nonlinear algebraic system are analyzed. Methods are developed to compute the solution for the special case of the wedge of vertex angle π . These methods are extended to a more general wedge and an example of the more general computation is given.

5628 Findley, W. N.; Stanley, C. A.: "Nonlinear Combined Stress Creep Experiments on Rigid Polyurethane Foam with Application to Multiple Integral and Modified Superposition Theory," Journal of Materials, JMLSA, Vol. 3, No. 4, Dec. 1968, pp. 916-949.

This investigation employs a multiple integral relationship as the constitutive equation for creep of nonlinear viscoelastic materials under stress. By retaining stress terms up to the third order, the constants for the multiple integral representation of constant tension and torsion were determined from seven creep tests under constant stress; two pure tension tests at different stresses, a compression test, two pure torsion tests at different stresses, and two combined tension and torsion tests at different stresses. Experiments included 20 combinations of constant tension and torsion on a single tubular specimen of polyurethane foam. Recovery following each experiment was nearly complete. The time-independent strain was found to be nearly linear, while the time-dependent strain was nonlinear for all stresses. Agreement between the multiple integral representation and experimental results for constant stress was very satisfactory.

Experiments included abrupt changes in stress. These results were compared with the prediction of a modified Boltzmann superposition principle. The agreement was reasonably satisfactory for all except experiments in which tensile stress was removed during shearing recovery. An observed synergistic effect was not predicted under this condition.

5629 Weber, Jean-Daniel: "Concerning the Properties of a Class of Nonlinear Viscoelastic Bodies with Hidden Parameters," Académie des Sciences (Paris), Comptes Rendus, Série A - Sciences Mathématique, Vol. 267, No. 16, October 14, 1968, pp. 565-568, (in French).

Definition of a class of nonlinear viscoelastic bodies which arise in the study of three-dimensional rheological models. These bodies have hidden parameters which behave according to a law which is compatible with the objectivity principle and the second principle of thermodynamics. The uniqueness of the deformations of these bodies in quasi-static and dynamic problems is treated.

5630 DeSilva, Carl N.; Kline, Kenneth A.: "Nonlinear Constitutive Equations for Directed Visco-Elastic Materials with Memory," Zeitschrift fuer angewandte Mathematik und Physik, Vol. 19, Jan. 25, 1968, pp. 128-139.

Development of nonlinear constitutive equations relating to the basic field equations and boundary conditions for a directed visco-elastic material with memory. These equations relate the double stress, double force, and stress tensor to certain kinematical measures felt to be appropriate for the theory. A brief review is given of the kinematics and governing equations related to the theory of a continuum with directors.

5631 McGuirt, C. W.; Lianis, G.: "Experimental Investigation of Non-Linear Viscoelasticity with Variable Histories," Fifth International Congress on Rheology, Kyoto, Japan, 1968.

In this paper more complicated time-dependent deformation fields are investigated. Theoretical expressions are developed for the two-step uniaxial history, the two-step equal biaxial history, the equal biaxial constant stretch-rate loading and unloading histories, the strip biaxial single-step history, and the strip biaxial constant stretch-rate loading and unloading histories. The stress histories for the above strain histories have been found through a 1620 IBM Computer.

These histories of deformation have been reproduced experimentally in an electronically controlled hydraulic loading unit. The specimen was enclosed in an environmental chamber in which the temperature and humidity were accurately controlled. The deformation history was programmed on a function generator while the stress history was recorded on a photographic recorder. A special relaxometer was designed for uniform biaxial strain.

4.5 General Time-Dependent Analysis

5632 Coleman, B. D.: "On the Use of Symmetry to Simplify the Constitutive Equations of Isotropic Materials with Memory," Royal Society (London), Proceedings, Series A, Vol. 306, Sept. 24, 1968, pp. 449-476.

This paper is concerned with general, compressible, isotropic materials, solid or fluid, characterized by functionals which give the stresses when the history of the strain is specified. It is shown that for certain broad classes of motions the requirements of material symmetry and frame indifference greatly simplify the form of constitutive equations. These simplefications are derived without invoking integral expansions or other special hypotheses of smoothness for material response. Among the motions considered in detail are those which are locally eqyivalent to pure extensions and sheared extensions.

4.6 Heat Conduction Analysis

5633 Walter, Wolfgang: "Heat Conduction in Systems with Several Components," Numerical Mathematics: Theory of Approximation of Differential Equations, ed. L. Collatz, G. Meinardus, H. Unger, 1968, pp. 177-185,(in German).

Investigation of heat conduction in a body consisting of two different materials. Two boundary conditions exist, an external condition against the environment and an internal condition between the two materials. Statements are proven for parabolic differential inequalities pertaining to the problem. The applied methods permit an essentially more general consideration of the problem, in terms of nonlinear differential equations, boundary conditions, and multiple components.

5634 Norwood, Frederick R.: "On Thermal Conductivities," Journal of Composite Materials, Vol. 2, Oct. 1968.

Comments on Behrens (1968) paper, in which a 'method of long waves' is used to determine the thermal conductivity of composite materials. It is recommended that this method not be used, because the equations treated in the paper do not admit propagating waves. The author answers that the use of the term 'wave' in his paper is admittedly unusual, since it implies that a 'wave' is not necessarily a time harmonic function.

5635 Ivanov, V. V.; Furman, A. V.: "On an Approximate Method of Solution of Nonlinear Heat-Conduction Problems," Journal of Engineering Physics, Vol. 9, No. 5, Nov. 1965, pp. 378-379.

An approximate method is presented for the solution of problems of transient heat conduction in solids with thermal conductivity and specific heat linearly dependent on temperature.

5636 Davis, Charles Alfred: "Boundary Value Problems for Wedges and Cones under Heat Conduction," North Carolina State University, Applied Mathematics Research Group, May 9, 1968.

Mellin integral transforms and the Wiener-Hopf techniques are used to obtain the temperature distribution in a semi-infinite wedge in which the temperature is specified on the boundary near the vertex and the remaining portion of the boundary is assumed to be insulated. Results are obtained in terms of infinite integrals.

Several boundary value problems are considered for the semi-infinite cone. First, the temperature distribution is obtained for the problem where a constant temperature is specified for the portion of the surface of the cone near the vertex and the remaining surface is at zero temperature. Next, the problem is considered where a temperature, dependent only upon the radial distance r, is specified on the boundary. This latter problem was for the half space or cone of angle $\pi/2$ and was solved using the Legendre transform of odd order.

Finally, the mixed boundary value problem for the cone, analogous to that of the wedge above, is considered with the method of solution including the Mellin integral transform and the Wiener-Hopf technique. The results for the cone of general angle, $0 < \alpha < \pi$, is in the form of an inversion integral. The temperature distribution is obtained as a residue series for the special case of $\alpha = \pi/2$.

4.7 Thermal Stress Analysis

5637 Steffens, Ed.: "Thermal Analysis by a Constant Heat Flow," Journal of Applied Polymer Science, Vol. 12, 1968, pp. 2317-2324.

A new method of and apparatus for thermal analysis is described, whereby the heat flow fed by the oven to the sample is kept constant as a function of time. The measurement gives the change of enthalpy in heating or cooling the sample. From this enthalpy-temperature relationship quantitative thermodynamic results are easily obtained. Transitions of first and second order in polymers can be measured in one run.

5638 Samoilovich, Yu. A.: "A Simplified Solution of the Problem of Elastoplastic Equilibrium of a Cylinder in a Nonuniform Temperature Field," Journal of Engineering Physics, Vol. 9, No. 5, November 1965, pp. 380-382.

A solution is given of the problem of thermal stresses in a solid circular cylinder, allowing for compressibility of the material and the Mises plasticity condition. It is shown that the radial and annular stresses are determined by simplified formulas with sufficient accuracy for engineering purposes.

5639 Weber, John Walter: "The Application of Characteristic Functions to Some Plane Problems in Thermoelasticity," Colorado University, Boulder, Ph. D. Thesis, 1967.

This thesis presents the application of characteristic functions to the solution of thermal stresses in a sector of a plane circle. The heat generated is independent of time and a function of the radial coordinate only. Two temperature distributions are investigated. Stresses for sectors of 20°, 40°, 60°, 80°, 90°, 120°, 150°, and 180° are also investigated. Maximum stresses and their locations are presented.

5640 Das, Bikas Ranjan: "Thermal Stresses in a Long Cylinder Containing a Penny-Shaped Crack," International Journal of Engineering Science, Vol. 6, Sept. 1968, pp. 497-516.

Analysis of the state of stress in a long circular cylinder of elastic material, when the inner surfaces of a concentric penny-shaped crack are subjected to a prescribed temperature distribution. The plane of the crack is perpendicular to the axis of the cylinder. By making a suitable representation of the temperature function, the heat-conduction problem is reduced to the solution of a Fredholm integral equation of the second kind. Then, using a suitable biharmonic function as the potential of thermoelastic displacements, the problem is reduced to the solution of a similar Fredholm integral equation, in which the solution of the earlier integral equation arising from the heat-conduction problem occurs as a known function. Iterative solutions of the integral equations are found which are valid for a certain chosen value of the ratio of the radius of the crack to that of the cylinder. The integral equations are also solved numerically by using a high-speed computer with the same value of the ratio. The stress intensity factor is calculated for both of these solutions, and the results are found to be in complete agreement.

5641 Oganov, E. P.; Siniukov, A. M.: "Thermal Stresses in an Inhomogeneous Cylinder of Finite Length," Mekhanika Polimerov, Vol. 4, July-Aug. 1968, pp. 710-715, (in Russian).

Development of an analytical method for calculating thermal stresses in circular cylindrical shells. A solution, obtained by the collocation method takes account not only of the finiteness of the cylinder but also any inhomogeneity it might contain. In particular, such an inhomogeneity may be caused by the effect of temperature on mechanical constants of the material, which is typical of polymers subjected to the influence of negative temperatures. The method is applied to the calculation of the stresses in a finite cylindrical shell with a variable modulus of elasticity.

5642 Sekiya, Tsuyoshi; Sumi, Seinosuke; Okamoto, Masaaki: "Analysis of Plane Thermoelastic Problem in Symmetrical Region under Asymmetrical Temperature Distribution by Mechanical Analog Procedure," Japan National Congress for Applied Mechanics, 16th, University of Tokyo, Japan, October 19, 20, 1966, Proceedings, 1968, pp. 96-108.

Description of a mechanical analog procedure for solving two-dimensional thermoelastic problems in a doubly connected symmetrical region with arbitrary (asymmetrical, in general) temperature distribution. The distribution of the thermal stress is obtained for a square region with a circular hole or a slot-shapedhole with an antisymmetrical temperature distribution. In order to assure the accuracy of the present method, a comparison between the experimental results obtained by this method and the theoretical ones is made for a circular region with a concentric circular hole.

5643 Gogotsi, G. A.: "Investigation of the Thermal Stability of Brittle Materials," Poroshkovaia Metallurgiia, Vol. 7, Dec. 1967, pp. 58-63, (in Russian).

Investigation of sensors (in the form of circular metallic strips) devised to determine the moments of fracture of brittle samples (the critical thermal gradients in the samples), as a means of testing the thermal stability of the samples. A method for investigating the behavior of the sensors under various applied thermal loads is proposed, together with recommendations regarding the proper practical utilization of the sensors.

5644 Mahalanabis, Ranjit Kumar: "Thermal Stresses in an Elastic Cylinder," Journal of Science and Engineering Research, Vol. 11, Jan. 1967, pp. 120-131.

The paper deals with the evaluation of thermal stresses in an elastic cylinder due to mixed thermal boundary conditions on its outer surface. The temperature and stresses are expresses in terms of the solution of a Fredholm integral equation of the second kind.

5645 Dhaliwal, R. S.; Chowdhury, K. L.: "Dynamical Problems of Thermoelasticity for Cylindrical Regions," Archiwum Mechaniki Stosowanej, Vol. 20, No. 1, 1968, pp. 47-66.

Study of the problems of thermoelasticity for an infinitely long cylinder and an infinite medium with a cylindrical hole. The medium is assumed to be undisturbed and initially at zero temperature. The inertial terms are included in the equations of motion. The solution is developed by the method of the variation of parameters and by Laplace transforms.

5646 Olesiak, Zbigniew: "Plastic Zone Due to Thermal Stress in an Infinite Solid Containing a Penny-Shaped Crack," International Journal of Engineering Science, Vol. 6, May 1968, pp. 113-125.

Dugdale's model is employed to find the width of the plastic zone surrounding a crack which is being opened by the application of a flux of heat or temperature acting on crack surfaces. It is shown that the ratio of the crack diameter to the diameter of the plastic zone varies depending on the initial diameter of the crack, material constants, and the ratio of the flux of heat to the yield limit of the material. The pertinent formulas for the components of the displacement vector have been derived for a constant flux and for a flux which is a function of radius represented in the form of a Fourier-Bessel series. The case of the precribed temperature is reduced to the case of the given flux of heat.

SEE ABSTRACT 5741

4.8 Wave Propagation Analysis

5647 Tokuoka, Tatsuo; Iwashimizu, Yukio: "Acoustical Birefringence of Ultrasonic Waves in Deformed Isotropic Elastic Materials," International Journal of Solids and Structures, Vol. 4, No. 3, March 1968, pp. 383-390.

The basic relations of the acoustoelasticity are deduced by means of the infinitesimal wave propagation in a deformed isotropic elastic material. The propagation equation is characterised by the acoustical tensor. This results in the three polarization directions, which are perpendicular to each other and, in general, do not coincide with the principal axes of the stress. When the propagation direction coincides with one of the principal axes of the stress, the former are identical to the latter and the so-called stress-acoustical law holds, which denotes that the magnitude of the acoustical birefringence is proportional to the difference of the secondary principal stresses.

5648 Bell, J. F.: "Large Deformation Dynamic Plasticity at an Elastic-Plastic Interface," Journal of the Mechanics and Physics of Solids, Vol. 16, No. 5, September 1968, pp. 295-313.

The diffraction grating measurements of finite strain nonlinear wave fronts are described for elastic-plastic interface experiments. Close agreement with theoretical prediction on both sides of the interface is shown to exist when the nonviscous finite deformation parabolic stress-strain function for annealed polycrystalline aluminium is introduced into the finite amplitude wave theory of Taylor, von Karman, and Rakhmatulin, and into the nonlinear unloading wave theory of Lee. Dynamic studies of interface lubrication, of Pochhammer-Chree oscillations in the hard bar, and of variations in the mode of unloading are included providing detailed experimental correlation with theory under these varied conditions. Diffraction grating surface-angle measurements in the elastic-plastic interface experiment are shown to provide a detailed demonstration that the nonlinear finite amplitude wave fronts are one-dimensional extending across the entire specimen diameter. These measurements also have demonstrated experimentally that finite amplitude wave propagation in dynamic plasticity is an incompressible distortional deformation.

5649 Bushnell, J. C.; McCloskey, D. J.: "Thermoelastic Stress Production in Solids," Journal of Applied Physics, Vol. 39, No. 12, November 1968.

Theoretical calculation of the consequences of the thermoelastic mechanism for production of stress in solids by pulsed energy input have been performed, and the effect of variations in the acoustic impedance of a transparent backup material and variations in the pulse duration as compared to the acoustic transit time across the penetration depth of the incident energy have been investigated. Experimental verification of the theoretical calculations has been done using a Q-switched ruby laser as an energy source with samples of absorbing glass as targets. It is found that the experimental results give good agreement in the shapes of the stress pulses produced, and fair agreement in the absolute amplitude of the stress, with no adjustable parameters being required. The calculations and experiments demonstrate the validity of the thermoelastic stress-production mechanism in solids when no phase transformation occurs.

5650 Dzygadlo, Z.; Kaliski, S.: "Instability Limits of Parametric Self-Excited Vibrations of Elastic and Aeroelastic Systems with Travelling Waves," Archiwum Mechaniki Stosowanej, Vol. 20, NO. 4, 1968, pp. 461-471.

Investigation of the parametric vibrations of self-excited mechanical systems with a traveling wave on the basis of examples involving an infinitely long plate in gas flow and a system of oscillators moving over an infinite beam. Relationships valid for nonstationary vibrations are used which make it possible to determine the boundaries of the regions of unstable vibration for velocities smaller and larger than the critical values. It is shown that quasi-periodic vibrations at the boundary of the regions of unstable vibration arise for flow velocities and oscillator motion larger than zero; periodic vibrations at the boundaries of these regions can arise only for velocities equal to zero.

5651 Bell, James F.: "An Experimental Study of Instability Phenomena in the Initiation of Plastic Waves in Long Rods," Mechanical Behavior of Materials under Dynamic Loads, Proceedings of a Symposium, San Antonio, Tex., September 6-8, 1967, ed. U. S. Lindholm, 1968, pp. 10-20.

A series of experiments are considered for stress-time histories at the impact face for wave propagation in long rods. From the data it is shown that the finite deformation mode and transition stability structure of the author's generalized parabolic stress-strain function is important in the problem of finite amplitude nonlinear wave initiation and growth at the impact face and in the three-dimensional first diameter when considering the symmetrical free-flight impact of identical long cylindrical rods.

5652 Reddy, Damoder Pati: "Propagation of Waves of Finite Strain in Elastic and Viscoelastic Solids," Northwestern Univ., Evanston, Ill., Ph. D. Thesis, 1967.

The propagation of one dimensional waves of finite strain in a semi-infinite elastic rod and in elastic and viscoelastic half spaces is studied. The material of the rod and the half space is incompressible. In each of the problems studied the transient wave motion is generated by a time dependent distrubance at the free boundary of the semi-infinite medium. The semi-infinite rod is subjected to a monotonically increasing longitudinal disturbance at its free end. An implicit solution for the wave motion in the region of simple waves is obtained by the method of characteristics. Conditions for shock formation are established. By employing the theory of propagating surfaces of discontinuity, an alternate and explicit solution in this region is obtained as a Taylor expansion about the time of arrival of the wave front.

5653 Sackman, J. L.; Kaya, I.: "On the Propagation of Transient Pulses in Linearly Viscoelastic Media," Journal of the Mechanics and Physics of Solids, Vol. 16, Sept. 1968, pp. 349-356.

A general procedure is developed for predicting the way in which transient pulses propagate through an arbitrary, linearly viscoelastic medium characterized by creep or stress relaxation functions. By use of the Laplace transform, different operations in transform space, and some asymptotic methods, the boundary-value in question is reformulated in terms of a Volterra integral equation, with the space variable playing the role of a parameter. This equation is readily resolved numerically, and results obtained by this procedure compare very well with solutions avaiblable in the literature.

5654 Liu, C. K.; Chang, C. H.: "Wave Propagation in Hollow Elastic Cylinders with End Constraints," Developments in Mechanics Vol. 3, 9th Midwestern Mechanics Conf., University of Wisconsin, Madison, Ws., Aug. 16-18, 1965, Proceedings, Part II, Dynamics and Fluid Mechanics, ed. T.C. Huang; M. W. Johnson, Jr., 1967, pp. 203-214.

Solution for the dynamic displacements (and stresses) in a thickwalled finite elastic cylinder, which is subjected to an internal blast-loading. The ends of the cylinder are well lubricated, but they are prevented from axial movement. The analysis has applications to some rocket-motor thrust chamber components, which are to withstand the transient loading of thrust buildup without interference with gimbaling.

5655 Tsai, Y. M.; Kolsky, H.: "Surface Wave Propagation for Linear Viscoelastic Solids," Journal of the Mechanics and Physics of Solids, Vol. 16, March 1968, pp. 99-109

(See Abstract 4686).

5656 Waterston, Robin J.: "One-Dimensional Evolutionary Discontinuities in Compressible Elastic Materials," Institute of Mathematics and Its Applications, Journal, Vol. 4, March 1968, pp. 58-77.

The paper analyses the one-dimensional discontinuities which can propagate in both isotropic and transversely isotropic compressible elastic materials and determine conditions for them to be evolutionary. It is found that for quasi-dilatational shocks, the evolutionary condition is equivalent to the entropy condition. This is true also for the circular discontinuities, which can propagate in isotropic materials only, except in the special case of the 180° circular discontinuity. However, in the case of quasi-transverse shocks, the evolutionary condition imposes conditions beyond those required by the entropy condition. We obtain results on how these waves propagate by considering the problem of an elastic half-space initially at rest, to whose surface is suddenly applied a uniform stress field.

5657 Tsai, Y. M.: "A Note on the Surface Waves Produced by Hertzian Impact," Journal of the Mechanics and Physics of Solids, Vol. 16, March 1968, pp. 133-136.

Calculation of the surface wave produced by Hertzian impact (where a sphere impinges on a half-space and an axisymmetrical wave is propagated over the free surface), by considering the variation of the normal stress and the area of contact with respect ot time. The predicted pulse shapes at four different distances from the center of the contact area were found to be in reasonable agreement with those determined experimentally.

5658 Dally, J. W.; Riley, W. F.: "Stress Wave Propagation in a Half Plane Due to a Transient Point Load," Developments in Theoretical and Applied Mechanics, 3rd Southeastern Conference on Theoretical and Applied Mechanics, University of South Carolina, Columbia, S. C., March 31-April 1, 1966, Proceedings, ed. W. A. Shaw, 1967, pp. 357-377.

Stress wave propagation in a half space, loaded at an interior point by a symmetric transient pressure pulse, was investigated by employing dynamic photoelasticity. A multiple spark gap camera was used to record the dynamic fringe patterns in the Columbia Resin (CR-39) model. The formation and development of the waves were analyzed before, during, and after their reflection from the free boundary. The dynamic fringe patterns were interpreted to provide data on the individual values of the principal stresses associated with the purely dilatational and purely distortional waves. Also a method was introduced to obtain dynamic displacements from dynamic fringe patterns.

5659 Grot, R. A.: "Relativistic Theory of the Propagation of Wave Fronts in Nonlinear Elastic Materials," International Journal of Engineering Science, Vol. 6, No. 5, June 1968, pp. 295-307.

Development of a relativistic theory of the propagation of a second-order singular surfaces in elastic-materials. Relations generalizing the classical results of nonlinear elasticity for the existence of wave fronts are derived. Specific results of the wave velocity propagating along a principal direction for isotropic materials are given.

SEE ABSTRACTS 5566, 5667

4.9 General Dynamic Analysis

5660 Hlavacek, B.; Kotrba, V.: "Numerical Iteration for the Calculation of Relaxation Spectra from Dynamical Measurements," Rheol. Acta, Vol. 6, 1967, pp. 288-294, (in German).

A method for calculation of the relaxation spectrum of a linear viscoelastic material from dynamic measurements is presented. The method is iterative, based on an iterative method of Roesler and Twyman for the solution of an integral equation. The initial approximation for the process is taken to be third approximation of Steverman and Schwarzl. The method enables the calculation to be done using measurements over a much smaller frequency range than would be required by the method of Roesler and Twyman, and compared with the method of Steverman and Schwarzl it has a greater power for resolving discrete relaxation times.

5661 Riddell, M. N.; O'Toole, J. L.: "Engineering Properties of Glass Reinforced Thermoplastics," Modern Plast., Vol. 45, No. 9, 1968.

The paper describes the torsion pendulum and drop weight impact tests as tools for investigating the rheology of glass reinforced thermoplastics and gives results, obtained for such materials, of creep, creep-rupture behaviour, and tensile and shear moduli.

5662 Toebes, Gerrit H.; Ramamurthy, Amruther S.: "Fluid Elastic Forces on Circular Cylinders," Jounral of the Enineering Mechanics Division, ASCE, Vol. 93, No. EM6, December 1967, pp. 1-20.

The fluidelastic behavior of a circular cylinder was studied. It is argued that improved empirical data on cylinders exposed to fluid flow are needed, and that it is better to impose cylinder motions and to measure the resultant fluid lift forces than to study the fluidelastic response directly. Accordingly, lift force data were collected, yielding direct evidence of fluidelastic force amplification and outline limits to the energy that may be extracted from the fluid flow and channeled into sustaining the more serious flow-induced vibrations. The application of fluid lift data at the design stage of cylindrical structures is most feasible when it comes to the question of trade-off between permissible amplitude and the damping to be provided. Use of lift force data in computing the complete structrual response is shown to be more problematic.

5663 Gruntfest, I. J.; Mueller, G. E.: "Transient in Model Viscoelastic Materials," Transactions of the Society of Rheology, Vol. 12, No. 3, 1968, pp. 469-478.

The dynamic behavior of a homogeneous slab subjected to a short pressure pulse on one face is explored from a simple rheological point of view. The analysis is one dimensional, but involves two strain modes in the material. The early response is shown to be controlled by the bulk viscosity which influences the distortion and attenuation of propagating disturbances. In particular, the peak stress at interior points is shown to be very sensitive to the duration of the pressure. This result is quite different from that usually applied in the analysis of impact data in which it is assumed that the controlling differential equations are hyperbolic and that the density pressure relation is not time dependent. It is also more compatible with some of the experimental results. Criteria for mechanical similarity are described which may be useful in the design and development of systems subjected to impacts. The uniaxial deformation generated in this type of experiment is contrasted with the uniaxial load condition generated in the usual tensile tendency toward strain homogeneity and strain stability can also be greatly enhanced. This is likely to be relevant to the understanding of material-forming processes.

5664 Bueche, F.; Tokcan, Güngör: "Range of Validity of the DTO Model," 39th Annual Meeting, The Society of Rheology, Inc., January 13 - 15, 1969.

Tobolsky and associates have pointed out that the dynamics of polymer molecules may be interpretable in terms of damped torsional oscillations (DTO) rather than by the conventional (Rouse-Bueche) entropic spring and intermolecular viscous friction factor, f. We have tested this supposition by measurement of the energy of activation for the alpha dipole resonance dispersion (E_d) and for viscous flow (E_v) for poly p-chlorostyrene solutions in the range of temperatures and concentrations -80 <T <40°C, 0.14< c <0.55 gm/cm^3 in toluene and chlorobenzene. For a hypothetical gaseous molecule, the damping factor, f, must by necessity correspond to that of the DTO model. In a glass, one suspects f to be intermolecular in origin. To find the transition point, we note that E_d/E_v should be about unity for the polymer used here if the RB model applies for f. As the matrix in which the polymer molecule is embedded becomes more fluid, the DTO model should become correct and $E_d/E_v>1$. Our experimental results find the transition occurs when $E_v \approx$ 13 kcal/mole. This is in the range where the system is already a rather 'slow' rubbery substance and the viscosity has started its rapid rise near the glass temperatue.

5665 Durelli, A. J.; Clark, J. A.; Kochev, A.: "Experimental Analysis of High Frequency Stress Waves in a Ring," The Catholic Universtiy of America, School of Engineering and Architecture, November 196?.

This paper deals with the photoelastic analysis of stress waves in a thick ring subjected to transient, high frequency loading. The device used to apply the loading is a piezo-electric transducer which initially produces four cycles of a 31.25 KHZ toneburst. The loading pulse can be reproduced with high precision. The ring is illuminated with a flash of approximately 0.5 microsecond duration which can be delayed in a continuously adjustable manner. Isochromatics and isoclinics and be directly observed as static patterns. Photoelastic data is supplemented by measurements obtained with a capacitance gage used as a dynamic lateral extensometer. Satisfactory agreement is found between tangential stresses near the free boundary of the ring determined from photoelastic data and those determined from capacitance gage measurements. As examples of complete determination of stress distributions, the separated principal stresses are obtained along an axis of symmetry and a vectorial representation of the principal stresses given. A wave interpretation of the data is developed and comparisons are made with available solutions of related problems.

5666 Reyhner, T. A.; Flügge-Lotz, I.: "The Interaction of a Shock Wave with a Laminar Boundary Layer," International Journal of Non-Linear Mechanics, Vol. 3, No. 2, June 1968.

A finite-difference solution to the problem of the interaction between an impinging shock wave and the laminar boundary layer on a flat plate is presented. The boundary-layer equations are used to calculate the flow with the Prandtl-Meyer formula being used to determine the pressure. Two different methods for calculating the region of separated flow are discussed. Comparison between this theory and experimental results show good agreement. The effects of the viscosity and heat-conduction relationships on the calculated results are determined. Diagrams show the influence of the Mach number and the displacement thickness of the boundary layer at the start of the interaction on the pressure distribution. The insulated plate and the plate with given temperature are considered.

5667 Pal'mov, V. A.: "Propagation of Vibrations in a Nonlinear Dissipative Medium," Applied Mathematics and Mechanics, Vol. 31, No. 4, 1967.

of strain or high pressures. The differential equations are then hyperbolic quasi-linear partial differential equations, a necessary wider formulation is possible in terms of characteristic equations, and in general their nonlinearity makes possible the existence of continuous and discontinuous solutions. Thus, nonlinear stress waves can show discontinuities; these may be either smoothed when present initially or formed during propagation, and examples of both cases are given. The situations discussed include longitudinal stress waves in bars, plane irrotational stress waves, and spherical stress waves.

5668 Kovalenko, A. D.; Karnaukhov, V. G.; Tiuptia, V. I.: "Propagation of Waves in an Infinite Viscoelastic Medium with Allowance for Thermomechanical Coupling," Prikladnaia Mekhanika, Vol. 4, Sept. 1968, pp. 1-8, (in Russian).

Study of the propagation of plane waves in an infinite viscoelastic medium, taking into account the mutual effects of the deformation and temperature fields. The problem is solved in a linear approximation for the most general form of interrelations between the stresses, strains and temperature, without taking into account the temperature dependence of the thermophysical and mechanical properties of the medium. The formulas obtained permit an estimation of the effects of viscosity on the phase velocity and damping coefficient of viscoelastic and thermal waves within the entire frequency range.

5669 Ross, Bernard: "The Perforation of a Porous Medium Due to Projectile Impact," Experimental Mechanics, Vol. 8, November 1968, pp. 488-495.

Impact tests with freely falling and rifle-powered projectiles were performed on Styrofoam slabs. Particular attention was devoted to studying the mechanisms of penetration and perforation. All tests were carried out at normal incidence. Results of the tests indicate that for slab-thickness/penetrator-diameter ratios large enough to preclude fracture due to bending, a cylindrical, blunt-end penetrator was more effective in perforation than a corresponding penetrator with a conical end. A mathematical model was constructed and a theoretical analysis developed from which the minimum impact velocity for perforation can be obtained. The critical velocity was found to be a function of projectile mass and diameter, and slab thickness, shear strength, tensile strength, and elastic modulus.

5670 Najar, J.:"Simple Waves in Plane Flow of a Perfectly Plastic Material," Archiwum Mechaniki Stosowanej, Vol. 20, No. 4, 1968, pp. 445-459.

Investigation of the possibility of the existence of solutions in the form of simple waves for a system of equations describing the rapid plane flows of an ideally plastic material. The general form of such solutions is constructed. It is shown that the velocity field of a simple wave corresponds to a time sequence of rectilinear fans of slip lines for which the paths of the particles are straight lines. The forces of inertia caused by the nonstationary nature of the flow are balanced by the convection components of the forces of inertia. Necessary and sufficient conditions of existence and singularity are found for the simple-wave class of solutions of the Cauchy problem. An example is given in the form of a solution to a problem involving the plane flow of a perfectly plastic material in the neighborhood of the involute edge of the tooth of a gear wheel revolving at constant angular velocity.

5671 Ariaratnam, S. T.: "Dynamic Stability under Random Excitation," Canadian Congress of Applied Mechanics, Laval Uni., Quebec, Canada, May 22-26, 1967, Proceedings, ed. B. H. Karnopp, 1967, pp. 3-163.

Outline of a few typical problems concerning the stability of structural systems subjected to random loading. The presence of small nonlinearities in the parametrically excited systems does not seem to affect the stability conditions obtained using the first approximation. It may be necessary to go to higher approximations to bring out the significance of these terms and also to discover whether the spectrum of the excitation at other multiples and combinations of the natural frequencies influence the stability. On the problems of dynamic snapping, several restrictive assumptions have been made to obtain the results. An estimate of the range of validity can be made only if a numerical method could be developed for integrating the Fokker-Planck equation.

5672 Rogge, Thomas R.: "Stable Elastic Waves in Anisotropic Materials," Zeitschrift fuer Angewandte Mathematik und Physik, Vol. 19, Sept. 25, 1968, pp. 761-770.

Investigation of the wave structure for a moving load on the surface of an anisotropic material in plane strain for the case of stable wave propagation. Loads moving along a boundary at a speed greater than the wave speeds in the material are studied. The problem is considered as one of plane strain in either an infinite half-space or an infinite slab. It is shown that the wave structure for a moving load on the surface of an anisotropic material in plane strain is qualitatively the same as that for an isotropic material.

5673 Sih, G. C.; Loeber, J. F.: "Flexural Waves Scattering at a Through Crack in an Elastic Plate," Engineering Fracture Mechanics, Vol. 1, August 1968, pp. 369-378.

Study of the dynamic stress distribution caused by the flexural motion of an elastic plate containing a through crack. The diffraction of a plane flexural wave by a through-the-thickness crack in an elastic plate is examined by application of Mindlin's (1951) theory of flexural motions of plates. In this theory, which takes into account the rotatory inertia and shear effects, an incident flexural wave passing through the crack is scattered into three types of flexural waves. By combining the incident and scattered waves, the complete stress distribution around the crack can be calculated. However, in the applications of the theory of crack propagation, it is only necessary to determine the intensity of the moment distribution in a small region surrounding the crack tip. It is found that this intensity decreases as the circular frequency of the input wave is increased. In other words, the magnitude of the local bending stresses is always lower in the dynamic case than in the static case. A dynamic moment-intensity factor is defined, whose critical value may be used to determine the onset of crack extension in brittle materials. Moreover, the problem of a cracked plate vibrating at steady state is discussed.

5674 Simpson, A.; Tabarrok, B.: "On Kron's Eigenvalue Procedure and Related Methods of Frequency Analysis," Quarterly Journal of Mechanics and Applied Mathematics, Vol. 21, Feb. 1968, pp. 1-39.

The Kron Eigenvalue Method is discussed and developed in terms of receptances. The formulation, which is quite general, illustrates the fact that the receptance matrix of a composite system cannot be obtained directly, by standard matrix transformation alone, from the 'primitive receptance matrix' which comprises the receptance matrices of the subsystems into which the composite system is assumed (for the purposes of analysis) to be subdivided. However, it is shown that such transformation leads to a matrix of 'receptance denominators' which, when its determinant is taken and equated to zero, yields a valid frequency equation for the composite system. Kron's procedure is thereby vindicated. A numerical (iterative) method, based on Newton's Process, for the eigenvalues of composite systems is propounded. This obviates the necessity of 'fine-mesh frequency scanning' when applying the Kron Method. In this respect, it is felt that the suggested procedure progresses a long way toward placing Kron's Method on a par with standard methods of numerical eigenvalue analysis.

The present paper concerns the propagation of harmonic vibrations in a semi-infinite rod with nonlinear properties. The problem is solved on the basis of the harmonic linearization method.

The problem of the propagation of vibrations in nonlinear media is of great practical interest. One encounters it both in nonlinear acoustics and in nonlinear optics. Further the important effect of internal friction in materials is generally describable by means of nonlinear equations. In describing the dynamic properties of complex structures it is possible in many cases to approximate the structure by a continuous medium. The properties of this medium often turn out to be nonlinear. In both of these cases it is the defining equations (i.e. the equations relating the stresses to the strains) which are nonlinear. This range of problems also includes those concerning vibrations in various classical nonlinear media (e.g., elastic-plastic, rigid-plastic, elastic-viscous-plastic media, reinforced media, etc.).

Problems on nonsteady-state perturbations in classical nonlinear media have been attracting the attention of numerous researchers over the past several years. However, to the author's knowledge vibrations have not been dealt with thus far.

We shall solve the problem of vibrations in the simplest case of a semi-infinite rod for certain types of nonlinearities. The solution will be approximate, giving a clear picture of the vibration field.

5675 Smol'nikov, V. A.: "Generalization of the Euler Case of Motion of a Solid," Applied Mathematics and Mechanics, Vol. 31, No. 4, 1967.

The motion of a free solid is Eulerian if it is not acted on by external moments. It can be shown, however, that even in the presence of an external moment a solid can engage in motion which differs from the Eulerian only in the character of the time dependence of the angles, while the geometry of motion remains exactly the same as in the Euler case. In order for this to happen the external moment acting on the solid must maintain a constant direction in the inertial field and must be parallel to the kinetic moment vector of the solid. The absolute value of this external moment can be an arbitrary function of time.

5676 Kil'chevskii, N. A.; Levchuk, E. F.: "On the Determination of Kinetic Stress Functions in Elastodynamics Problems," Applied Mathematics and Mechanics, Vol. 31, No. 4, 1967.

The purpose of the paper is the development of a new method of solving dynamic problems of elasticity theory by introducing kinetic stress functions. Equations which the kinetic stress functions satisfy are presented here, and the form of the general solution of these equations is found.

5677 Saidel, Gerald M.; Katz, Stanley: "Dynamic Analysis of Branching in Radical Polymerization," Journal of Polymer Science, Part A-2, Vol. 6, 1968, pp. 1149-60.

A method for the theoretical analysis of branching in radical polymerization is presented which includes the dynamics of the process. In particular, the method is applied to a polymerization that occurs by decomposition of initiator, propagation, termination by radical combination, and chain transfer with polymer. By a numerical solution of the kinetic equations (suitably transformed), the time dependence of the number-average degree of polymerization (DP), the weight-average DP, the mean number of branches, and the monomer conversion are obtained. The parameters of the process, that is the rate coefficients and initial concentrations, have the following effects: (1) An increase in the chain transfer coefficient increases the ratio of weight-average to number-average X_w/X_n and the mean number of branches X_b, but does not change the number-average X_n, (2) For a given value of the chain transfer coefficient, a change in the parameters of the process such that Xn increases, causes X_w/X_n and X_b to increase also. (3) Chain transfer with polymer seems to produce relatively few polymer molecules having many branches and a large number of smaller polymer molecules having no branches; consequently, the polymer size (or molecular weight) distribution broadens.

5678 Plaut, Raymond Herman: "A Study of the Dynamic Stability of Continuous Elastic Systems by Liapunov's Direct Method," California University, Berkeley, Ph.D. Thesis, 1967.

Liapunov's direct method is used to derive dynamic stability and instability criteria for some elastic and aeroelastic systems. Domains of asymptotic stability are also obtained. The systems considered are continuous and autonomous, and include columns, arches, plates, and shallow shells. Some nonlinear and nonconservative problems are treated. One-dimensional systems are considered first. The dynamic stability of columns with various end conditions under axial loading is examined. Then necessary and sufficient stability conditions are found for a simply-supported arch and a clamped arch under distributed static loads. The nonconservative problem of a curved panel in an airstream also is investigated and a sufficient condition for stability is established. Two-dimensional systems are studied next. Clamped systems which are investigated include plates and shallow shells under uniform normal forces at the edges.

5679 Hornsey, Edward Eugene: "A Theoretical Investigation of Elastic and Voigt Transient Spherical Waves, and Plane Three-Element Viscoelastic Waves," Missouri University, Ph.D. Thesis, Rolla, 1967.

Spherical waves in elastic and Voigt media were investigated. Series solutions for plane waves in a three element viscoelastic medium were obtained. A dual exponential pressure pulse was assumed because it can exhibit significant features of real pressure pulses while avoiding instantaneous rise time, which is an objectionable feature of some of the models frequently employed in the literature. It was concluded that elastic and Voigt spherical waves, and three element viscoelastic plane waves are not sufficient to represent explosive generated waves in rock. On the basis of this and other investigations cited in the literature it appears that a mechanism for attenuation other than, or in addition to, viscosity will be needed to satisfactorily represent waves in rock.

5680 Pnueli, D.: "An Extension of the Rayleigh-Ritz Method to Obtain Exact Values for the Natural Frequencies and Exact Modes of Vibrations," Israel Journal of Technology, Vol. 6, July-Sept 1968, pp. 200-204.

Development of an iterative method which solves the eigenvalue problem associated with the solutions of problems of natural frequencies and modes of vibrations of strings, rods, beams, membranes, plates, shells, etc., of variable cross section and arbitrary boundary shape. This method has an advantage over the Ritz method in that it does not require a priori knowledge of a complete orthogonal set of functions over the considered region in order to obtain an exact solution. When the region is irregular (but physically possible)-e.g., for membranes or plates - the method becomes numerical, but can still be put directly into a computer.

5681 Hopkins, H. G.: "The Method of Characteristics and its Application to the Theory of Stress Waves in Solids," Engineering Plasticity; Conference, Cambridge University, Cambridge, England, March 1968, ed. J. Heyman; F. A. Leckie, 1968, pp. 277-315.

Introductory account of applications of the method of characteristics to the theoretical analysis of one-dimensional situations of stress-wave propagation. Attention is given chiefly to circumstances where the elastic limit is exceeded and the mechanical behavior is affected by either high rates

4.9 General Dynamic Analysis (contd.)

5682 Shaw, Richard Paul: "Discontinuities in One-Dimensional Thermoelastic Wave Propagation in an Inhomogeneous Medium," AIAA Journal, Vol. 6, August 1968, pp. 1627-27.

Analytical determination of the mechanical and thermal discontinuities in a suddenly loaded inhomogeneous half space. The determination is made separately from the remainder of the solution, using coupled linear thermoelastic theory. It is concluded that although the results represent not the actual values of the variables involved, but their discontinuities, this information would be valuable in any numerical approach to such problems.

5683 Soós, E.: "Thermoelastic Waves Produced by a Point Force in an Unbounded Material," Revue Roumaine de Mathematiques Pures et Appliquees, Vol. 13, No. 2, 1968, pp. 261-272.

Determination of the displacement and temperature fields in an unbounded thermoelastic material for the case where an external force is acting on the body at a point. The solution is obtained by the use of Laplace, Fourier, and Hankel integral transforms and is expressed as a series of functions. The results are compared with those obtained previously by the author (1966) by an approximation method based on a theorem of Abel type. It is noted that the present result can be used as a solution of Green type.

SEE ABSTRACT 5572

4.10 Granular Analysis

5684 Pietsch, W. B.: "Tensile Strength of Granular Materials," Nature, London, Vol. 217, 1968.

Further theoretical examination of the strength of packings of moist granular materials by consideration of the liquid bridge theory. The effect of percentage liquid saturation is discussed.

5685 Smalley, I. J.: "Tensile Strength of Granular Materials," Nature, London, Vol. 216, 1967.

Discussions of equations derived for the tensile strength of granular materials, in which the tensile strength is related to some function of the particle diameter.

5686 Forkin, A. G.; Shermergor, T. D.: "Correlation Functions of the Elastic Field of Quasi-isotropic Solid Bodies," Prikladnaia Matematika i Mekhanika, Vol. 32, July-August 1968, pp. 660-71, (in Russian).

Application of correlation functions to the quantitative evaluation of the microstresses and distortions occuring in the grains of inhomogeneous materials subjected to large strains. A second-order correlation function for the elastic moduli tensor is selected for an inhomogeneous medium with well defined interfaces between the grains. The grain distortions are described by binary correlation functions of the stress and strain tensors and the angles of rotation. The nature of the grain distortions is determined from an analysis of these correlation functions.

5687 Parks, V. J.; Durelli, A. J.; Ferrer, Luis: "Constant Acceleration Stresses in a Composite Body," The Catholic University of America, School of Engineering and Architecture, October 1968.

This paper is a contribution to the experimental stress analysis of composite structures subjected to gravitational forces. It is proved, generally, that the immersion analogy can be used to analyze these stresses in composite bodies provided all the materials of such bodies have the same weight per unit volume. Applications are described in two dimensional problems immersing urethane rubber models bonded to epoxy shells in a thallium formate solution. Photoelasticity is used to determine stresses. The method increases the response obtained, and will have application in the solution of problems where constant acceleration stresses are important as in dams and solid propellant rocket grains.

SEE ABSTRACTS 5550, 5720, 5778

4.11 Systems Analysis

5688 Ciuffi, Renzo: "Calculation of Stresses and Strains in Constant-Thickness Conical Shells Loaded with Variable Pressure Along the Cone Axis," L'Aerotecnica, Vol. 47, October 1967, pp. 177-192, (in Italian).

Investigation of stresses and strains in conical shells loaded with variable pressure in the case where the pressure is expanded by a polynomial with integral exponents as a function of the distance from the cone vertex. Resolving functions are given with tabulated coefficients. A numerical example dealing with the divergent section of a rocket nozzle is given. A comparison is made between the stresses in the nozzle resulting from the actual gas pressure and the stresses due to the constant pressure that the same axial thrust might cause on the shell. It is found that the stresses calculated for the two cases differ appreciably from each other.

4.12 Thermodynamic Analysis

5689 Valanis, K. C.: "The Viscoelastic Potential and Its Thermodynamic Foundations," Journal of Mathematics and Physics, Vol. 47, September 1968, pp. 262-275.

Revaluation of the Onsagerist theories in regard to the work of Coleman (1964) on the thermodynamics of materials with memory. A general theorem and its corollary are developed, establishing the existence of a viscoelastic potential from which the stress tensor and the entropy density are derivable. The constitutive equations are derived for a viscoelastic material with an initial elastic response and in the presence of large deformation and a time-varying, spatially inhomogeneous thermal field. The constitutive equations are also found for the case of small deformation.

5690 Nowacki, W. K.; Raniecki, B.: "Remarks on the Solutions for Some Dynamic Problems of Thermo-Viscoelasticity," Archiwum Mechaniki Stosowanej, Vol. 20, No. 3, 1968, pp. 337-346.

Description of a method for obtaining the particular solution of the basic equation of thermoviscoelasticity for a fairly broad class of dynamic problems. The absence of body forces and heat sources is assumed, and homogeneous initial conditions for the temperature field and for the quantities characterizing the strain state are introduced. Particular solutions are obtained using the elastic-viscoelastic analogy, and the discussion is based on the results of Nowacki and Raniecki (1967) concerning an elastic medium. The particular solution in the space of transforms for a medium described with polynomial differential operators is presented. The inverse transforms are determined for both Voigt and Maxwell models. The general solution of the one-dimensional problem for a half-space with an arbitrary boundary condition for the temperature field is presented.

5691 Truesdell, Clifford: "Thermodynamics of Deformation," Canadian Congress of Applied Mechanics, Laval University, Quebec, Canada, May 22-26, 1967, Proceedings, ed. B. H. Karnopp, 1967, pp. 3-207, 3-231, (in French).

Discussion of deformation thermodynamics on the basis of the mechanics and thermokinetics of continuous media. The importance of the results obtained by this approach are illustrated by the solution of a central problem of wave propagation. Finally, a theorem is formulated showing the close links that exist between thermostatics and thermokinetics.

5692 Reiner, Markus: "Dynamical Strength of an Ideal Solid with Definite Constitutive Equation," Mechanical Behavior of Materials under Dynamic Loads; Proceedings of a Symposium, San Antonio, Tex., Sept. 6-8, 1967, ed. U. S. Lindholm, 1968, pp. 1-9.

The mechanical behavior of a solid is in general determined by the parameters of instantaneous elasticity, delayed elasticity with retardation time, flow with relaxation time and strength, the latter including resistance to plastic yield or fracture. A mechanical model which can represent these properties was proposed by Burgers (1935). Its constitutive equation was derived by Reiner (1958). In the present paper the thermodynamic theory of strength by Reiner and Weissenberg (1939) is applied upon the strength behavior of a solid cylinder under the action of dynamic deformation by axial loads increasing in time at a given rate. According to this theory, failure will occur when the conserved part of the strainwork reaches a certain limit. It is examined how the corresponding stress is affected by the rate of stress. It is known that, in general, with increased rate of stress the strength increases. This assertion is examined under the conditions mentioned above.

5693 Capriz, Geinfranco: "On the Thermodynamics of Viscoelastic Continua," Meccanica, Vol. 3, Sept. 1968, pp. 143-147.

Treatment of the thermodynamic foundations of a theory of permanent deformations, relating to certain thermomechanical axioms where an appropriate definition of free enthalpy plays an essential role. The outlined developments are parallel (and in a certain sense dual) to those which occur in an earlier theory of viscoelastic materials by Coleman and Noll (1963).

5694 Smith, E.: "Crack Bifurcation in Brittle Solids," Journal of the Mechanics and Physics of Solids," Vol. 16, No. 5, Sept. 1968, pp. 329-336.

Classic thermodynamic considerations are employed to derive the condition for bifurcation of a crack situated within a brittle solid deforming in an anti-plane strain mode. Criteria are determined for bifurcation along circular segments at right angles to the initial crack, and also along planar segments inclined at an arbitrary angle with respect to the original crack, the results being used in a brief discussion of physical situations where bifurcation occurs.

5695 Day, W. A.: "Thermodynamics Based on a Work Axiom," Archive for Rational Mechanics and Analysis, ed. C. Truesdell; J. Serrin, Vol. 31, No. 1, Oct. 1968.

In recent years rational theories of thermodynamics for materials with memory have been constructed, first by Coleman, and later by Coleman and Mizel, Gurtin, and Wang and Bowen. Each of these theories adopts the Second Law, as a fundamental axiom. In this paper it is shown that, for a broad class of materials, all the results given by these theories concerning relationships between stress, entropy and free energy can be obtained by a different approach. This approach involves taking an axiom about work as fundamental in place of the Clausius-Duhem inequality.

5696 Mandel, J.; Brun, L.: "Thermodynamique et Ondes Dans les Milieux Viscoelastiques," J. Mech. Phys. Solids, Vol. 16, 1968, pp. 33-58, (in French).

Les relations de Coleman liant les contraintes et l'entropie aux dérivées partielles de l'énergie libre par rapport aux déformations et à la température ne s'appliquent qu'aux corps viscoélastiques doués d'une élasticité instantanée complète (6 degrés de liberté). On établit ici des relations analogues mais valables pour tous les milieux, pourvu qu'il n'y ait pas de déformations instantanées irréversibles. Pour obtenir ce résultat, il est nécessaire de substituer les contraintes aux déformations comme variables indépendantes. Ce mode de définition de l'état thermodynamique est comparé au mode classique, notamment dans le cas des fluides.

Les relations obtenues permettent d'étudier en toute généralité les propriétés des ondes de discontinuité ordinaires dans un milieu viscoélastique et en particulier de préciser le nombre des ondes possibles pour une même direction de normale.

5697 Staverman, A. J.: Thermodynamics of Rheological Behaviour," Fifth International Congress on Rheology, Kyoto, Japan, 1968.

Thermodynamics can be applied to rheological problems in different ways. This paper deals with the information given by thermodynamics about molecular processes behind rheological phenomena.

The first quantity of interest in this connection is the 'relaxation strength'; that is the amount of free energy dissipated per unit deformation per molecule or per characteristic group of atoms in a relaxation process. Besides the free energy also other fundamental quantities like the internal energy and the volume are of interest. A complete understanding of rheological properties implies that these quantities as derived from rheological measurements are in quantitative agreement with those derived from data on molecular dynamics.

A quantitative value of the relaxation strength has been proposed only for the very simple model of the ideal entropy chain. For this model the relaxation strength is assumed to have the value of k T for every normal mode, the internal energy is assumed to vanish.

5698 Lianis, G.: "Non-Linear Thermorheologically Simple Materials," Fifth International Congress on Rheology, Kyoto, Japan, 1968.

This paper generalizes the notion of thermorheologically simple materials which has been used in the past in infinitesimal viscoelasticity. This generalization is obtained by introducing a restricted class of functionals for the specific free energy in which the temperature history is combined with the time parameter into a 'reduced time'. While the dependence on the strain history is not restricted, this history is expressed through the reduced time. The smoothness and continuity hypotheses inherent to Coleman's studies lead to an algorithm for the stress and entropy functional which resembles the constitutive equations for isothermal deformations. The same hypotheses are also used to derive approximations amenable to experimental verification, and prove that the error magnitude is of the same order as in isothermal viscoelasticity. It is finally shown that our hypothesis is confirmed by tests under variable temperature and/or deformation history.

5699 Crochet, M. J.; Naghdi, P. M.: "A Class of Simple Solids with Fading Memory," California University, Berkeley, College of Engineering, Report No. AM-68-9, December 1968.

This paper is concerned with non-isothermal constitutive equations and related thermodynamical results for a class of simple solids with fading memory. Our development is partly motivated by, and also bears on, 'thermo-rheologically simple' materials. After motivating and developing the forms of the constitutive relations (and the expression for internal dissipation) within the framework of the theory of simple materials with fading memory, detailed attention is given to the construction of a non-isothermal finite linear theory of viscoelasticity. Some remarks on simplification of the results and their forms when the deformation is infinitesimal are also included.

5700 Lemprier, B. M.: "Poisson's Ratio in Orthotropic Materials," AIAA Journal, Vol. 6, November 1968, pp. 2226-2227.

Investigation of the thermodynamic limitations of positive strain energy for orthotropic materials. The investigation is made to add credulity to large measured values of Poisson's ratio.

5.0 Failure

5701 Smith, T. L.: "Strength and Extensibility of Elastomers," Fifth International Congress on Rheology, Kyoto, Japan, 1968.

The strength and extensibility of unfilled noncrystallizable elastomers in simple tension ordinarily change 100-fold and 10-fold, respectively, as the test temperature and extension rate are varied over a wide range. In contrast, the ultimate properties of elastomers containing a colloidally dispersed phase commonly depend less on temperature and time (e.g., extension rate), as illustrated by data on: noncrystallizable and crystallizable elastomers, both unfilled and filled with carbon black; elastomeric styrene-butadiene-styrene triblock copolymers: and high strength polyurethane elastomers. The ultimate properties of such elastomers are considered in terms of the rupture mechanism, which involves the slow growth of a crack or cavity (either pre-existent or stress induced) until an instability criterion for self-sustained high-speed crack-growth is satisfied.

5702 Fulmer, G. E.: "Kinetics of Environment Stress Cracking," Fifth International Congress on Rheology, Kyoto, Japan, 1968.

Kinetic studies of material failure give insight into failure processes and mechanisms of failure of polymers in aggressive environment. Eyring's kinetic theory, amplified by Saibel and best interpreted by Coleman was used to study failure processes of polymers in various environments.

Failure under constant load is described by equations of the form log t_b=bf where t_b is the time to failure and f is the applied force. The value a is the zero force intercept and is related to the free energy and b is the slope which is related to the size of the moving element in the flow process. Not well understood are experimental observations that three or more failure mechanisms may exist during reasonable time scales. This is shown by straight line segments of the log time to failure vs. force graphs.

5.1.1 Microscopic Mechanisms

5703 Corten, Herbert T.: "Micromechanics and Fracture Behavior of Composites," Modern Composite Materials, ed. L. J. Broutman; Krock, R. H., 1967, pp. 27-105, 523-528.

Study of internal stresses and fracture occurring in composite engineering materials and structures. The study of micromechanics analysis and fracture behavior is concerned with the relationship loads, deformations, crack initiations, and flaw and crack extension leading to partial or complete separation of the material or structure. In terms of fracture prevention, the various circumstances by which subcritical cracks initiate and grow toward critical size are important. The state of internal stresses and strains in a composite is considered. The modes of fracture of homogeneous materials and the individual constituents of a composite are reviewed. The modes of tensile behavior and fracture of both particulate and fibrous composites are treated. Fracture of fibrous composites subjected to loads other than simple tension is discussed.

5704 Kausch-blecken von Schmeling, H. H.; Hsiao, C. C.: "Behavior of Elastic Networks of Various Degrees of Orientation in the Kinetic Theory of Fracture," Journal of Applied Physics, Vol. 39, Oct. 1968, pp. 4915-4919.

The paper describes a kinetic theory of fracture initiation using a liner elastic network as an approach to represent the strength and elastic properties of oriented materials. Emphasis has been places on the questions as to whether the assumptions of small strains and invariant molecular orientational distribution are valid for the whole period of fracture initiation. The decrease of the modulus of elasticity resulting from the breakage of molecular elements during this period was found to be less than 1%. For brittle materials with high velocities of crack tip propagation the initiation period covers most of the lifetime of a sample. The logarithms of time to break calculated accordingly for network systems of different degrees of orientation are linear functions of applied stress over a wide range of stress. The slopes of these linear curves are inversely proportional to the modulus of elasticity of the network at zero time. Therefore, if the calculated curves of the logarithm of time are plotted vs the applied stress divided by the initial modulus of elasticity the linear portions of all curves reduce to one. For very small or large stresses the curves deviate from linearity.

5.1.2 Macroscopic Fracture Surface Propagation

5705 Kenny, P.; Campbell, J. D.: "Fracture Toughness: An Examination of the Concept in Predicting the Failure of Materials," Progress in Materials Science, Vol. 13, No. 3, 1968, (Oxford, England, Pergamon Press Ltd.)

The development of the concept of fracture toughness is explained along with its use in predicting low-stress failure of materials, caused by sharp notches or cracks. Low-stress failure is used in this context to describe the onset of rapid crack propagation at a stress level below the material yield stress. A brief account is given of the experimental work which has verified the applicability of the concept of high-strength metallic materials. Because of the use made of linear elasticity theory in the development of the concept, there appears to be no limitation of particular geometric situations or to particular modes of crack extension. The progress made in the treatment of the different stages of crack development is described. Of the three stages involving slow growth, rapid propagation, and crack arrest, the first of particular importance in connection with fatigue. Possible application of this concept to lower strength metals, mild steel in particular, is of greatest importance. The problems associated with this application are described in some detail.

5706 Tomkins, B.: "Fatigue Crack Propagation - An Analysis," Philosophical Magazine, 8th Series, Vol. 18, November 1968, pp. 1041-1066.

A simple theory is developed to assess quantitatively the mechanism of fatigue crack propagation in metals. The basic laws governing fatigue are derived theoretically for failure in both the high- and low-stress regions, and the material parameters controlling crack propagation are determined. The theory is compared with that developed in recent years using linear fracture mechanics.

5707 Shioiri, J.; Ishida, R.: "Dynamic Crack Propagation in Rubbers," Fifth International Congress on Rheology, Kyoto, Japan, 1968.

Crack propagation velocities in natural rubber and styrene-butadiene rubber were measured at temperatures from 0° to 100°C. The so-called 'pure shear specimen', a narrow rectangular sheet specimen chucked at longer edges, was adopted to obtain the steady-propagation state. The propagation velocities increase as the temperature is raised, and approach asymptotically to finite values. In rather lower velocity range, the Arrhenius plots of the velocities fall on straight lines which give apparent activation energies of about 10 kcal/mole. These values are close to the apparent activation energy of the viscosity due to the second order force among the segments of long-chain molecules. This indicates that the rate determining factor in crack propagation is the viscous resistance of the substance to the rapid extension at the crack tip. The deviations of the Arrhenius plots from the straight lines in higher velocity range can be attributed to the dynamic effects.

5708 Wraith, A. E.: "A Photographic Method for the Recording of Specimen Behaviour During Rapid Fracture Tests," J. Sci. Instrum., Vol. 44, 1967, pp. 873-874.

Time delay twin flash photography has been applied to the observation of small scale impact test specimens during fracture. Incremental changes in delay time in successive identical tests yield a series of photographs from which a continuous surface behaviour throughout fracture can be implied.

5709 Gent, A. N.; Hirakawa, H.: "Solvent-Induced Crack Growth in Rubbery Block Polymers," Journal of Polymer Science, Part A-2, Vol. 6, 1968, pp. 1481-1492.

The rapid cracking of lightly stressed rubbery block polymers of styrene and isoprene in certain liquids and vapors has been examined experimentally, by using model test pieces containing a single crack. Solvents which preferentially dissolve the rigid molecular end blocks rather than the rubbery center blocks are efficient cracking agents. The stress required for crack growth to occur is shown to be in accord with a simple energy criterion: the stored elastic energy must be sufficient to provide a characteristic energy for the newly formed surface. This characteristic energy ranges from values close to the surface energy of simple liquids up to about 100 times this value for thicker test pieces or slowly diffusing vapors, when some tearing of an incompletely swollen core is inferred. 'Induction times,' before the initial crack starts to grow, are shown to be due to a progressive increase in stored energy under a constant stress as the material absorbs solvent and softens until the critical energy criterion is met. Thus, a time-dependent fracture process is shown to be in accord with a constant energy criterion. Above the critical condition the rate of crack growth depends strongly upon stress, like tearing of amorphous elastomers, and the crack then accelerates rapidly.

5710 Koryavov, V. P.: "Crack Zone and Crack Front in an Elastic Body under Pressure," Journal of Applied Mechanics and Technical Physics," No. 6, Nov.-Dec. 1965, pp. 58-63.

A description was given of the crack zone and crack front in a brittle elastic body under high pressure at the wall of a cavity inside the body. In the present paper, this description is analyzed and an approximate solution of the problem of the propagation of the crack front and the motion of the medium is proposed.

5711 Bergen, R. L., Jr.: "Stress Cracking of Noncrystalline Plastics," SPE (Soc. Plast. Eng.) J., Vol. 24, No. 8, August 1968.

This article describes various stress cracking tests and constant stress vs constant strain techniques as well as the influence of time and temperature on the stress cracking of plastics.

5712 Cherepanov, G. P.: "Cracks in Solids," Internation Journal of Solids and Structures, Vol. 4, No. 8, August 1968.

The subject of this paper is the application of basic ideas and methods of continuum mechanics to the crack propagation processes. The crack extension is governed by an additional condition at the crack-tip. As a consequence of this a problem of 'fine' structure of the crack-tip is considered. The general additional condition for any model of continuum is obtained making use of the energy conservation law and of the physical concept about the fracture energy. Dynamic cracks in elastic solids and quasi-static cracks in elastic- and rigid-plastic solids are briefly considered, as well as a problem of the crack extension in dissipating viscoelastic bodies. The general approach is also applied to the case of fatigue and 'fluctuation' cracks.

5713 Erdogan, Fazil: "Dynamics of Propagating Shear Cracks," Engineering Fracture Mechanics, Vol. 1, No. 2, August 1968.

The energy balance theory for the fracture propagation in brittle and quasi-brittle materials is discussed in a toroidal region around the crack periphery. A simple form requiring the dynamic solution valid only around the crack front and the knowledge of the fracture energy is presented. The results are applied to the fracture of an infinite medium containing a central through crack and subjected to anti-plane shear loads at infinity.

5714 Wnuk, Milosz: "Criteria of Ductile Failure Caused by an Axisymmetric Crack Loaded by Hydrostatic Pressure," Rozprawy Inzynierskie, Vol. 15, No. 4, 1967, pp. 595-616, (in Polish).

Study of the mechanism of ductile failure on the basis of the energy balance during failure of a perfect elasto-plastic medium with an axisymmetric crack loaded by hydrostatic pressure. The existence of a localized plastic zone constituting a narrow layer in the plane of the crack is assumed. An equation is derived for the energy balance before and during failure. The critical pressure causing the crack to propagate is calculated from the energy condition and is compared with the value obtained from the condition of maximum strain. The results are compared with the theory of the failure of brittle bodies. It is shown that the loading scheme has a significant influence on the load limit and the type of failure.

5715 Dooley, L. W.; Howell, A. D.; Yusuff, S.: "Yielding Zones and the Mechanism of Fracture," Symposium on Nondestructive Evaluation of Aerospace and Weapons Systems Components and Materials, 6th, San Antonio, Texas, April 17-19, 1967, Proceedings, 1967, pp. 60-78.

Discussion of three theories concerned with the nature of yielding at the ends of a crack and with the relation betweenplastic yielding and external load. These theories are compared with test data obtained by measuring the yielding zone by strain etching and photoelastic coating, as a result of which Yusuff's theory of yielding is verified.

5716 Segedin, C. M.: "A Note on Geometric Discontinuities in Elastostatics," International Journal of Engineering Science, Vol. 6, No. 5, June 1968, pp. 309-312.

Extension of the Kassir andSih (1967) investigation on the problem of a three-dimensional elliptical crack in an infinite elastic medium, when the faces of the crack are subjecte to a variety of normal loadings. Using partial differentiation to generate new harmonic functions, a more general presentation of the problem is given.

5717 Ivlev, D. D.: "Theory of Quasi-Elastic Rupture Cracks," PMTF-Zhurnal Prikladnoi Mekhaniki i Tekhnicheskoi Fiziki, Nov.-Dec. 1967, pp. 88-128, (in Russian).

Survey of the theory of cracks due to quasi-elastic rupture, including a review of the development of the theory and a description of its current status. The development of the fundamental concepts is outlined in terms of the mathematical principles, the origin of the Griffith-Irwin theory and several other approaches, and the interrelationships with the theory of stress concentration. Models for crack propagation based on the redistribution of stresses caused by plastic deformations are examined, and the chief conclusions of some significant concepts are analyzed. A short survey is given of the solutions to problems in the mathematical theory of cracks based on a model for a linear elastic body. The problems considered include an isotropic elastic body (plane problem), axisymmetric and dimensional problems, torsion, longitudinal displacement, bending, anisotropic materials, inhomogeneous materials, and bending of plates and shells.

5718 Miyamoto, Hiroshi: "Stress and Strain Distribution at the Tip of Cracks," Tokyo, University, Faculty of Engineering Journal, Series A, No. 5, 1967, pp.20-21, (in Japanese).

Study of stress and strain distribution at the tip of cracks by calculation and experimentation. The forms of elastic-plastic boundary and stress distributions at the tips of cracks in circular and rectangular shafts were obtained by the relaxation method under longitudinal shear. In the steady test, a photo-interference method was used, and in the fatigue test the Cu-plating method was used.

5.1.2 Macroscopic Fracture Surface Propagation (contd.)

5719 McClintock, Frank A.: "Local Criteria for Ductile Fracture," International Journal of Fracture Mechanics, Vol. 4, June 1968, pp. 101-130.

Strain distributions in specimens suitable for studying the initiation of fracture are reviewed, and distributions are developed for the steady-state propagation of cracks in plane strain tension of fully plastic materials. The functional forms of local fracture criteria are discussed for different metallurgical mechanisms. It is concluded that (1) pure Mode I (normal) fracture is unlikely to exist except in cleavage; (2) there is both theoretical and experimental evidence for the development of both sharp and flat-bottomed cracks; and (3) simultaneous diffuse and concentrated (Dugdale-Muskhelishvili) flowfields can occur in torsion of longitudinally grooved bars if the stress-strain curve has a maximum which causes band formation, so that a displacement criterion becomes appropriate for final fracture.

5720 Lardner, R. W.: "The Effect of Crystal Orientations on Fatigue Crack Growth," Canadian Journal of Physics, Vol. 46, Oct. 1968, pp. 2225-2226.

A previous theory of fatigue crack growth in metals was based on an analysis of the plastic zone at the tip of a crack in terms of coplanar dislocation arrays. This analysis is presently extended to the case of oblique slip planes. It is shown that, for the case of a crack growing in mode 2 through a polycrystalline material, the average rate of growth through the differing orientations of many grains is almost identical with that obtained by the coplanar analysis.

5721 Lindborg, U.: "Creep Cracks and the Concept of Damage," Journal of the Mechanics and Physics of Solids, Vol. 16, Sept. 1968, pp. 323-328.

Mechanisms for creep damage and fracture are analyzed and compared with phenomenological creep rupture theories for an austenitic stainless steel. The most common form of damage in this material appears to be the formation of sharp grain boundary cracks. A model has recently been proposed for the gradual growth of one of these cracks to infinite size. It is shown that the model is consistent with the Kachanov-Odqvist theory for creep rupture and, under certain conditions, with the Robinson life-fraction rule for the summation of creep periods of different stress levels. Ductile creep theories appear to be applicable only in rare cases for these materials.

SEE ABSTRACTS 5536, 5646, 5694

5.2 Elastic Macroscopic Failure

5722 Matsuo, M.; Imasawa, Y.; Kondo, Y.: "Fracture Behaviors in Plastic/Rubber Two-Phase Polymer Systems," Fifth International Congress on Rheology, Kyoto, Japan 1968.

Fracture behaviors of several plastic/rubber two-phase polymer systems were observed under the electron microscope by the ultrathin sectioning method using osmium tetroxide staining and hardening procedure. Samples used were ABS polymer, high-impact polystyrene, and several PVC/rubber blends including high-impact PVC.

It has been conclusively evidenced that stress-whitening induced under the tensile stress in all of these systems obviously results from the stress-crazing, and that the crazes are not mere cracks but contain oriented polymer chains aligned in the direction of tensile stress applied as observed in glassy polymers.

Other characteristic crazing behaviors in rubber-toughened plastics were summarized.

5.2.1 Uniaxial Failure

5723 Bikerman, J. J.: "The Rheology of Brittle Rupture," Fifth International Congress on Rheology, Kyoto, Japan, 1968.

Two erroneous beliefs longer prevented our understanding of the mechanism of brittle fracture. One was, that no work is spent if only elastic deformations are involved, and the other, that the work dW done in creating a fracture surface dA is equal to $\gamma \cdot dA$, γ being the specific free energy of the solid. In reality the work of rupture dW is the work needed to deform (elastically) a column of the solid, of the cross-section dA, in front of the growing crack until the total relative elongation is exceeded and the column snaps.

The new theory is an improvement over the old in four respects. It preserves the continuity between the macroscopical and the microscopical phenomena; macroscopically, it is clear that the work of fracture is not determined by the increase in surface area achieved, either for solids or for liquids; in numberless instances, the area is smaller after than before rupture. Then, it avoids the notion of the surface energy of solids which was severely criticized recently (Bikerman, 1965). Thirdly, it accounts for the heat liberated during the fracture; in published experiments, this heat amounted to 70% or 90% of the total work spent. Finally, it explains why materials whose surface energies, theoretically, are very similar (for instance, glass and rubber) require very different magnitudes of dW/dA (e.g., 1000 times as much for rubber as for glass); this difference is caused by the fact that the total relative elongation of rubber is so much greater than that of glass.

5724 Halpin, J. C.; Whitney, J. M.; Meinecke, E. A.: "Delayed Instability (Buckling) of Viscoelastic Materials," Fifth International Congress on Rheology, Kyoto, Japan, 1968.

It is commonly observed that when a sufficient compressive load is administered to a slender bar it collapses. If the bar consists of a viscoelastic material, their will be a delay, in time, between the application of the steady compressive load and the catastrophic collapse of the bar. This phenomena, of a delayed instability, is the simplest of a family of such phenomena which underlie such physical processes as time-temperature dependent fracture, delayed yielding, etc. Because such processes are poorly understood, if at all, and are of paramount importance in modern technology, a critical examination of this class of phenomena is most timely. A satisfactory analysis of the kinetic processes leading to a delayed instability can be achieved through a study of the creep buckling of elastomeric rods.

5725 Sneddon, Ian N.; Tweed, J.: "The Stress Intensity Factors for a Griffith Crack in an Elastic Body in which There is an Asymmetrical Distribution of Body Forces," North Carolina State University, Applied Mathematics Research Group, April 2, 1968.

5726 Irwin, G. R.: "Linear Fracture Mechanics, Fracture Transition, and Fracture Control," Engineering Fracture Mechanics, Vol. 1, No. 2, August 1968, pp. 241-258.

As an analysis viewpoint, fracture mechanics treats the leading edge of a crack as a line disturbance zone in a manner similar to the treatment of dislocation lines in dislocation mechanics. Linear fracture mechanics analysis is adequate for most practical applications and permits estimates of two new length factors: the approximate size of the plastic zone 2ry, and the crack border opening displacement, $\delta = G/\sigma_Y$. Studies of crack extension behaviors as a function of the stress field parameter K and G, and their interpretation with the assistance of length factors, have clarified general understanding of fracture in ways which impinge strongly on various fields of investigation such as stress corrosion cracking, fatigue, brittle transition temperature, and fracture control methods. As an example, the paper discusses interpretation of the brittle-ductile transition in terms of relative plastic zone size, and allowable-load estimates which include fracture strength in a rational way. Fracture control methods which do not rely on prior fracture failure experience are needed for new structures now under consideration. Correspondingly, the need for training and experience in fracture mechanics is urgent.

5727 Shah, R. C.; Kobayashi, A. S.: "On the Parabolic Crack in an Elastic Solid," Engineering Fracture Mechanics, Vol. 1, No. 2, August 1968, pp. 309-326.

This paper is concerned with the distribution of stresses near an embedded flat parabolic crack in a body of infinite extent when the crack surface is subjected to uniform normal loading. It is shown that the crack opening shape for the flat parabolic crack is an elliptic paraboloid. Also, it is shown that the stresses possess a singularity of $r^{-\frac{1}{2}}$ near the parabolic crack front and the dominant state of stress is plane strain near the crack front. The stress intensity factor for the opening mode of fracture k_I, is obtained for this configuation of the crack.

5728 Matczynski, M.; Sokolowski, M.: "On a Certain Case of Equilibrium Cracks Under Harmonic Loads," Academie Polonaise des Sciences, Bulletin des Sciences Techniques, Vol. 16, No. 1, 1968, pp. 13-23.

Study of the stability of an unbounded elastic medium weakened by an infinite number of semiinfinite, parallel and equidistant cracks. Each crack is loaded by a self-equilibrated system of forces harmonically varying in time. The stability of the cracks is estimated as a function of stress concentration at the tip and the modulus of cohesion. Special cases of the stress intensity factor are considered.

5729 Loeber, J. F.; Sih, G. C.: "Diffraction on Antiplane Shear Waves by a Finite Crack," Acoustical Society of America, Journal, Vol. 44, July 1968, pp. 90-98.

The scattering of polarized harmonic shear waves by a sharp crack of finite length under antiplane strain is considered. Use is made of integral tansforms, which reduce the problem to the evaluation of a system of coupled integral equations. Special emphasis is placed on obtaining the detailed structure of the crack-front stress and displacement fields, which control the instability behavior of cracks in brittle materials. While the dynamic stresses around the singular crack point are found to be qualitatively the same as those encountered under statical loading, they differ quantitatively in that the intensity of the dynamical stress field, which may be regarded as a measure of the force tending to cause crack propagation, depends on the incident wavelength. At certain wavelengths, this intensification is shown to be larger than the static case. The method of solution described applied equally well to boundary value problems in electromagnetic and acoustic theory.

5730 Wnuk, Milosz; Knauss, Wolfgang G.: "Delayed Fracture in Viscoelastic-Plastic Solids," California Institute of Technology, Pasadena, Firestone Flight Sciences Lab., NASA-CR-97582, September 1968.

Using the viscoplasticity model of Crocket, the growth of a penny-shaped crack in a linearly viscoelastic solid was studied in an attempt to elucidate (1) the load carrying ability of glass-like polymers having potential application as structural materials and (2) the fracture behavior of materials possessing relaxation and creep responses which span several decades of time. The Crocket model attempts to generalize the elastic-plastic stress-strain law by replacing the elastic portion by a linearly viscoelastic one and makes the yield stress dependent on the rate of deformation during the initial, linearly viscoelastic deformation phase. Stress and strain distribution around the crack, effect of time dependent yield, and delayed fracture for time-independent yield are evaluated using the prescribed model. Comments on failure behavior in two dimensional stress fields are included.

5731 Lebedev, A. A.: "Possible Combination of Conditions of Plasticity and Brittle Fracture," Prikladnaia Mekhanika, Vol. 4, August 1968, pp. 85-93, (in Russian).

Theoretical demonstration of the expediency of rational combination of conditions of plasticity and brittle fracture. The study is based on modern concepts concerning the mechanism of strain and destruction of materials. A new type of invariant function is proposed. The strength criteria including the parameters of this function are investigated. A comparison is made between the criteria offered and experimental results. The limiting surfaces which interpret the strength criteria in the stressed space have a logical shape according to an earlier work.

5732 Podil'chuk, Iu. N.: "Plane Elliptic Crack in an Arbitrary Homogeneous Stress Field," Prikladnaia Mekhanika, Vol. 4, August 1968, pp. 94-100, (in Russian).

Investigation of a plane elliptic crack in an infinite elastic medium. A solution to this problem has been given by Lur'e (1952). However, of his three solutions to the Lamé equilibrium equations only two are linearly independent. In this work a third linearly independent solution is obtained.

5733 Moser, Alma Porter: "Elastic Stress Fields and Stress Intensity Factors for Finite Bodies with Single Edge Cracks and Notches," Colorado University, Boulder, Ph.D. Thesis, 1967.

This dissertation is concerned with elastic stress fields and stress intensity factors for finite bodies with single edge cracks and notches. The solutions are obtained by the use of Airy stress functions given by a truncated biharmonic eigen-function series. The satisfaction of the homogeneous boundary conditions along the faces of the notch or crack is ensured by the use of a set of eigenvalues which are the solutions of a characteristic equation. It was found in this study that the stress fields could best be found by specifying boundary tractions and that the stress intensity factors could best be arrived at by specifying the boundary values of the stress function and its normal derivative. Thus, it was necessary to solve each problem twice in order to obtain both the stress field and reliable stress intensity factors.

5734 Novikov, N. P.: "One of the Features of the Structure of the Zone Near the Tip of a Crack," International Journal of Solids and Structures, Vol. 4, No. 12, December 1968.

It is known that in polymers (such as nylon, polyethylene, polypropylene, etc.), as the uniaxial loading reaches a definite value, orientation occurs and the strength of an oriented polymer is much higher. It may be assumed that in such materials, as the crack moves along as a result of large stresses, orientation of the polymer occurs in the vicinity of the tip zone. Therefore, the development of a crack in these polymers will be strongly connected with fracture of an oriented polymer as it exists near the tip of the crack.

With the example of development of incisions (seed cracks) in films of polyethylene and polypropylene, it was established that the assertion stated above indeed is valid. In the experiment, films of thickness of 30 to 50 μ were used with different supermolecular structure. The extension was observed with a microscope in polarized light which permitted to detect changes in the supermolecular structure.

SEE ABSTRACTS 5640, 5756

5.3 Viscoelastic Macroscopic Failure

5.3.1 Uniaxial Failure

5735 Kamins'kii, A. O.: "Kinetics of the Development of Cracks in Viscoelastic Materials," Akademiia Nauk Ukrains'koi RSR. Dopovidi. Seriia A - Fiziko - Tekhnichi i Matematichni Nauki, Vol. 30, Sept. 1968, pp. 849-852, (in Ukrainian).

Derivation of an equation describing the steady propagation of a crack tip in a viscoelastic plate. This equation is used as a basis for obtaining an analytical expression describing the propagation rate of a crack tip in an infinite viscoelastic strip. A distinctive feature of the solution obtained is that it does not require the introduction of new material constants characterizing the progessive failure of the material.

5.4 Internal Composite Failure

5736 Chen, P. E.: "Stress Fields Around Interior Cracks," Fifth International Congress on Rheology, Kyoto, Japan, 1968.

This paper describes the mathematical approach for calculating the stress fields around interior cracks and the experimental verification based on the photoelasticity technique. A computer program was used to carry out the numerical calculations for the mathematical model. The stress fields around a single interior crack as well as two and three parallel interior cracks in tensile specimens have been calculated and compared with the experimental results. It has been found that both the overlap and spacing between the parallel interior cracks have significant effects upon the stress fields around such cracks. A basic mechanism which may contribute to stop the crack growth is expounded.

5737 Kawabata, S.; Tatsuta, S.; Kawai, H.: "A Phenomenological Approach to the Failure Mechanism of Elastomers," Fifth International Congress on Rheology, Kyoto, Japan, 1968.

A phenomenological theory on creep failure of elastomers is improved. Three assumptions are presented here. That is, (1) there are many latent defect points all over the volume of solid specimen at random and each of them has possibility to grow to a crack during given time interval if the specimen is placed in stressed state defined by ϕ, where ϕ takes zero when the solid is not in stressed state and fracture chance increases with increasing ϕ, (2) the probability that a small cell which is taken in the specimen produces a crack during unit time is determined as a function of ϕ , (3) as soon as any one of defect points grows to crack, the specimen falls into failure.

5738 Sneddon, I. N.: "Crack Problems in the Theory of Elasticity," Developments in Theoretical and Applied Mechanics, Vol.3, Southeastern Conference on Theoretical and Applied Mechanics, 3rd., University of South Carolina, Columbia, S.C., March 31-April 1, 1966, Proceedings, ed. W. A. Shaw, 1967, pp. 73-103.

Account of calculations in the mathematical theory of elasticity relating to Griffith cracks and their three-dimensional analogs and having some relevance for the theory of brittle fracture. The physical considerations which indicate the need for the calculation of certain features of the stress field are discussed. The results for an isolated Griffith crack and an isolated penny-shaped crack in an infinite solid are derived. The modifications which must be made to these results to include the effect of cohesive forces as suggested by Barenblatt are examined, and problems associated with 'external' cracks in infinite solids are considered. Accounts of two- and three-dimensional problems with more complicated geometry, and of solutions of dynamical crack problems are given. Attention is restrictred to internal cracks.

5.5 External Interface Failure

5739 Wu, E. M.; Thomas, R. L.: "Interfacial Fracture Phenomena," Fifth International Congress on Rheology, Kyoto, Japan, 1968.

Experimental comparison of theoretical observations are presented. Specimens are formed by edgewise joining of two flat plates with different material properties. Stiffness ratios of 75, 25, 2, 1.5 and 1 are investigated by casting epoxy on steel, alumin and silicon filled epoxys respectively. A flaw is introduced in the interface and the specimens are subjected to a tensile load. In the cases where mis-match is large, the trajectory of propagation is repelled from the interface due to the aforementioned coupling effect. The initial angles of the trajectories are predictable from the elastic stress analysis. For several mis-match ratios, when the cracks are of the theoretical decoupling lengths, the crack indeed propagages along the interface as predicted. The experimentally observed strain energy release rate calculated from the theoretical expression appears to be a constant.

5.6 Repeated Cycle Failure

5740 Berg, C. A. : "Kinematic Reversibility in Plane Deformation," Fifth International Congress on Rheology, Kyoto, Japan, 1968.

The phenomenon of kinematic irreversibility which was reported by McClintock (1962) and others, and which is suspected to play an important role in fatigue, is re-examined analytically and experimentally. It is found that the motion of a free surface in a body which undergoes plane deformation and which is made of an icompressible isotropic material having no history effects in its rheology (e.g. a nonlinear fluid), is always kinematically reversible. A slight extension of these results shows that nonhardening plastic deformation in the absence of Bauschinger effect also provides kinematically reversible free surface motion. Experiments on plasticine specimens show very strong kinematic irreversibility of the motion of transverse cylindrical holes bored through large rectangular parallelepiped blocks which were made to deform in the plane of one pair of faces by cyclic pure shear loading.

5741 Coffin, L. F., Jr.: "Introduction to High-Temperature Low-Cycle Fatigue," Experimental Mechanics, Vol. 8, May 1968, pp. 218-224.

Discussion of significant areas in the field of high-temperature low-cylce fatigue to point up that a detailed knowledge of the problem is important to the reliable performance of the component involved. Some of the metallurgical aspects involved in the use of materials at high temperature are emphasized. It is noted that there is a need to relate more closely the observed results with existing knowledge of metallurgical processes. This can best be done by a closer working relationship between designer, the materials engineer, and the metallurgist.

5.7 Accumulative Damage

5742 Hori, M.: "Superposition Principles in the Stochastic Process Theory of Fracture," Fifth International Congress on Rheology, Kyoto, Japan, 1968.

The stochastic process theory of fracture, sometimes called the statistical theory of breaking kinetics, was designed to account for the time dependence of the rupture process, as well as its statistical variability. The essential feature of this approach is that it regards fracture phenomenon as a kind of stochastic process associated with thermal fluctuations. Stochastic process theory has so far been applied to various types of failure in glasses, metals, concretes, and polymers.

Since the rupture behavior is strongly non-linear, Boltzmann's superposition principle is not considered to be valid. Superposition principles in the theory of non-linear viscoelasticity, developed by Leaderman, Findley, Pipkin, and other investigators, are applied to the fracture process under randomly changing loads. Theoretical results derived from these theories are discussed and criticized.

Furthermore, a comparison of the present model with Coleman's theory of breaking kinetics is given. Miner's damage accumulation law for metal fatigue is also re-interpreted from the standpoint of stochastic processes.

5743 Younger, Dewey G.: "Cyclic Plasticity and Fatigue at Stress Concentrations," Society for Experimental Stress Analysis, Spring Meeting, Albany, N. Y., May 7-10, 1968.

Study of the effects of cyclic plasticity on the magnitudes of stress- and strain-concentration factors at geometric discontinuities. Procedures are presented for predicting notch-fatigue curves from unnotched fatigue data through an application of Stowell's formula and the cyclic stress-strain curve. A survey of previous work is presented and new methods are introduced for defining the notch-fatigue curve of the power-law relationships which relate fatigue failure to mechanical tension properties and cyclic strains. The important implication of the procedure is that fatigue failure in structures can be predicted from a minimum of information derived from smooth laboratory specimens and an estimate of the effective stress-concentration factor.

5744 Kudriavtsev, P. I.: "Method for Investigating the Kinetics of the Development of Fatigue Cracks," Industrial Laboratory, Vol. 34, January 1968, pp. 108-110.

Discussion of a method of inve igating the origin and the development kinetics of fatigue cracks based on fatigue test specimens with several stress raisers. The stress raisers on the specimen are located in zones with different stress levels. Testing of a single specimen can yield simultaneously data concerning the fatigue strength of the material under variable loads of different magnitudes.

5745 Forrester, E. R.; Thevenow, V. H.: "Designing For Expected Fatigue Life," Annals of Assurance Sciences; Proceedings of the Seventh Reliability and Maintainability Conference, San Francisco, Calif., July 14-17, 1968.

Discussion of some of the processing and operational factors which reduce fatigue strength. Emphasis is placed on the finite fatigue life region, often called low-cycle fatigue, because in many lightweight, high-performance systems, hardware cannot be designed for finite life. An approach for estimating the probability of fatigue failure on the basis of the scatter inherent in material properties and fatigue life is described.

5746 Sweet, A. L.; Kozin, F.: "Investigation of a Random Cumulative Damage Theory," Journal of Materials, JMLSA, Vol. 3, No. 4, December 1968, pp. 802-823.

A cumulative damage theory for fatigue is presented, which takes account of the randomness of the time-to-failure and the fact that the failure process can be said to possess memory. This is accomplished by correlating the failure process with the change in hysteresis-loop area that a specimen undergoes during fatigue testing.

An experimental program designed to investigate the theory is discussed. Specimens of SAE 1020 steel were tested sinusoidally, under stress control, with a mean stress equal to zero, in a tensile-compressive mode. Specimens were subjected to a single stress amplitude-to-failure, and also to mixtures of two and three amplitudes-to-failure. Hysteresis-loop areas were monitored 'on-line' during all tests.

The data is used to evaluate the theory, and comparisons with the Miner-Palmgren theory are shown.

5747 Osgood, Carl C.: "Allowable Fatigue Stresses for a Given Lifetime," International Council of the Aeronautical Sciences, Congress, 6th, Munich, West-Germany, Sept. 9-13, 1968.

Correlation of the dynamic response stress with a function of fatigue damage as caused by sine or random loading. The prediction of fatigue life or an allowable stress involves the concept of the gradual accumulation of damage during the loading period. The evaluation on the basis of available data, minimal assumption, and acceptable accuracy suggests that a linear function in the form of the Palmgren-Miner hypothesis is adequate for the method employed here. The arrangement of equations expressed in a form of a power law allows them to be written for any incremental length of the log S-log N curve. thus determining the slope, or exponent with an accuracy dependent only on that of the data itself. As a further characteristic of the method, the dynamic transfer functions is introduced to accommodate properly the relation between the external forcing function and the response stress at any chosen location.

5748 Bills, K. W.,Jr.,et al.: "Solid Propellant Cumulative Damage Program," Final Report, AFRPL-TR-68-131, Air Force Rocket Propulsion Laboratory, Research and Technology Division, October 1968.

A comprehensive laboratory and theoretical analysis program was conducted to provide increased understanding of linear cumulative damage concepts for solid propellants, with emphasis upon the statistical characteristics of propellant failure. Mechanism of damage studies on model material showed that failure is controlled by a mechanical instability behavior in the binder, which is not a tearing process. The linear cumulative damge (LCD) relation and the maximum principal stress (MPS) failure criterion were described and shown to hold for uniaxial, strip-biaxial and triaxial (poker-chip) tensile tests. The effects on the time-to-failure data were evaluated in terms of the superimposed pressure, relative humidity, statistical variability, aging and sensitivity to variations in the environmental test conditions.

5749 Birnbaum, Z. W.; Saunders, Sam C.: "A Probabilistic Interpretation of Miner's Rule," SIAM Journal on Applied Mathematics, Vol. 16, May 1968, pp. 637-652.

(See Abstract 4744).

5750 Johnson, Leonard G.: "The Probabilistic Basis of Cumulative Damage," American Society for Quality Control, Annual Technical Conference, 22nd, Philadelphia, Pa. May 6-8, 1968, Transactions.

5.7 Accumulative Damage (contd.)

Discussion of the problem of assessing cumulative damage. Cumulative damage is most conveniently measured by cumulative probability of failure. A complete S-N-P (stress, cycles of life, probability) diagram is required for a complete solution to the cumulative-damage prediction problem. Approximations such as Miner's rule are valid only under restricted conditions.

SEE ABSTRACT 5561

6.1.3 Test Methods for Mechanical Characterization

5751 Bollenrath, F.; Feldmann, H.; Happek, G.: "Criteria for Carrying out Tensile and Creep Tests in Vacuum at High Temperatures," Metallwerk, Plansee, 6th Plansee Seminar, Reutte, Austria, June 24-28, 1968, Reprints, Vol. 2, 1968, (in German).

Discussion of criteria for conducting tensile and creep tests in vacuum at high temperatures, taking into account the influence of measurement and control failures on the material characteristics. Results of different tests at different test institutes are comparable only when the failure parameters characteristic for each method are known. The differences in the observed stresses are described as functions of the relative failures of the experimental parameters. They are also given in the form of dimensionless failure moduli.

5752 Taprogge, R.: "Research to Determine Permissable Mechanical Stress of Thermoplastic Plastics by Static and Vibratory Tensile and Load Tests. II," Kunststoff-Rundschau, Vol. 15, No. 6, June 1968, (in German).

The critical curves showing the viscoelastic behavior of thermoplastics are determined under constant and alternating stress conditions. A literature survey is included.

5753 Taprogge, R.: "Studies to Determine Permissible Mechanical Stress of Thermoplastic Plastic by Static and Vibratory Tensile and Load Tests,IV," Kunststoff-Rundschau, Vol. 15, No. 8, August 1968, (in German).

Creep curves determined experimentally for samples of PVC at 20° C are given along with a discussion of creep behavior of thermoplastics. Similar data are also given for polyoxymethylene and polypropylene. Stress-strain curves are also determined, and the testing procedure is described.

6.1.4 Ultimate Property Tests

5754 Bridle, C.; Buckley, A.; Scanlan, J.: "Mechanical Anisotropy of Oriented Polymers, Part 1: A Yield Criterion for Uniaxially-Drawn Poly(ethylene terephthalate)," Journal of Materials Science, November 1968, pp. 622-628.

Measurements of tensile and shear yield stress have been made on strips cut at various angles to the draw direction from films of drawn amorphous poly(ethylene terephthalate). The data were well fitted by a criterion of the von Mises type but with modifications to allow for the anisotropy of the samples and also for a built-in compressive stress in the draw direction. In the tensile experiments a sharp neck is usually formed at an angle to the tensile direction and this angle is predicted with good accuracy by an application of the theory of plastic potential.

The built-in stress is closely related to the retraction stress which develops when the films are heated but not allowed to contract. In general the tensile yield stress and the tensile modulus are also closely correlated.

5755 Lim, C. K.; Tschoegl, N. W.: "Tensile Strength and Stress-Strain Behavior of Swollen Elastomers under Superposed Hydrostatic Pressure," Fifth International Congress on Rheology, Kyoto, Japan, 1968.

Rubber rings swollen in hydrocarbon solvents were stretched in uniaxial tension at a crosshead speed of 1.45 inches per minute under superposed hydrostatic pressures up to 2000 psi. Two elastomers were examined: a moderately cross-linked compression molded styrene-butadiene rubber, and a more tightly cross-linked cast polyurethane rubber. Both materials obeyed the stress-strain relation predicted by the kinetic theory of rubber elasticity under all pressures. The tests were carried out at room temperature and were corrected to 25°C. The superposed hydrostatic pressure had no effect on the tensile strength of the two rubbers. Within the experimental scatter the stress-at-break appeared to depend on the octahedral shear stress alone and thus followed the Henchy-von Mises failure criterion. The failure surface of the swollen rubbers in principal stress space could therefore be described by a cylinder coaxial with the hydrostatic axis.

6.2.1 Biaxial Tests

5756 Sharma, M. G.: "Some Observations on Yielding and Fracture of Polymeric Materials under Biaxial Stresses," Fift. International Congress on Rheology, Kyoto, Japan, 1968.

The paper describes an extensive experimental program for the study of yielding and fracture of several polymeric materials under various types of biaxial loading. Effect of rate of applied stresses and temperature on yielding and fracture behavior has been investigated. An apparatus specially suited for this study has been developed and is described in this paper. The important feature of this apparatus is that the effect of rate of biaxial loading on yielding and fracture behavior of polymeric materials can be simultaneously studied for different biaxial stress fields. The biaxial stress apparatus as such consists of a top head that is common for all biaxial stress field tests and a lower head that is variable depending upon the biaxial stress field under consideration. The apparatus is equipped with several lower heads to cover the various stress fields corresponding to biaxial stress ratios $\alpha=\sigma_{22}/\sigma_{11}$ (σ_{11},σ_{22} are the nominal principal stresses) in the tension-tension quadrant of principal stress co-ordinate plane. The apparatus makes use of cylindrical specimens. The specimen in a particular biaxial stress experiment is subjected to a predetermined pressure history by a closed loop feed back control system. The specimen is enclosed in a thermal cabinet to study the yielding and fracture behavior of polymeric materials at various constant temperatures.

6.2.2 Shear Tests

5757 Sigmon, William M.; Parr, Charles H.; Ignatowski, Albert J.: "Development of a Ball Indentation Test for Samples of Finite Thickness," Rohm and Haas Co., Redstone Research Laboratories, December 1968, Technical Report S-182.

A spherical indentation test for small quantities of low modulus materials is described and experimentally validated. The data analysis takes into account finite sample thickness. Comparison with the Hertz contact theory is made, and extension to viscoelastic characterization is discussed.

6.3.1 Free Vibration Tests

5758 Gajendar, N.: "Free Vibrations of Composite Elastic Systems," Journal of Science and Engineering Research, Vol. 11, January 1967, pp. 45-50.

Extension of Wah's analysis of the dynamic problem of a plate with attached masses to the case of free vibrations of composite elastic systems such as plates with concentrated mass, spring, and dashpot systems. The results are presented in terms of the modal functions of the plate alone. Some of the particular cases have been deduced.

5759 Feng, Chuan C.; Bajan, Robert L.: "Free Vibration Analysis by the Modal Substitution Method," Space Projections from the Rocky Mountain Region; Proceedings of the Symposium, Denver, Colorado, July 15-16, 1968, Vol. 2, 1968, 40p.

The modal substitution method is an iterative technique developed for determining accurate natural modes and frequencies of large discrete undamped dynamic systems. The system is considered to be subdivided into a number of subsystems, each of which is amenable to analysis. Formulation of the system equations for free vibration is based on an incomplete modal coupling using exact displacement modes calculated from the constitutent subsystems. Approximate natural modes and frequencies are computed from the incomplete eigenvalue problem associated with the system. A prescribed number of these modes, in conjunction with a selected set of previously unused subsystem modes, are used in successive model substitution cycles. Improvement is guaranteed in the approximate system modes utilized, and their corresponding frequencies. Criteria for the optimal selection of the unused subsystem modes in modal substitution and a numerical example verifying the developed concepts are presented.

5760 Dean, Thomas Scott; Plass H. J., Jr.: "A Dynamic Variational Principle for Elastic Bodies, and its Application to Approximation in Vibration Problems," Developments in Mechanics, Vol. 3, Midwestern Mechanics Conference, 9th, University of Wisconsin, Madison, Wis., August 16-18, 1965, Proceedings, Part II, Dynamics and Fluid Mechanics, ed. T. C. Huang; M. W. Johnson, Jr. 1967, pp. 107-118.

A variational principle is presented which embodies both Hamilton's principle and Reissner's principle as special cases. Its form is such that upon postulated independent variations on stresses, displacements, and particle momenta, the associated Euler equations are the equations for the relation between momentum and velocity, the stress-strain relationship for an elastic material, and the equation of motion. Further, stresses, displacements, and moments may be both time- and spatially-dependent. The paper is devoted to an exposition of the principle in one dimension and the approximate solution of linear and nonlinear one-dimensional problems. In the appendix the general three-dimensional development is presented.

6.3.2 Forced Vibration Tests

5761 Danek, O.: "Forced Vibrations of Linear Systems," Journal de Mècanique, Vol. 6, December 1967, pp. 461-479, (in French).

Study of the trajectories of points of a structure subjected to natural or forced vibrations. The structure considered is a system of bars. The natural mode of this system is represented by a controlled surface (e-face), while the forced mode is represented by a more complicated surface formed, for example, by the elliptical trajectories of the points considered (q-face). The q-faces associated with the harmonic excitation (monofrequency) or periodic (polyfrequency) are studied. The variation of the q-face of the system subjected to excitation of the varied mode was observed.

5762 Marinescu, Al.: "Concerning the Oscillations of the Rocket," Revue Roumaine des Sciences Techniques, Serie de Mecanique, Applique, Vol. 12, No. 5, 1967, pp. 1145-1164, (in German).

Examination of a model rocket which has the shape of a rod with one free end and is characterized by variable mass and rigidity. The free oscillations of the rod are investigated by means of the bending theory, as well as from the standpoint of rotational inertia, shear forces, inner damping, aerodynamic damping, and axial forces. Finally, forced oscillations arising from the combined action of harmonic, accidental, and unsteady perturbations are studied. Numerical examples of these three types of perturbing force are presented.

5763 Laura, Patricio A.; Shahady, Paul A.: "Longitudinal Vibrations of a Solid Propellant Rocket Motor," Developments in Theoretical and Applied Mechanics, Vol. 3, Southeastern Conference on Theoretical and Applied Mechanics, 3rd, University of South Carolina, Columbia, S. C., March 31-April 1, 1966, Proceedings, ed. W. A. Shaw, 1967, pp. 623-633.

Study of the problem of calculating the lower natural frequency of a long clamped circular cylinder with a star-shaped stress-free internal perforation vibrating in axial-shear mode. This problem is interpreted as a first approximation for a typical long, solid-propellant rocket motor. It is pointed out that the method described is directly applicable in determining the cutoff frequencies of wave-guides of very general cross section.

6.4.1 Uniaxial Cyclic Load Tests

5764 Swanson, S. R.: "Random Load Fatigue--A State of the Art Survey," Matl. Res. Stand., Vol. 8, 1968, pp. 10-44.

An extensive review of the present state of work in the field of random load fatigue testing. Sections covered include ones on programmed constant amplitude cycles in random sequence, industrial cycles in randomised sequence, testing by analogous random process, acoustic fatigue tests, crack propagation under random loading, and other work currently in progress. An extensive bibliography and glossary are included.

5765 Slot, T.; Stentz, R. H.: "Experimental Procedures for Low-Cycle-Fatigue Research at High Temperatures," Experimental Mechanics, Vol. 8, March 1968, pp. 107-114.

Summary of testing procedures for low-cylce fatigue experiments on hydraulic fatigue machines operated with closed-loop servo control of the strain in inductively heated test specimens of the hourglass type. Typical equipment performance data and fatigue-test results are presented. In this type of testing, transverse strain is measured and controlled at the minimum specimen diameter, and heating of the specimen is accomplished by means of an induction coil around the gauge section.

SEE ABSTRACT 5793

6.6 Analogue or Model Tests

5766 Marvin, R. S.: "Rheological Models and Measurements," Fifth International Congress on Rheology, Kyoto, Japan, 1968.

The evaluation of the rheological properties of a material requires certain assumptions from which the form of a constitutive equation can be deduced. The term model, whether molecular or phenomenological, here denotes the body of assumptions used on the development of a particular theory. The testing of these assumptions and the evaluation of the constants or functions in the resulting constitutive equation require the design and performance of various measurements. A single type of measurement may be adequate to evaluate functions occuring in a constitutive equation, but it is seldom sufficient to establish the validity of the assumptions on which that equation is based. Such results may simply establish an equation as a good empirical representation, a useful accomplishment, but one quite different from establishing the validity or adequacy of a model.

In carrying out measurements intended to check a model or some of the assumptions on which a model is based, certain factors which are deliberately ignored in the model (always an idealization of an actual material) must be considered, as must the effect of deviations from boundary conditions assumed in the measurement. And, a consideration often ignored, both the measurement and the manner in which the results are analyzed should be chosen to provide as sensitive check of the assumption or model. The history of experiments stimulated by the Weissenberg hypothesis about the equality of normal stress differences illustrates both the difficulty of satisfying these criteria and the danger of judging the correctness of a hypothesis or a model from the results of a single type of measurement.

5767 Sobotka, Z.: "Two-Dimensional and Three-Dimensional Rheological Models for Orthotropic Viscoelastic Bodies," Fifth International Congress on Rheology, Kyoto, Japan, 1968.

The author has introduced the two-dimensional rheological models which represent schematically the rheological configuration of unit surface or of unit volume of orthotropic viscoelastic bodies. These models corresponding to the real rheological materials at the two-dimensional and three-dimensional state of stress and strain consist of the orthotropic elastic and viscous two-dimensional or three-dimensional regions, respectively, which have rectangular straight boundaries lying in the principal directions of orthotropy. By various arrangements of such regions, all kinds of viscoelastic bodies may be represented.

5768 Baer, A. D.; Ryan, N. W.: "An Approximate but Complete Model for the Ignition Response of Solid Propellants," AIAA Journal, Vol. 6, No. 5, May 1968, pp. 872-77.

Early theories of ignition, describing events leading to a bootstrapping exothermic reaction, cannot be extended to describe the complete ignition process terminating in steady deflagration. The complete description requires consideration of surface regression. If the regression rate of the propellant is described by simple, feasible relationships and the rate of energy release by temperature-dependent reactions is limited to a maximum value, the complete ignition transient, which starts with the cold, passive solid and ends at a condition of steady-state regression, may be simulated. Such a simulation is achieved by a model that treats the solid as homogeneous, considers the effect of all reaction to be approximated as surface heat fluxes, and employs a simplified description of the steady-state burning process. Qualitative agreement is obtained between predictions of the model and laboratory ignition results for the effect of igniter flux and pressure on ignition times. Values assumed for the net heat of gasification of the propellant, a steady-state burning parameter, and the manner in which the igniter heat flux is terminated are found to have critical effect on the transition to stable deflagration.

6.7 Local Strain Measurement Tests

5769 Archbold, E.; Ennos, A. E.: "Observation of Surface Vibration Modes by Stroboscopic Hologram Interferometry," Nature, Vol. 217, March 9, 1968, pp. 942-43.

Description of a method for real-time analysis of a surface shape based on the findings of Powell and Stetson (1965) that holography can be used to study the vibration modes of a surface. Interference effects can be obtained between the object and its holographically recorded image if the two are superimposed, by replacing the processed plate in exactly the same position in which it was recorded, and viewing the object through the hologram plate using the same illuminating conditions. A slight displacement of the surface of the object will then give rise to a pattern of interference fringes. For a surface vibrating normal to its plane, the interference fringes will sweep across it in synchronism with the frequency of vibration, so that by pulsing the illumination at this frequency, their motion can be arrested and the distortion of the surface, measured relatively to the rest position, can be deduced.

5770 Riera, J. D.; Mark, R.: "The Optical-Rotation Effect in Photoelastic Shell Analysis," Experimental Mechanics January 1969, pp. 9-16.

A difficulty commonly encountered in the three-dimensional photoelastic analysis of thin-shell structures is the so-called optical rotation effect which, in spite of some noteworthy efforts, has not yet been fully elucidated. The objective of this paper is to show how modern description of polarized light can be advantageously used to predict the influence of the rotation effect on optical observations. Use will be made of the Poincaré sphere representation of polarized light and of the associated Mueller calculus. Because these subjects may be unfamiliar, the fundamental concepts involved are briefly discussed in each case and readily available supplementary references are given.

5771 Aben, Hillar: "Optical Theory of the Multilayer-Refelction Technique for Three-Dimensional Photoelastic Studies," Experimental Mechanics, January 1969, pp. 25-30.

Using the theory of characteristic directions developed previously by the author optical phenomena by the multilayer-reflection technique in the general case are studied. Recursive formulas which enable successive determination of the parameters of all the photoelastic layers without any complication of the experimental technique are derived.

6.7.1 Birefringent Tests

5772 Rankilor, P. R.; McNicholas, J. B.: "The Preparation and Use of a Stress-Sensitive Material in Multi-Layer Photoelastic Models," Rock Mechanics and Mining Sciences, Vol. 5, No. 6, November 1968, pp. 465-474.

There are many applications for a stress-sensitive material in research and teaching when considering photoelastic problems. The particular material selected by the authors is a polyurethane rubber sold under the trade name 'Solithane'. Engineers reading existing technical publications might feel that Solithane is too difficult and too expensive to use as a research tool. The authors hope to show in this article that, for very little cost, and with a modicum of care, it can be prepared and used in the most modest space. The basic composition and preparation of the final rubber under laboratory conditions are described including practical aspects of model preparation. A range of rubbers of differing elasticity were prepared, their properties tested, and the results of these tests are given. It is suggested how and why this material should lend itself to the construction of multi-layer models with particular reference to geological and mining problems. Photographs are included of apparatus used, and of problems being investigated.

5773 Onogi, Shigeharu et al.: "Time-Temperature Superposition of Time-Dependent Birefringence for Low-Density Polyethylene," Journal of Polymer Science, Part A2, Vol. 5, 1967, pp. 1067-1078.

The time-dependent birefringence has been measured simultaneously with the stress relaxation on quenched and annealed low-density polyethylene at various temperatures from 10 to 70°C. The strain-optical coefficient increases generally with increasing time, and approaches the equilibrium value, which depends upon the temperature. When the strain-optical coefficient at a fixed time is plotted against temperature, it first increases and then decreases after passing through a maximum at T_{max} with increasing temperature. The higher the degree of crystallinity, the higher are the equilibrium values of the strain-optical coefficient and T_{max}. The curves for strain-optical coefficient vs. time and relaxation modulus vs. time below T_{max} can be superposed well by a horizontal shift along the abscissa. The optical shift fact obeys the original WLF equation, while the mechanical shift factor is much larger than the optical one. The molecular mechanisms corresponding to this dispersion of the strain-optical coefficient and visco-elastic α_c absorption near T_{max} are discussed.

5774 Pelzer-Pawin, G.: "Application of Photoelasticity to the Resolution of Hyperstatic Systems," Société Royale des Sciences de Liège, Bulletin, Vol. 37, No. 3-4, 1968, pp. 172-181, (in French).

Analysis of processes which widen the scope of applications of photoelasticity, especially in the hyperstatic region. The numerous applications which have thus far been made have shown their validity and simplicity. The experimenter can choose the method which lends itself most exactly and most easily to the problem which interests him. It is considered that the 'photelastic visualization' of the hyperstatic benavior is very instructive for the design engineer.

5775 del Rio, Carlos: "Application of 3-D Photoelasticity to Axi-Symmetrical Problems," Strain, Vol. 4, July 1968, pp. 30-31.

Description of a special approach using photoelasticity to treat the experimental analysis of stresses and strains in three-dimensional photoelastic problems. A model is made of material suitable to 3-D photoelasticity and tested in the frozen-stress technique to determine the state of stress. Specifically examined is a loaded structural component with axisymmetrical shape and loading in a cylindrical coordinate system. Since many practical problems are characterized by axial symmetry, application in industry might be of interest.

5776 Lord, P. R.: "High Speed Photography and Photo-Elasticity," High-Speed Photography, International Congress for High-Speed Photography and High-Speed Cinematography, 7th, Zurich, Switzerland, Sept. 12-18, 1965, Proceedings, ed. Othmar Helwich, 1967, pp. 543-547.

Study of dynamic photoelasticity and high-speed photography, with comments on the field of information storage. It is shown that, when the stress gradient is linear and the direction of the principal stress is known, it is possible to use a bent-beam compensator previously described by the author. It is shown how the gap between static and dynamic work can be bridged by the use of filters with various patterns of retardation frozen into them in conjunction with an image-dissection technique.

5777 Nazarenko, P. V.; Zaitsev, O. V.; Kostetskii, B. I.: "Effect of the Initial Dislocation Density on the Friction Force and the Ratio of Elastic to Plastic Deformation," Soviet Materials Science, Vol. 2, Nov.-Dec. 1966, pp. 471-473.

Description of strain measurements carried out on a specially constructed machine to determine the elastic and plastic strain components from the illumination intensity of double refraction bands during friction under both static and dynamic conditions at various normal pressures in single-crystal specimens of alkali metal halides. It is shown that the initial dislocation density of materials in friction has a substantial effect on the ratio of elastic to plastic strains produced during friction, that materials which undergo heavier plastic deformations during friction have larger friction coefficients, and that the initial dislocation density affects the friction force to the extent that it affects the magnitude and the ratio of the elastic to plastic strain components during friction, the effects of plastic strains being predominant.

5778 Hackett, R. M.; Krokosky, E. M.: "A Photoviscoelastic Analysis of Time-Dependent Stresses in a Polyphase System," Experimental Mechanics, December 1968.

The method of photoviscoelastic, stress analysis is used to predict time-dependent stress redistributions in a polyphase-material system having a viscoelastic binder and subjected to applied external-loading conditions. The polyphase-

6.7.1 Birefringent Tests (contd.)

material model studied is composed of a photoviscoelastic matrix material and contains rigid inclusions and voids, thus simulating a three-phase composite system.

In order to perform the study, a photoviscoelastic model material is developed. An epoxy-resin system consisting primarily of Shell Epon 828 and Epon 871, optimized to display the properties desirable for such application, is utilized.

The time-dependent stress distributions obtained by the photoviscoelastic analysis are compared with results obtained by applying the 'correspondence rule' to finite-element solution for the elastic stress field of a mathematical model of the three-phase material system. The comparison of results indicated that the technique of photoviscoelastic stress analysis is extremely applicable to complex models such as the one studied. The feasibility of this application to more complex polyphase models with varying loading conditions is indicated.

5779 Brillhart, L. V.; Dally, J. W.: "A Dynamic Photoelastic Investigation of Stress-Wave Propagation in Cones," Experimental Mechanics, Vol. 8, April 1968, pp. 145-153.

The embedded-polariscope method was employed to isolate the central plane in cylindrical and conical models subjected to axial loads. Light-field isochromatic-fringe patterns associated with each of the five models studied were recorded by using a multiplegap camera. Results obtained indicate that the maximum stress decays with distance propagated approximately as indicated by the elementary one-dimensional wave theory.

5780 Iosipescu, N.; Huidu, T.: "Observations on the Problem of Tests of Materials in Pure Shear, Deduced from Some Photoelastic Studies," Bucuresti, Universitatea, Analele, Seria Stiintele Naturii-Matematica, Mecanica, Vol. 15, No. 2, 1966, pp. 113-122, (in Rumanian).

Description of some supplementary photoelastic studies made with a view to completing previous studies on the new Rumanian process of testing materials in pure shear. These studies deal with the influences of variation of the notch angles and of variation of the radii of curvature of the bottoms of the notches on the mode of distribution of the tangential stresses over the pure-shear cross section. It is shown that only 90° notches, with sharp bottom angles, can lead to a uniform distribution of these tangential stresses, as had been established previously.

5781 Hunter, A.; Schwarz, M.: "Development and Application of a 3D Photoelasto-Plastic Method to Study Stresses Around a Crack," Weld Imperfections; Proceedings of a Symposium, Palo Alto, Calif., Sept. 19-21, 1966, ed. A. R. Pfluger; R. E. Lewis, 1968, pp. 543-565.

(See Abstract 3388).

SEE ABSTRACTS 5528, 5658, 5665, 5736

6.7.2 Moiré Fringe Technique

5782 Jenkins, Christopher J.: "Diffraction Gratings for Moire-Fringe Strain Analysis," Experimental Mechanics, Vol. 8, July 1968, pp. 331-332.

Description of a method for the fabrication and use of inexpensive diffraction-grating replicas for accurate moiré-fringe strain analysis. The replicas are composed of thin Lucite films suited for gluing onto model surfaces. The grids have good mechanical strength and toughness, and give results having errors of 3% or less. Gratings are discussed having 3000 lines/in.; apparently even finer grids can be produced with this method.

5783 Pelzer-Bawin, G.: "A Photographic Peculiarity in the Moire Domain," Société des Sciences de Liège, Bulletin, Vol. 37, No. 3-4, 1968, pp. 182-185, (in French).

Demonstration that although, in principle, whole orders of a moiré are given by white fringes, this can never be made into a general rule. The moiré is inverted as desired by a small variation of the exposure time. It is recommended that the terms 'whole orders' and 'half-orders' be used, instead of speaking of black and white fringes.

5784 Hinton, Ernest; Irons, Bruce: "Least Squares Smoothing of Experimental Data Using Finite Elements," Strain, Vol. 4, July 1968, pp. 24-27.

A program for interpreting moiré fringe data using a digital computer is described. The finite element technique overcomes certain intrinsic defects of existing methods which use polynomials, and promises to give better results, especially where stress concentrations are present. An experimental example compares the technique with the polynomial technique.

5785 Ross, Bernard E.: "Objective Experimental Stress Analysis Using the Moire Method," Developments in Theoretical and Applied Mechanics, Vol. 3, Southeastern Conference on Theoretical and Applied Mechanics, 3rd., University of South Carolina, Columbia, S. C., March 31-April 1, 1966, Proceedings, ed. W. A. Shaw, 1967, pp. 397-418.

Discussion of research into the further development of the moiré method of experimental stress analysis. Particular emphasis is placed on achieving complete objectivity in reducing the strain information from the moiré pattern. The application is to the thermal-stress problem of a ring under an axisymmetric temperature distribution. The maximum temperature reported is 1120°F. The results indicate that new levels of sensitivity and accuracy are achieved even though coarse gratings are used. The theory of the process is discussed, and a photo-reading device is described. A computer program is developed to reduce the moiré data. Techniques for using the moiré method in thermal stress problems at moderately high temperatures are devised.

5786 Ave, Masaru: "Stress Analysis by Moiré Methods. I.--Application to the Analysis of Two Dimensional Problems," Hosei University, Technical College, Bulletin, March 1967, pp. 22-34, (in Japanese).

Study of the applicability of the moiré method to stress analysis by solving two two-dimensional problems with this method and comparing the results with those obtained by analytical methods. The problems concern a plate with a hole subjected to pure tension and a rigid frame corner with deep members subjected to antisymmetrical bending. In the first problem, the diameter of the hole is varied and the measured stresses for each case are compared with the values obtained by Howland. In the second problem, by changing the ratio between the opening and the frame dimensions, the change in

6.7.2 Moirè Fringe Technique (contd.)

rigidity of the frame is examined and the stress distribution in the cross-panel is measured. Adaptability of simplified analytical methods for rigid frames with deep members is examined by the results obtained in the second problem.

6.7.3 General Strain Measurement Techniques

5787 Chiba, Mitsumasa; Shimada, Heihachi: "On Rosette Gage Factor of Photoelastic Strain Gage-Dependence on Strain, Temperature and Fringe Order," Tohoku University, Technology Reports, Vol. 32, No. 2, 1967, pp. 179-197.

Experimental and theoretical study of the mechanical behavior of the photostress rosette strain gauge. The photostress rosette gauges are tested under various loading conditions at various testing and bonding temperatures. It is found that the rosette gauge factor is not constant, but varies with strain and testing and bonding temperatures; this factor depends, moreover, on the order of the fringe pattern. This 's verified by theoretical analyses. A theoretical solution is obtained for the stresses in a circular hollow disk bonded along its outer rim to the surface of a structural part under biaxial strain. Numerical calculations carried out on this solution reveal some interesting and important characteristics of the gauge.

6.8 Systems Tests

5788 Nakano, Akira: "The Effects of Malalignment on the Aeroplastic Behavior of Unguided Rockets." Tokyo, University, Institute of Space and Aeronautical Science, Report No. 421, Vol. 33, Feb. 1968, pp. 73-96.

Study of bending loads produced in unguided rockets by misalignment caused by initial deflection of the rocket body and maladjustment of the fins and the nozzle. Equations of perturbed motion are derived for modal analysis and discrete mass analysis of such rockets. Expressions are also given for the bending-load factor as a linear function of each type of misalignment. The flight behavior of unguided single-stage rockets vs their misalignment characteristics is discussed.

5789 Achenbach, J. D.: "The Structural Dynamics of Solid Propellant Rockets," Applied Mechanics Reviews, Vol. 21, June 1968, pp. 542-555.

Examination of the structural dynamics of solid-propellant rockets, with emphasis on a description of several types of service loads, vibrations, and acoustic instability. The following loads or load conditions are considered: (1) transportation and handling; (2) aerodynamic loads; (3) combustion loads; (4) acceleration loads; (5) explosive loads; and (6) shock loads from nuclear blasts. An analysis of the free-standing vibrations of a hollow cylinder of a homogeneous, isotropic, elastic solid is carried out by writing general solutions of the elasticity equations for the cylinder in the form of products of Bessel functions governing radial dependence and trigonometric functions governing dependence on the circumferential and axial coordinates and on time.

5790 Viles, Joe M.: "Measurement of Erosive Burning Rates," Technical Report S-213, Rohm and Haas Co., January 1969.

A new technique for measuring average erosive burning rates of a propellant fired under realistic motor conditions is described. By utilizing a small test motor attached as a blast tube to a large gas generator, a minimal amount of test propellant is required. Hence the technique is attractive for evaluating or ranking the erosive-burning tendencies of compositions in a propellant development program. Erosive burning rates were measured for a CTPB-based composite propellant. Excellent correlation was found between the erosive burning rate, Mach number at the tail end of the propellant grain, and chamber pressure. The erosive burning rates measured in the test motors were independent of the composition of the gas-generator propellant. Application of the data in the design of an erosive-burning propellant grain has not been made.

5791 Tanis, Charles: "Large Segmented Reinforced Plastic Rocket Motor Case," Research & Technology Briefs, No. 10, October/November 1968, pp. 17-18.

5792 Thrasher, Durwood I.: "Structural Analysis of a Test-Weight Minuteman (Wing I), Second-Stage Aft Closure for Project NOMAD," Air Force Rocket Propulsion Lab., AFRPL-TR-68-186, October 1968.

The analysis reported was performed in support of an AFRPL in-house project utilizing surplus Second-Stage Minuteman motors as a low-cost test vehicle for contractor-furnished and in-house-designed nozzles.

A structural analysis was performed on the NOMAD test assembly, which consists of a Minuteman (Wing I) Second-Stage rocket motor, a redesigned single-nozzle aft closure, and the AFRPL-designed NOMAD nozzle. The critical safety margin was found to occur near the forward flangeof the aft closure; the safety margin was -0.272 at that point. For reasons discussed in the report, the test assembly is considered safe as designed in spite of the computed negative margin of safety. Input data generation, program utilization, and analysis results are fully documented in the report.

6.9 New Test Equipment

5793 Kaiser, W. D.; Cress, H. A.: "A Simple, High Capacity, Rotating Load, Fatigue Testing Machine," Matl. Res. Stand., Vol. 8, No. 1, 1968, pp. 12-16.

A reliable and simple high capacity, rotating load fatigue testing machine was designed on the principle of mechanical resonance. The machine can test six large, symmetrical cantilever type specimens, either pipes or solid shafts, simultaneously, they need not be identical. It has been used for rapid fatigue testing of 2 and 4 in. pipe specimens, with internal pressure up to 1300 psi. With slight modification it can accomodate specimens of a wide range of size and impose rotating moments on them as high as 1,500,000 in. lb.

5794 Saada, A. S.: "A Pneumatic Computer for Testing Cross-Anisotropic Materials," Matl. Res. Stand., Vol. 8, No. 1, 1968, pp. 17-23.

A testing machine suitable for applying multiaxial states of stress to thin hollow cylinders is described. A pneumatic analogue computer performs the operations necessary for testing at any desired rate of true stress and for changing at will the directions of the principal stresses with respect to the axis of rotational symmetry of the material. An application is given for the case of cross-anisotropic clay tested under pure deviatoric conditions with the major principal stress at a fixed angle with the axis of rotational symmetry.

5795 Duvdevani, I. J.; Biesenberger, J. A.; Gogos, C. G.: "A New Concept in Thermo-Mechanical Measurements," Fifth International Congress on Rheology, Kyoto, Japan, 1968.

A sensitive (approx. 0.2 millicalories/sec)dynamic flow calorimeter, new in concept and design, has been constructed in which instantaneous stress-strain and instantaneous (lag time of 2 sec) heat-effect measurements are made and recorded. It is capable of straining specimens, in the form of thin films, at various strain rates (10^{-3} to 10^{+3} inches/min) as well as sinusoidally (10^{-3} to 10^{+3} cycles/min) with variable amplitude and at various temperatures(from room temperature to about 100°C).

5796 Birnboim, M. H.; Burke, J. S.; Anderson, R. L.: "A Computer Approach to Instrumentation in Viscoelasticity," Fifth International Congress on Rheology, Kyoto, Japan, 1968.

This basic processing instrument is used in conjunction with the apparatus specific to the experiment, namely, sample, force and response transducers, thermometers, and environmental chamber, to form a complete experimental system. The instrument is being used with a cryogenic torsion pendulum as a system for viscoelastic studies on crystalline polymers in the frequency range from 10^{-3} Hz to 10^{3} Hz and temperature range from 4°K to 400°K. Results for a high molecular weight polyethylene fraction will be presented. The basic instrument performs these automatic functions: determines phase and amplitude from d.c. to 500 KHz with noise rejection capabilities and an accuracy of 10^{-3} radians and 0.1% through the use of cross-correlation and signal averaging techniques; generates sine waves 10^{-3} Hz to 10^{3} as well as other waveforms; programs a frequency synthesizer; determines temperature; through oscilloscope and other displays it provides the experimenter with a basis for instant judgement of each measured point; enormously reduces data handling and processing.

5797 Tuijnman, C. A. F.; Janssen, P. H.; Sieswerda, B. S.: "Equipment for Measuring Stress Relaxation and Torsional Vibration in a Large Frequency Range," Fifth Interntl. Congress on Rheology, Kyoto, Japan, 1968.

A stress relaxation apparatus measuring the decay of stress of a viscoelastic sample after application of a torsional step deformation has been developed. The stress relaxation takes place under conditions where a variation of the deformation of at most 0.5% is allowed. Under these conditions, the use of servo systems can be avoided, which allows of a stable and simple construction of the apparatus by using only one measuring device. This consists of a bending strip supported on one end and carrying semi-conductor strain gauges arranged in a bridge circuit.

The principle used for the design of the second apparatus is similar to that described by Lord and Wetton. With the aid of a capacitance transducer, the phase and amplitude of the torsional oscillation of an electromagnetically driven specimen are measured. The forced oscillation is applied in a frequency range of 0.5 to 1000 c/s, in which the storage modulus and loss tangent of the material of the specimen can be obtained.

5798 Gangi, A. F.; Thomson, K. C.: "Wide-Band Transducer for Seismic Modeling," Journal of Geophysical Research, Vol. 73, No. 14, July 15, 1968.

A linear piezoelectric transducer with a wide-band frequency response has been designed for use as a seismic model source. The wide bandwidth is achieved by a transducer configuration that is constant for discrete scaling changes. This gives a log-periodic design that is a subclass of frequency-independent designs. A six-step log-periodic transducer with a scaling ratio of 1.25 was constructed and tested. The measured electrical impedance compares favorably with a theoretical electrical impedance obtained using an approximate analysis. The electrical impedance of the transducer mounted on an aluminum semicircle was measured and found to be relatively independent of frequency over the frequency range from 90 to 300 kHz. The elastic waveform from the transducer compared with that from a standard simple transducer shows that the wideband transducer is more efficient in electromechanical conversion over a broader frequency band.

5799 Coppa, A. P.: "Application of a Pneumatic Gun Apparatus to Structural Impact Studies at High Velocity," Applied Polymer Symposia, No. 5, 1967, pp. 257-283.

Description of experimental research in high-speed structural impact. The discussion of these studies is intended to serve two purposes: (1) to illustrate several applications of a pneumatic gun apparatus to research studies and materials behavior under high-speed loading; and (2) to present results obtained from these studies, which show some interesting effects due to high-speed loading. A gun apparatus is described in sufficient detail to point out important design features which result in satisfactory high-speed performance. Such features produce an accurate alignment between specimen and impacting projectile, a sage recovery of specimens intact for post-impact examination, and dissipation of impact energy for safe operation under normal laboratory conditions. Results of three studies are reported.

5800 Shippy, David J.; Gillis, Peter P.; Hoge, Kenneth G.: "Computer Simulation of a High Speed Tension Test," Applied Polymer Symposia, No. 5, 1967, pp. 311-324.

Description of a relatively simple mass-spring system designed to gain insight into the vibrational response of a load-cell coupling a tensile specimen and a high-speed testing machine. The machine and load cell are represented by linear springs and the specimen by a nonlinear spring that closely models the static stress-strain behavior of many metals. These are connected in series with two masses representing the testing machine and the load cell-specimen combination. It is assumed that during a test the ends of this mass-spring series separate at a constant velocity. A numerical analysis of the system was carried out on a digital computer with values considered appropriate for such tests. Since the system has two degrees of freedom, two vibrational modes were observed, corresponding approximately to the natural fre-

6.9 New Test Equipment (contd.)

quencies of the machine and load cell. Vibrational amplitudes were usually of the same order of magnitude in the two modes. While the study was designed primarily to investigate the effects of specimen characteristics on load-cell response, the most interesting result was that the period of the lf vibrational mode was usually long compared with the time-required for the specimen to fracture. This implies that the hf vibrations can have a mean value displaced in a given direction from the specimen force during the entire test.

5801 Melton, R. B., Jr.: "Mohr's Circle Presentation on an Oscilloscope," Experimental Mechanics, January 1969, pp. 41-44.

An instrument is described which operates from a single three-element rosette strain gage and displays the diameter of Mohr's circle for stress or strain on an oscilloscope with proper length, position and angle for the determination of principal stress or strain magnitudes and direction. The device combines simplicity of construction and calibration with low cost and versatility of operation. Its useful frequency range is from static to a reasonable fraction of the system carrier frequency. The present design employs a-c gage excitation but the basic concept may be extended to d-c excitation for high-frequency work. Recording of dynamic strains is possible by photography of the oscilloscope trace. Uses have included instruction in elasticity as well as conventional stress analysis.

5802 Schroeer, Rudi: "Research on Exploratory Development of Nondestructive Methods for Crack Detection," Air Force Materials Laboratory, Air Force Systems Command, Technical Report AFML-TR-67-167, Part II, November 1968.

Results of a research study devoted to exploratory development of a nondestructive method for crack detection are reported in this document, covering the period from June 1967 to July 1968. The method investigated is based upon an acoustic impact technique, which consists of the analysis of the vibrations in the test specimens produced by mechanical pulses. Frequency shifts and damping times were the primary factors evaluated. Some theoretical concepts are discussed in this report.

Test methods and levels were established for various sample configurations and jet engine components. The test results presented indicate that fatigue cracks hidden beneath fasteners can successfully be detected with the acoustic impact technique. Probe configurations for this application have been tested. A final breadboard system has been assembled into a portable package.

Extensive studies were performed to investigate the applicability of the acoustic impact technique for crack detection on jet engine components, especially turbine wheels, compressor disks and blades. Laboratory results show that the acoustic impact technique is not only capable of detecting small cracks, but also seem to be superior to other methods presently used, with respect to sensitivity and required test time.

5803 Glukhov, E. E.; Shelion, A. V.: "Apparatus for Testing Plastics for Deformability in Tension," Plast. Massy, No. 5, May 1968, (in Russian).

The apparatus is intended for the short-term tensile testing of plastics with constant loading and temperatures of from -50 to 100°C, It provides for rapid attachment and removal of the specimen. Results are given for plasticized PVC, PTFE, oriented and unoriented polyethyleneterephthalage film and various PE/polyisobutylene compositions.

SEE ABSTRACT 5637

7.1 Interaction Between Curing Conditions and Mechanical Behavior

5804 Shimazaki, A.: "Viscoelastic Changes of Epoxy Resin-Acid Anhydride System During Curing," J. Appl. Polymer Sci., Vol. 12, No. 9, September 1968.

The changed viscoelastic properties of the epoxy resin-acid anhydride system, Epikote 834-HHPA, are followed to the gel point at 130, 140, and 150°C with a dynamic viscoelastometer. The viscosity increases with curing time through two inflections designated A and B. The point A is interpreted (from the reference to the chemical changes reported in the previous paper) as the termination of the initial state of this curing reaction, and point B coincides with the gel point determined by the torsion method. The resonance frequency remains constant value up to the point B, followed by a rapid increase. The extents of reaction for epoxide, anhydride, and initial OH are 15, 45.8 and 100% at the point A; 27.8, 63.7, and 100% at the point B, respectively. The apparent activation energies for viscosity are 7.5 kcal/mole for point B (gel point). The overall apparent activation energies of this curing reaction are obtained from the Arrhenius plots for the curing time required for the resin mixture to reach the state of the points A and B; these values were 8.9 kcal/mole for point A and 16.2 kcal/mole for point B.

7.3 Effects of Aging

5805 Williams, Bernard L.; Weissbein, Leonard: "Torsional Braid Analysis of Antioxidant Activity in Elastomer Systems, I. Initial Studies," Journal of Applied Polymer Science, Vol. 12, 1968, pp. 1439-47.

The torsional braid apparatus as originally described by Lewis and Gillham has been explored as a means of providing a quantitative measure of antioxidant activity of selected compounds when formulated with certain elastomer systems prone to oxidative crosslinking on heat aging. With this technique the time dependence of the sharp torsional modulus increase corresponding to a change from a rubbery to a highly crosslinked state, is determined. This time dependence is taken as a measure of the rate of oxidative crosslinking in heat-aged elastomer films coated on a fiber-glass braid. In this manner an assessment of the activity of antioxidants can be made. To illustrate the application of this technique, two initial studies will be cited. In one study the relative protective effect on a carboxylated styrene-butadiene latex system of a series of antioxidants was found to be in the following order: α,α'-2,6-bis(2-hydroxy-3-tert-butyl 5-methylphenyl)xylenol > the reaction product of nonylated paraethylphenol and formaldehyde > 2,2'-methylene bis(6-nonylparacresol). In another study, with cis-polybutadiene as the elastomer, the effectiveness of a series of antioxidants was found to be in the following order: 2,2'-methylene bis(6-tert-butyl paracresol) >1,3,3,5-tetramethyl-1-m-tolylindane-4',6-diol > 4,4'-methylene bis (2,6-di-tert-butylphenol). In addition, the effect of concentration and temperature was studied with the most efficient antioxidant in this last series.

5806 Martirosyan, M. M.: "Effect of Aging on Creep of Svam Glass-Reinforced Plastic in Tension with Allowance for the Orientation of the Fibers," Polymer Mechanics, Vol. 1, No. 6, November-December 1965.

The author presents the results of an experimental study of the effect of aging under room conditions on the creep deformation of SVAM glass-reinforced plastic. It is established that with prolongation of the aging period up to two years the resistance of the material to creep deformation increases. The effect of aging is investigated in relation to anisotropy.

7.3 Effect of Aging (contd.)

5807 Pavlov, N. N.; Akopdzhanyan, Z. A.: "Aging of Various Plastics under Various Climatic Conditions," Plast. Massy, Vol. 5, No. 72, May 1968, (in Russian).

Results are presented and discussed on the aging of plasticized PVC, polyamides and epoxy compositions in certain cases using stabilizers, in temperature continental, humid subtropical, and dry continental subtropical climates.

7.4 Effects of Binder-Filled Chemical Interactions

5808 Baumgartner, W. E.; Myers, G. E., et al.: "Double-Base Binder Improvement," Air Force Rocket Propulsion Laboratory, Research and Technology Division, 14 October 1968.

Investigation of means to upgrade the mechanical properties of slurry cast CMDB propellants has continued. Emphasis is being placed upon the use of nitrocellulose derivatives (particularly the acetate) to improve plasticization, crosslinking, and binder-solids adhesion. No significant changes in tensile behavior were produced by using enzyme-treated and non-treated ball powder or by adding acceptable quantities of highly active plasticizers. Low molecular weights of some nitrocellulose derivatives resulted in potlife problems; higher molecular weight materials are being prepared. Even in highly purified plasticizers a substantial portion of isocyanate crosslinkers is consumed in non-crosslinking reactions. The effect upon binder-solids adhesion of additives capable of adsorption upon solids and reaction with curatives is bein examined.

INDEX OF AUTHORS REFERRED TO IN THIS ISSUE
(NUMBERS USED ARE SERIAL NUMBERS OF ABSTRACTS)

INDEX OF AUTHORS REFERRED TO IN THIS ISSUE
(NUMBERS USED ARE SERIAL NUMBERS OF ABSTRACTS)

INDEX OF AUTHORS REFERRED TO IN THIS ISSUE
(NUMBERS USED ARE SERIAL NUMBERS OF ABSTRACTS)

INDEX OF AUTHORS REFERRED TO IN THIS ISSUE
(NUMBERS USED ARE SERIAL NUMBERS OF ABSTRACTS)

INDEX OF AUTHORS REFERRED TO IN THIS ISSUE
(NUMBERS USED ARE SERIAL NUMBERS OF ABSTRACTS)

UNCLASSIFIED

Security Classification

DOCUMENT CONTROL DATA - R&D

(Security classification of title, body of abstract and indexing annotation must be entered when the overall report is classified)

1. ORIGINATING ACTIVITY (Corporate author)	Solid Rocket Structural Integrity Information Center University of Utah, College of Engineering	
2a. REPORT SECURITY CLASSIFICATION	UNCLASSIFIED	
2b. GROUP		
3. REPORT TITLE	SOLID ROCKET STRUCTURAL INTEGRITY ABSTRACTS	
4. DESCRIPTIVE NOTES (Type of report and inclusive dates)	Vol. 6, No. 2	
5. AUTHOR(S) (Last name, first name, initial)	Wagner, F. R. Cluff, E. D. (editors)	
6. REPORT DATE	April 1969	
7a. TOTAL NO. OF PAGES	97	
7b. NO. OF REFS	286	
8a. CONTRACT OR GRANT NO.	F04611-67-C-0042	
b. PROJECT NO.	3059	
c.		
d.		
9a. ORIGINATOR'S REPORT NUMBER(S)	UTEC SI 69-016	
9b. OTHER REPORT NO(S) (Any other numbers that may be assigned this report)	AFRPL-TR-69-57	
10. AVAILABILITY/LIMITATION NOTICES	Qualified requestors may obtain copies of this report from DDC. No foreign distribution without approval of sponsoring military activity.	
11. SUPPLEMENTARY NOTES		
12. SPONSORING MILITARY ACTIVITY	Air Force Rocket Propulsion Laboratory Edwards, California 93523	

13. ABSTRACT

Vol. 6 No. 2 of the Solid Rocket Structural Integrity Abstracts contains a comprehensive coverage of "The Ballistic Interface in Grain Configuration for Structural Analysis" as the lead article. This paper represents several years work by John S. Billheimer, Senior Engineering Specialist at the Research and Technology Department of Aerojet-General Corporation, Sacramento, California. This issue also contains a Calendar of Conferences and Short Courses, reviews of seven technical books, 286 Abstracts, and an Author Index.

DD FORM 1 JAN 64 1473

UNCLASSIFIED

Security Classification

UNCLASSIFIED
Security Classification

14. KEY WORDS	LINK A		LINK B		LINK C	
	ROLE	WT	ROLE	WT	ROLE	WT
Solid Propellant Grain Design Solid Propellant Rocket Engines Solid Rocket Abstracts						

INSTRUCTIONS

1. ORIGINATING ACTIVITY: Enter the name and address of the contractor, subcontractor, grantee, Department of Defense activity or other organization *(corporate author)* issuing the report.

2a. REPORT SECURITY CLASSIFICATION: Enter the overall security classification of the report. Indicate whether "Restricted Data" is included. Marking is to be in accordance with appropriate security regulations.

2b. GROUP: Automatic downgrading is specified in DoD Directive 5200.10 and Armed Forces Industrial Manual. Enter the group number. Also, when applicable, show that optional markings have been used for Group 3 and Group 4 as authorized.

3. REPORT TITLE: Enter the complete report title in all capital letters. Titles in all cases should be unclassified. If a meaningful title cannot be selected without classification, show title classification in all capitals in parenthesis immediately following the title.

4. DESCRIPTIVE NOTES: If appropriate, enter the type of report, e.g., interim, progress, summary, annual, or final. Give the inclusive dates when a specific reporting period is covered.

5. AUTHOR(S): Enter the name(s) of author(s) as shown on or in the report. Enter last name, first name, middle initial. If military, show rank and branch of service. The name of the principal author is an absolute minimum requirement.

6. REPORT DATE: Enter the date of the report as day, month, year; or month, year. If more than one date appears on the report, use date of publication.

7a. TOTAL NUMBER OF PAGES: The total page count should follow normal pagination procedures, i.e., enter the number of pages containing information.

7b. NUMBER OF REFERENCES: Enter the total number of references cited in the report.

8a. CONTRACT OR GRANT NUMBER: If appropriate, enter the applicable number of the contract or grant under which the report was written.

8b, 8c, & 8d. PROJECT NUMBER: Enter the appropriate military department identification, such as project number, subproject number, system numbers, task number, etc.

9a. ORIGINATOR'S REPORT NUMBER(S): Enter the official report number by which the document will be identified and controlled by the originating activity. This number must be unique to this report.

9b. OTHER REPORT NUMBER(S): If the report has been assigned any other report numbers *(either by the originator or by the sponsor)*, also enter this number(s).

10. AVAILABILITY/LIMITATION NOTICES: Enter any limitations on further dissemination of the report, other than those imposed by security classification, using standard statements such as:

(1) "Qualified requesters may obtain copies of this report from DDC."

(2) "Foreign announcement and dissemination of this report by DDC is not authorized."

(3) "U. S. Government agencies may obtain copies of this report directly from DDC. Other qualified DDC users shall request through
______________________________."

(4) "U. S. military agencies may obtain copies of this report directly from DDC. Other qualified users shall request through
______________________________."

(5) "All distribution of this report is controlled. Qualified DDC users shall request through
______________________________."

If the report has been furnished to the Office of Technical Services, Department of Commerce, for sale to the public, indicate this fact and enter the price, if known.

11. SUPPLEMENTARY NOTES: Use for additional explanatory notes.

12. SPONSORING MILITARY ACTIVITY: Enter the name of the departmental project office or laboratory sponsoring *(paying for)* the research and development. Include address.

13. ABSTRACT: Enter an abstract giving a brief and factual summary of the document indicative of the report, even though it may also appear elsewhere in the body of the technical report. If additional space is required, a continuation sheet shall be attached.

It is highly desirable that the abstract of classified reports be unclassified. Each paragraph of the abstract shall end with an indication of the military security classification of the information in the paragraph, represented as *(TS), (S), (C), or (U)*.

There is no limitation on the length of the abstract. However, the suggested length is from 150 to 225 words.

14. KEY WORDS: Key words are technically meaningful terms or short phrases that characterize a report and may be used as index entries for cataloging the report. Key words must be selected so that no security classification is required. Identifiers, such as equipment model designation, trade name, military project code name, geographic location, may be used as key words but will be followed by an indication of technical context. The assignment of links, rules, and weights is optional.

UNCLASSIFIED
Security Classification